

# Numerical and Experimental Researches in Engineering

EDITOR  
HASAN KÖTEN

## **BIDGE Publications**

Numerical and Experimental Researches In Engineering

**Editor:** Hasan KOTEN

ISBN: 978-625-372-219-7

Page Layout: Gözde YÜCEL

1st Edition:

Publication Date: XXXX

BIDGE Publications,

All rights of this work are reserved. It cannot be reproduced in any way without the written permission of the publisher and editor, except for short excerpts to be made for promotion by citing the source..

Certificate No: 71374

Copyright © BIDGE Publications

[www.bidgeyayinlari.com.tr](http://www.bidgeyayinlari.com.tr) - [bidgeyayinlari@gmail.com](mailto:bidgeyayinlari@gmail.com)

Krc Bilişim Ticaret ve Organizasyon Ltd. Şti.

Güzeltepe Mahallesi Abidin Daver Sokak Sefer Apartmanı No: 7/9 Çankaya /  
Ankara



## **PREFACE**

There has been a growing significance placed on disciplines like engineering and pure sciences when it comes to determining the most efficient system points in engineering studies. The parameters utilized in optimization studies serve as boundary values for identifying the most efficient points. The implementation of these boundary values relies on fundamental elements such as production methods, heat treatments, and energy techniques. Our publication focuses on the latest research in this field, including special production and heat treatment techniques, as well as theoretical, numerical, experimental and optimization. We firmly believe that these production techniques will serve as a valuable reference for both researchers and technical personnel involved in practical applications. We extend our gratitude to the authors of the chapters in this book, with the hope that it will prove beneficial to both our industry and research centers.

**Editor**

Hasan KOTEN, Professor

## Content

PREFACE .....	3
Parametric Design and Static Analysis For Solar Energy Panel Bracket Application .....	6
Güllü AKKAŞ .....	6
An Overview of the Substantial Outputs of Forging Processes and the Generation of Loads Affected by Forging Parameters in Closed-Die .....	36
İsmail GÜRBÜZ .....	36
Seyit Murat Altunç .....	36
Abdulmecit GÜLDAŞ .....	36
Replacement of Cross-Car Beam Steel Parts with a Carbonfibered Composite Material in a Vehicle .....	92
Cem İÇİER .....	92
Tevfik Can ÖZGÜR .....	92
Gökay PİRLEPELİ .....	92
Gökçe EKEN .....	92
Living Hinge Design on Automative Glovebox Mechanism.....	100
Gökay PİRLEPELİ .....	100
Abdullah HELVACI .....	100
Gökçe EKEN .....	100
Cem İÇİER .....	100
Additive Manufacturing in Plastic Injection Moulding .....	109
Mehmet ALTUĞ .....	109
Yunus ASLAN .....	109
Yakup YILMAZ .....	109

Performance Improvement of Vapor Compression Refrigeration System Using Nanofluid .....	141
Metin YILMAZ .....	141
Canan CİMŞİT .....	141
Elif ÖĞÜT .....	141

# CHAPTER I

## Parametric Design and Static Analysis For Solar Energy Panel Bracket Application

Güllü AKKAŞ<sup>1</sup>

### 1. Introduction

Modern 3D CAD (Computer Aided Design) has many positive effects on accelerating product development processes. One of these effects is the efficient and relatively easy reuse of existing models. In addition, the ability to make changes to these models is also very effective in accelerating the processes. In modern engineering approaches and especially in product development processes, the ability to apply previous designs and processes to new situations is extremely important (Camba, Contero, & Company, 2016; Iyer, Jayanti, Lou, Kalyanaraman, & Ramani, 2005; Jackson & Buxton, 2007). Most design information is stored digitally in CAD models. The preference for model-based engineering approaches is

---

<sup>1</sup> Asst. Prof. Dr., Kayseri University, Vocational School of Technical Sciences, Department of Machine and Metal Technologies, Kayseri/Turkey, Orcid: 0000-0001-7836-9746, gullu.akkas@kayseri.edu.tr

becoming increasingly widespread. At this stage, if CAD can be reused, design can be reused. CAD models are central to development processes. They are also widely used within manufacturing processes among process stakeholders. In addition, they are the main source of data for the process (Camba et al., 2016).

Feature-based parametric CAD is a common design tool in most engineering fields. It creates models and assemblies. Industrially, it is the industry standard technology for model and assembly creation. Non-geometric features, called parameters based on geometry, are the controllers of a parametric design (Shah, 1991). These parameters are defined based on dimensional, geometric and algebraic constraints. As a result of the proper use of CAD systems, design semantics are added to the model. Design semantics allows the designer to easily update existing models quickly and accurately by adjusting some parameters (Camba et al., 2016).

The parametric CAD systems used today are characterized by a history-oriented approach. According to this approach, how the model was created is automatically recorded. At the same time, it is made available while the model is being created. History-based parametric modeling systems keep relational three-dimensional information of certain aspects of the model. This information is based on a parent/child relationship. All features in the model are linked hierarchically. Each node represents one feature. Each link shows the dependency between two features. In this way a network structure is created. This structure is often referred to as a design tree, feature tree or history tree in different notations. The design tree has an adaptive structure. Thanks to this feature, CAD users gain the ability to easily model complex parts. The major advantages of this

gain are flexible design and reusability. Feature dependencies must be properly defined. This means that changes and innovations in parent nodes are automatically transferred to child nodes. This means that the CAD model reacts to changes and innovations in a predictable format (Bodein, Rose, & Caillaud, 2014; Camba et al., 2016). With all these advantages, however, there are still parent/child dependencies between traits. This form of coupling is the source of many regeneration problems in parametric modeling. The size and complexity of a parametric CAD model is common in industrial design. This complexity can grow rapidly and significantly depending on the application. Increasing the number of drawing relationships and dependencies means increasing the interconnectedness of the design tree. This is a major obstacle to maintainability and model reuse. For a stable CAD design, the dependencies between features must be correctly defined. An unstable CAD model poses a challenge to designers. The designer may have to rebuild the design (Branoff, 2014; Camba et al., 2016).

The finite element method (FEM) is a numerical technique that subdivides a system into smaller, simpler components to approximate the solution of a boundary value problem. This method is employed for conducting structural analysis. The process begins with defining the geometry of the structure, which is dictated by the specific type of simulation analysis to be conducted (Vardaan & Kumar, 2022).

Nowadays, various software has been developed to perform finite element analysis. Each of these software are powerful new tools for engineers. The development of the Internet has opened the door to moving CAD/CAE software to the cloud. As a result, high-



quality design tools have become globally available. This has made CAD/CAE software indispensable for engineering. Despite these developments, the human factor still plays a leading role in all product design processes. Computers today are still only auxiliary tools that help people to design. In this design mode, people use various tools to design and analyze a product. These tools fulfill different design requirements, from the creation of geometric shapes to the evaluation of structural performance (Yingjun Wang, Xiao, Xia, Li, Li, & Gao, 2023). In fact, CAD and CAE modules were originally separate software that needed to be harmonized with each other (Yingjun Wang et al., 2023). Based on current developments, today CAD software can produce basic solutions for FEM analysis by using CAE plug-ins.

The current way to create high quality products is to apply computer-aided intelligent structural optimization methods to design processes. Structural optimization processes have certain constraints such as stress and displacement (Yingjun Wang et al., 2023). The aim of the optimization process is to computationally find the optimal material distribution for a design under these constraints (Huang & Xie, 2010; Le, Norato, Bruns, Ha, & Tortorelli, 2010). In today's technology, designers no longer need a wealth of knowledge and experience. Because with the use of topology optimization, designers can obtain a high-performance design scheme (Yingjun Wang et al., 2023).

The widespread use of solar panels is becoming a key component in promoting sustainable development by providing clean and renewable energy for social development. The main task of a bracket is to bear the weight of the solar panel and at the same

time ensure that the panels are fixed. If the bracket structure is not strong, it can have a number of bad consequences. In the case of a weak solar panel, the solar panel may deform or break. As a result of these deformations, energy production efficiency decreases and equipment damage can also occur. Therefore, analyzing the strength of solar panel bracket structures is of great importance in improving the reliability and safety of solar systems (Xu, Xie, & Li, 2023).

This study involves a parametric design and static analysis based on the example of a solar panel bracket. The commands used to perform parametric design are explained in detail. Also, detailed information is given on static analysis procedures. The SolidWorks CAD and CAE modules were used for the design and analysis stages.

## **2. Related Studies**

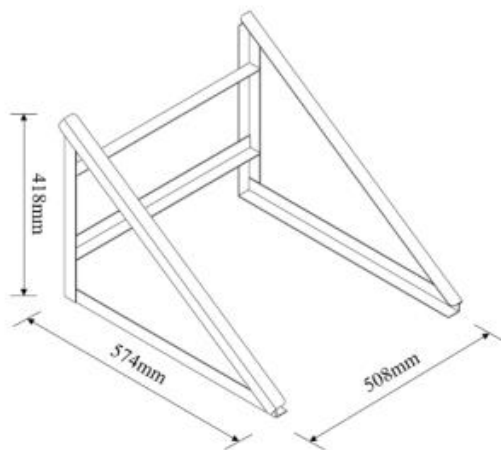
In a 2002 study, a new airplane was developed that encompassed all areas of aeronautical engineering. The focus of the design is on geometric modeling. Innovative technologies were incorporated into new configurations and therefore each new idea was modeled in an understandable way. Feedback from the analyzed models was easily integrated into subsequent iterative cycles. The primary goal in aircraft design is to investigate the configuration as a whole. As a result, there should be a single geometric model that is frequently updated and accessible to each discipline with its own tools. For this purpose, a parametric geometric model has been created for the various disciplines in order to keep the effort of developing the necessary interfaces low. The aircraft is divided into logical components that reflect the modules used. These components are successively divided into sub-assemblies until the aircraft parts are defined with useful parameters. This step was repeated down to

the rivets to reach the required level of detail. This process requires a large amount of effort, know-how and computing power due to the parameterized interconnections (Richter, Mechler, & Schmitt, 2002).

In another study, a simple solar panel bracket was designed and investigated to improve the performance of solar panel brackets. Ansys Workbench software was used to perform finite element analysis on the bracket. The response surface method was applied to optimize the design of the bracket structure. The models of the bracket before and after optimization were analyzed and compared. The optimized bracket has a section height of 32 mm, a section width of 21.6 mm and a section thickness of 2 mm. Compared to the original stent, the weight of the optimized stent was reduced by 0.4365 kg and the weight loss rate was calculated as 11.02%. Furthermore, the maximum displacement of the optimized bracket was reduced by 0.0531 mm and the maximum stress was reduced by 1.587 MPa. These results show that the solar panel bracket improves its overall performance while providing light weight (Xu et al., 2023).

In their paper, Camba et al. presented an analysis of formal CAD modeling strategies and best practices of history-based parametric design. These strategies are Delphi horizontal modeling, open reference modeling and flexible modeling. Among the considerations in the study is the rationale to avoid unnecessary feature dependency. The order and selection criteria of these features were also examined. The effects of parent/child relationships on model change are also considered. They conducted a series of experiments using industrial CAD models with three different levels

of complexity. They presented a comparative evaluation of the strategies in these experiments. By analyzing the internal structure of the models, they compared their robustness and flexibility when the geometry is changed. The results showed significant advantages of formal modeling methodologies. In particular, flexible techniques outperformed unstructured approaches. It was also shown that in many modeling situations the horizontal strategy leads to unexpected problems (Camba et al., 2016).



*Figure 1: 3D model of the solar panel bracket*

*Source: Xu et al., 2023*

A wide variety of definitions have been proposed for features used in the CAD and computer-aided manufacturing (CAM) domains. They are initially modeled according to machining features that can be used to integrate CAD and CAM packages (Ma & Tong, 2003). After many years of development in feature-based design or manufacturing, most of the implemented features are still CAD-oriented and related to machining processes (e.g., holes, slots, and pockets) or design geometry (e.g., drafting angle). Their definitions

are based on predefined parametric templates that lack the flexibility for extension or reconfiguration as required by some design processes such as mold cooling channel design. Otto (Harald E., 2001) [16] identified three groups of information consistency breakdowns to be addressed by feature technology: static, dynamic, and hybrid breakdowns. Efforts have been made to overcome these problems through features such as CAD and CAE feature information sharing (Deng, Britton, Lam, Tor, & Ma, 2002). For example, when analyzing plastic components with CAE applications, walls, ribs, and midplanes are defined as features. More recently, the concept of feature has been expanded to encompass any meaningful grouping schema related to geometric entities. In fact, feature definition largely depends on the application objectives. Otto (Harald E., 2001) described the role of features as relating (product or part) geometry to an engineering discipline in order to represent a specific meaning. Feature modeling represents a special application of information modeling (Ma & Tong, 2003).

Initially, efforts to define formal parametric design methodologies focused on assembly modeling. Some strategies were developed on the organization of components in the assembly context and the constraints and relationships that should be established between components. These strategies were based on a top-down design approach. For example, Aleixos et al. (Aleixos, Company, & Contero, 2004) propose a top-down assembly modeling methodology based on the integration of semantic elements with CAD models. The work of Hui et al. (Hui, Dong, Guanghong, & Linxuan, 2007) uses semantic elements to develop an "assembly semantic modeling" theory for use in assembly sequence planning. More recently, software systems and algorithms, such as the graph-

based system proposed by Patalano et al. (Patalano, Vitolo, & Lanzotti, 2013), aim to assist users and partially automate some aspects involved in the design of constraint-based mechanical assemblies (Camba et al., 2016). The main objective of the effective application of parametric modeling methodology is to generate design trees with a small number of parent/child dependencies, which are easy to understand and accurately express the design intent (Wang & Nnaji, 2005).

This study provides a detailed explanation of how a parametric design application can be implemented based on the example of a solar energy panel bracket. The study also explains in detail how to calculate the resistance of brackets that protect solar panels against wind load through a static analysis scenario.

### **3. Parametric Design Process for the Solar Panel Bracket**

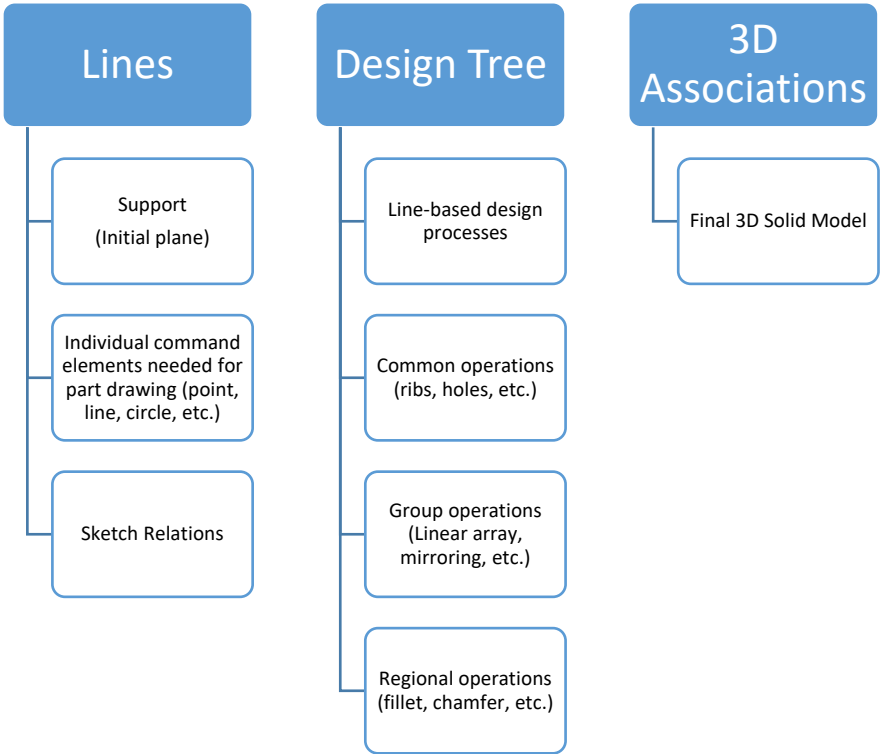
Parametric design is, in a sense, a rather limited term; while it refers to the use of parameters to describe a form, it is really about the use of relationships. The term can be used in a broad sense to encompass concepts found in the literature under headings such as relational modeling, variational design or constraint-based design. These topics will be touched upon to some extent in the following paragraphs. From a fundamental point of view, it should also be noted that the boundary between parametric design and computer-aided design or modeling is not clear. In these cases, forms are created by combining basic entities that are added to the model after a template containing their basic parameters has been filled in. For example, a line becomes part of a model after two parameters, its length and direction, have been specified. A polygon is a series of lines that meet at their vertices, and their position parameters need

to be specified when they are created. With a prismatic mesh, the volume is added to the model with four parameters: position, length, width and height (Monedero, 2000).

For the parametric design of the bracket, the drawing parameters of the fastener were first determined using conventional methods. Then a parametric section was obtained by using line commands. Following the parametric section drawing, the design tree would begin to be created. The aim here is to move from line-based design processes to a solid model of the fastener. This is where the solid modeling commands in SolidWorks features come into play (create solids by extrusion, create solids by rotating, create solids by sweeping, as well as detail commands such as fillet and chamfer). In the last stage, the final solid model is obtained with 3D associations. Figure 2 presents a systematic overview of modeling operations and sub-operations (Aranburu, Camba, Justel, & Contero, 2023).

The brackets are panel fixing elements that protect solar panels against the wind force during use. They are capable of functionally resisting the wind force, thereby preventing the panels from being displaced by the wind. The brackets consist of four elements. The first one is the upper bracket element. This element is designated as bracket element 1 in Table 1. The other one is the lower bracket element. It is named bracket element 2 in Table 3. These two elements are specially designed to protect against the wind force. One of the other two elements is the Allen head bolt, one of the standardized fasteners. The last element of the bracket is the spring element, which supports the bracket to remain in an elevated position, facilitating assembly. This last design unit is also modeled using the Helix command, taking into account the spring standards.

Table 1 and Table 2 show all the commands used in the bracket parametric design process and the visual stages reached after these commands. The purpose of this part is to ensure that the solar panels can remain stable against the moving forces caused by the wind.


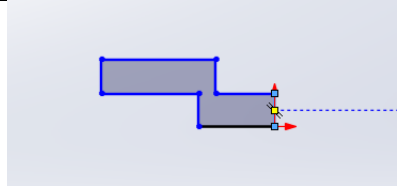
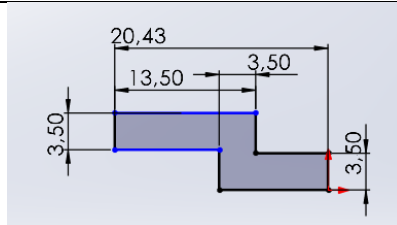
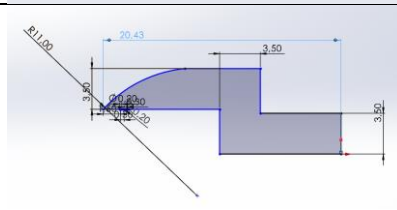



*Figure 2: Modeling operations and sub-operations*

*Source: Aranburu et al., 2023*

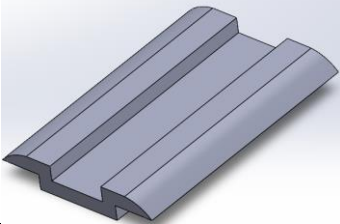
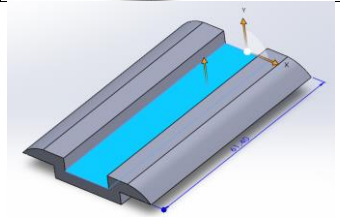
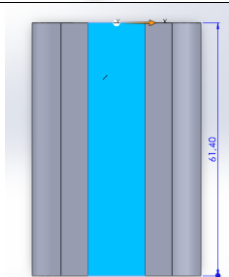
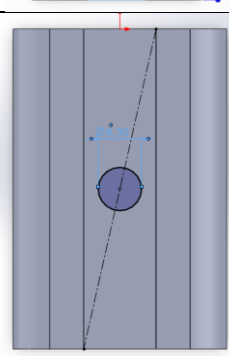


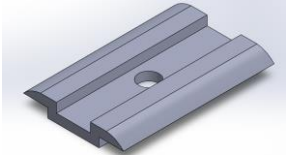
*Table 1: Linear design stages of the 1<sup>st</sup> part of the bracket*

Numbering of the Design Stages of Bracket Element 1	Command Used	Visual Developments
1	Selecting the initial plane (Feature Manager-Front plane)	
2	Sketch-Line	
3	Sketch-Smart dimension	
4	Sketch-3point arc-Circle-Smart dimension	
5	Sketch-Mirror	

*Source: Created by the author.*

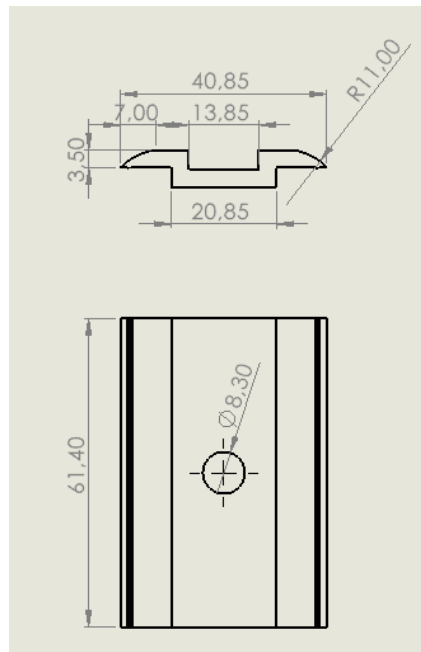
*Table 2: Solid Model Design Stages of the 1<sup>st</sup> Part for the Bracket*

Numbering of the Design Stages of Bracket Element 1	Command Used	Visual Developments
1	Features-Extruded Boss/Base	
2	Plane selection	
3	View Orientation-Normal To	
4	Sketch-Center line-Circle-Smart dimension	

5	Features- Extruded Cut	
---	---------------------------	---

*Source: Created by the author.*

Parametric modeling allows for the reuse of existing products and rapid modification of the design based on the results of engineering analysis. In a feature-based modeling system, the level of detail is important for feature classes. Decisions need to be made about the levels of detail across which they will be manipulated. The different levels of detail include form features, functional features, and manufacturing features (Myung & Han, 2001).

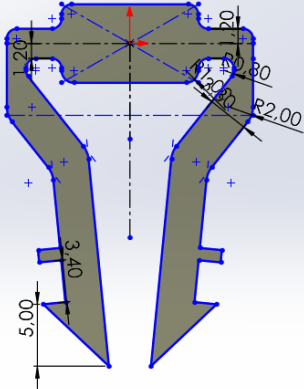
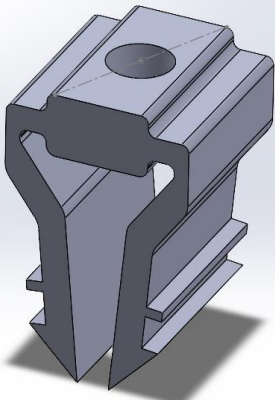


*Figure 3: Section parameters of bracket element 1*

*Source: Created by the author.*

Table 3 shows the design processes of the part that allows the panel bracket to be fixed to the panel carrier section.

*Table 3: Drawing and solid modeling of the second part for the bracket*

Numbering of the Design Stages of Bracket Element 2	Command Used	Visual Developments
1	Sketch-Line-Offset Entities	 <p>A 2D technical drawing of a bracket. The drawing shows a central vertical section with a horizontal top flange. Dimensions include a top flange width of 60.0, a central hole diameter of 30.0, a fillet radius of R2.00, a vertical section width of 3.40, and a base thickness of 5.00. Construction lines (dashed blue lines) and offset entities (solid blue lines) are used to define the geometry.</p>
2	Features-Extruded Boss/Base  Features-Hole wizard-Advanced hole	 <p>A 3D isometric view of the bracket. The model shows the top flange, the central vertical section, and the base. A circular hole is visible on the top flange. The model is rendered in a light blue color with a shadow on the base.</p>

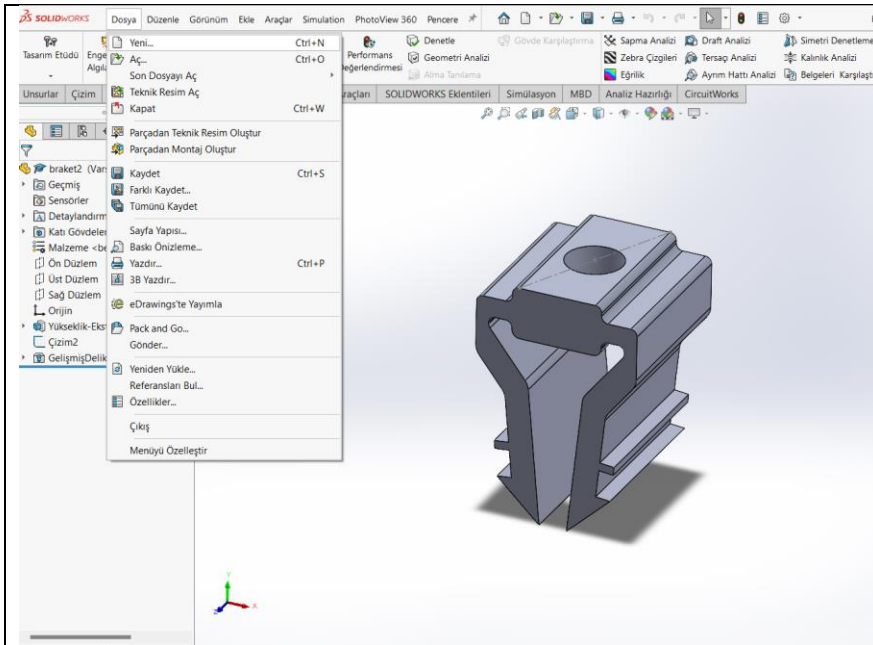
*Source: Created by the author.*

As seen in Table 1, Table 2, and Table 3, two different assembly elements were designed for the solar panel bracket design.

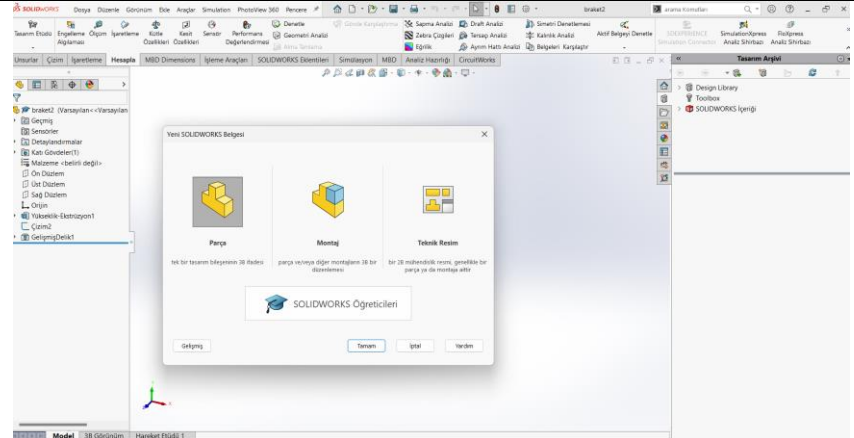
After this stage, these two separate design units are saved as SLDPRT. Following the saving process, the assembly screen is opened. The first part to be fixed is called by using the add component command on the assembly screen.

In this study, bracket element 1 is called as the part desired to be fixed on the assembly screen. Immediately afterwards, bracket element 2 is brought to the assembly screen. At this point, coaxiality is defined between the upper bracket element and the lower bracket element by referencing the holes on them. After the definition of coaxiality, an Allen head bolt that can work with the two design units is retrieved from the design library, ensuring the assembly of these two parts. Table 4 shows the assembly processes of the design units in stages.

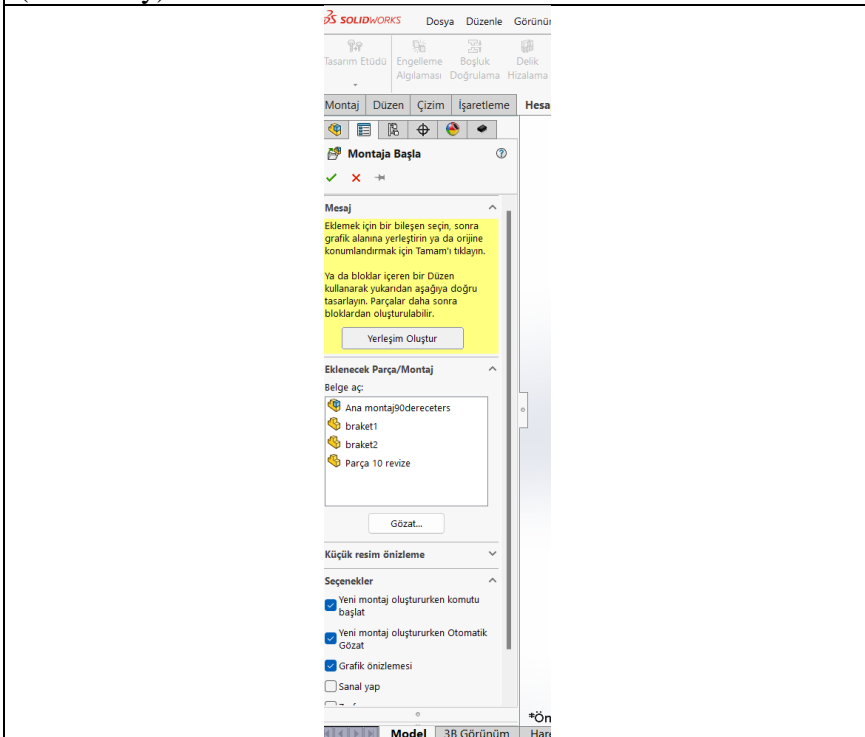
*Table 4: Assembly process stages of the design units*



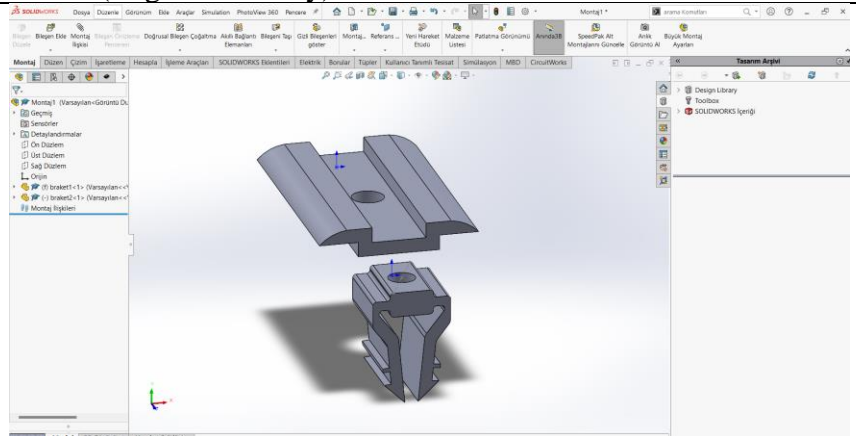
1. A new design page is opened on the SolidWorks screen. (New)



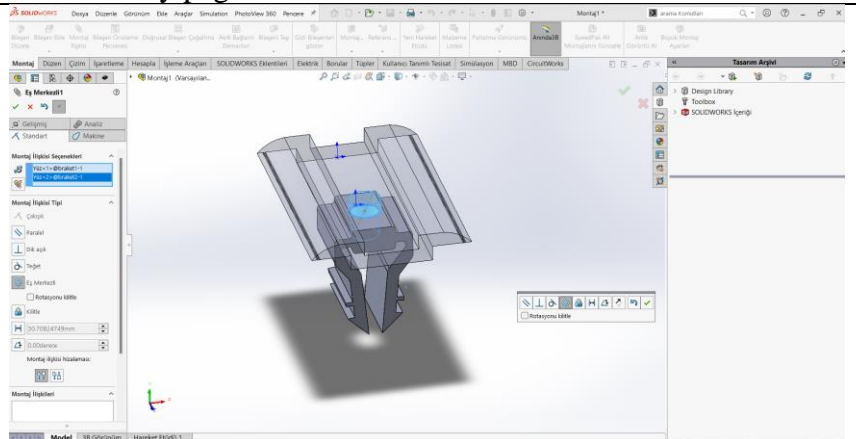
2. The assembly interface begins to be used on the screen above (Assembly).



3. The bracket elements 1 and 2 are retrieved onto the assembly screen (Begin Assembly).



4. The unassociated state of the bracket design units appears on the assembly page .



5. Assembly association takes place. At this stage, coaxiality to the holes and parallelism between the two surfaces on the front side are defined as assembly relationships (Mate-Concentric).



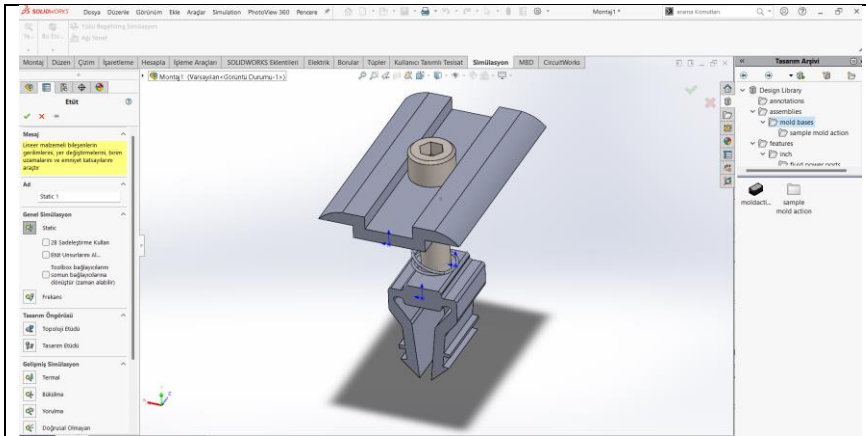


said to demonstrate safe resistance to wind impact when four brackets are used per panel, depending on the application.

In this book chapter, a scenario has been planned for rooftop panel connection under the influence of wind force. According to this scenario, four brackets are used for each panel. The panels are secured with these brackets at four points. Under this condition, each bracket bears an average load of 125 kg when there is an average distributed wind load of 500 kg. Within this scenario, the strength value of the bracket design unit when produced from AA 6063-T6 aluminum extrusion material was investigated. The analysis part of the SolidWorks software was used for this investigation.

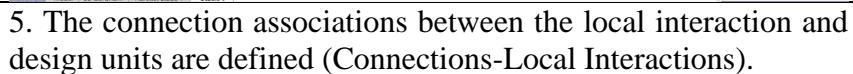
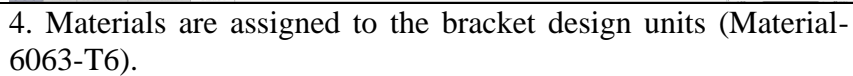
Table 5 explains, step by step, the FEM analysis process for determining the solar panel bracket strength values.

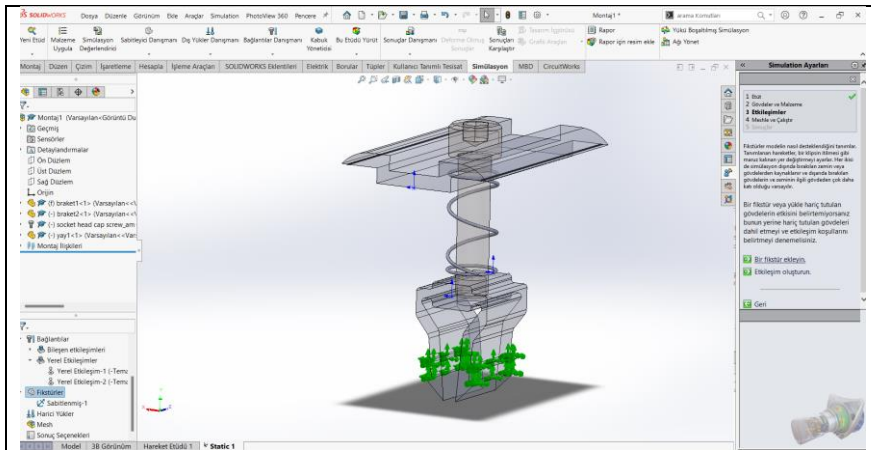
*Table 5: Bracket analysis stages*



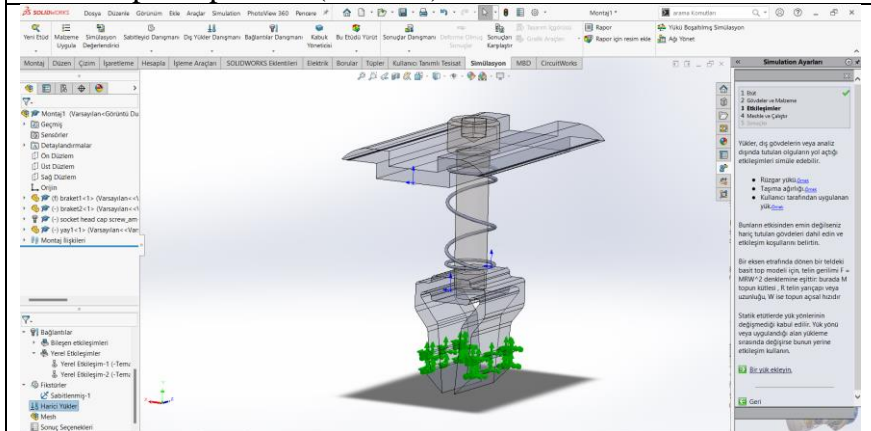
1. The simulation-new study command is selected, and the screen above is opened. Here, the static analysis is selected, and the analysis is named (Simulation-New Study-Static1).



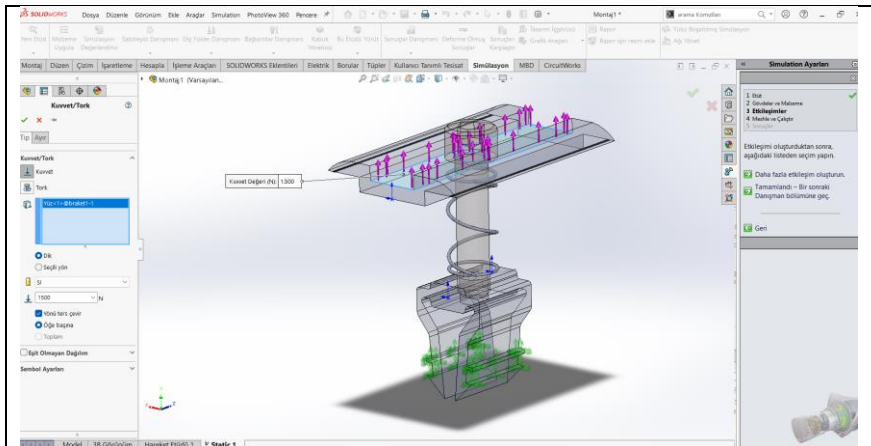




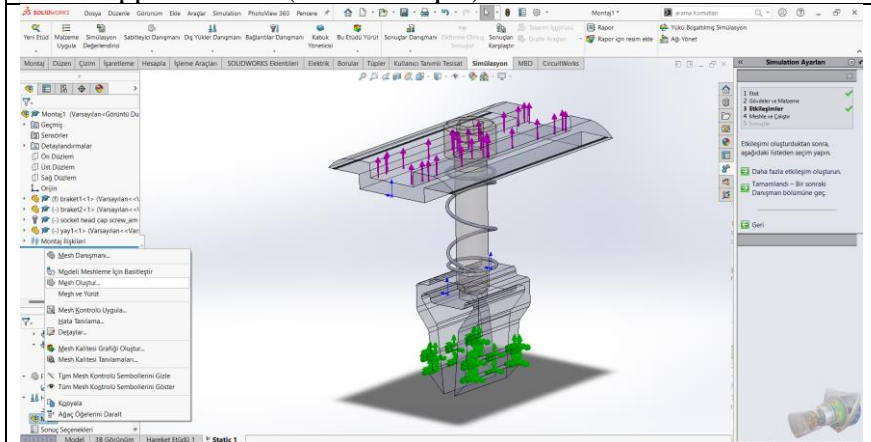
6. Fixation is defined at the points where bracket 2 makes contact with the panel profiles (Fixtures).



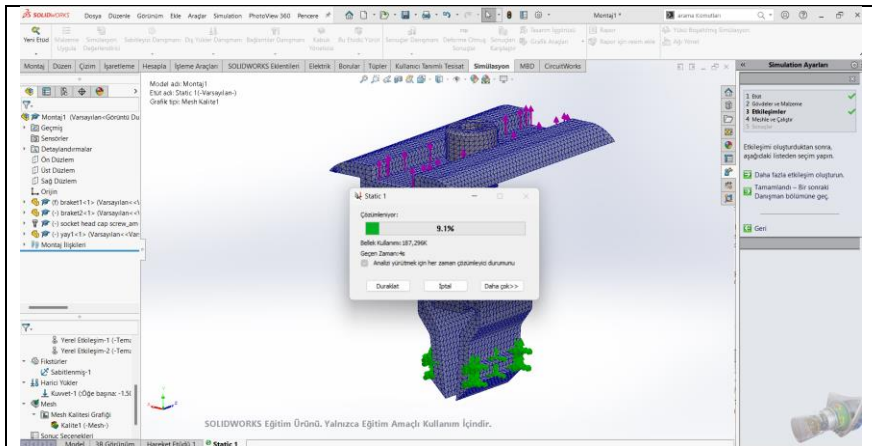
7. With the selection of the external loads section, the amount of load to fall on the design unit affects the simulation settings (External Loads).



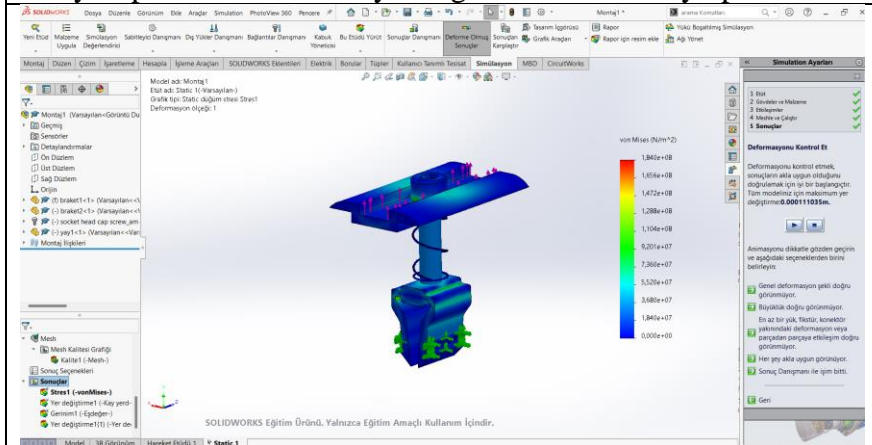
8. A distributed wind load of 150 kg is applied to the top surface of the upper bracket (Force-Torque).



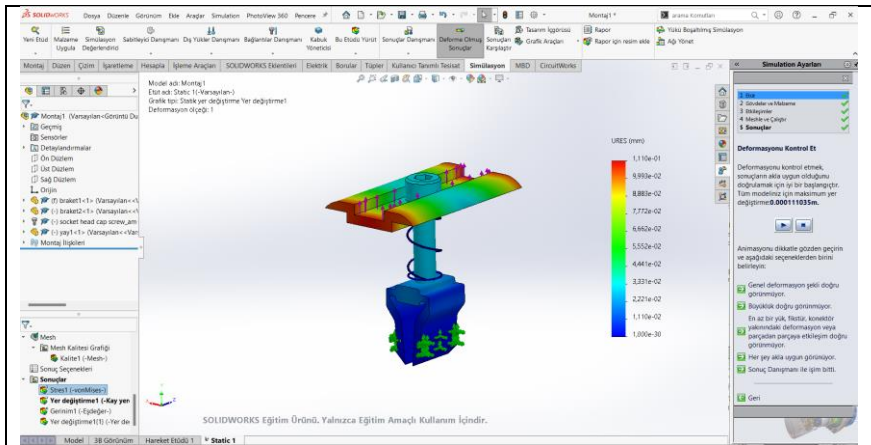
9. Mesh assignment is performed with the create mesh option (Mesh>Create Mesh).



10. After the mesh is created with the fine mesh setting, the analysis process is started by using the execute study option.



11. Information about the strength of the bracket is obtained based on the analysis results. According to the Von Mises values, it can be said that the design unit will operate safely under the created analysis scenario (Results).



12. The displacement values are also acceptable. The parts colored red are the areas with the highest displacement (Results-VonMises).

*Source: Created by the author.*

## 5. Conclusion

In today's technology, utilizing solar energy has become an indispensable part of a sustainable life and a responsible manufacturing process in every aspect. For this reason, every detail, from panel production to the production of assembly elements and even the on-site applications of solar panels, is open to development and thus needs to be thoroughly researched. While elaborating such research and design processes, it is necessary to make use of technological developments and basic principles. Parametric design with CAD programs is one of the greatest opportunities that technology offers in the process of creating and optimizing new products. This chapter has focused on how parametric design processes can be operated on brackets, which are solar panel fasteners. CAD models were created for bracket design units using reverse engineering techniques, and then they were assembled to bring them into their real-life working form. The progression of solid

modeling processes has been explained in detail. Based on the wind force scenario created after the assembly process, the strength analysis of the design unit was performed in the case of using AA 6063-T6 material. The SolidWorks program was preferred for the design and analysis processes. Based on the analysis results, the study concludes that the solar panel brackets will be able to function safely under a possible wind force of 150 kg for the current design.



## References

Aleixos, N., Company, P., & Contero, M. (2004). Integrated modeling with top-down approach in subsidiary industries. *Computers in Industry*, 53(1), 97–116.

Aranburu, A., Camba, J. D., Justel, D., & Contero, M. (2023). An Improved Explicit Reference Modeling Methodology for Parametric Design. *Computer-Aided Design*, 161, 103541. doi:<https://doi.org/10.1016/j.cad.2023.103541>

Bodein, Y., Rose, B., & Caillaud, E. (2014). Explicit reference modeling methodology in parametric CAD system. *Computers in Industry*, 65(1), 136–147.

Branoff, T. J. (2014). *Examining the constraint-based modeling strategies of undergraduate students*. In *Proceedings of the 69th midyear conference engineering design graphics division ASEE* (pp. 54–66).

Camba, J. D., Contero, M., & Company, P. (2016). Parametric CAD modeling: An analysis of strategies for design reusability. *Computer-Aided Design*, 74, 18–31. doi:<https://doi.org/10.1016/j.cad.2016.01.003>

Deng, Y.-M., Britton, G. A., Lam, Y. C., Tor, S. B., & Ma, Y. S. (2002). Feature-based CAD-CAE integration model for injection-moulded product design. *International Journal of Production Research*, 40(15).

Harald E, O. (2001). From concepts to consistent object specifications: translation of a domain-oriented feature framework

into practice. *Journal of Computer Science and Technology*, 16, 208–230.

Huang, X., & Xie, Y. M. (2010). Evolutionary topology optimization of continuum structures with an additional displacement constraint. *Structural and Multidisciplinary Optimization*, 40, 409–416.

Hui, W., Dong, X., Guanghong, D., & Linxuan, Z. (2007). Assembly planning based on semantic modeling approach. *Computers in Industry*, 58(3), 227–239.

Iyer, N., Jayanti, S., Lou, K., Kalyanaraman, Y., & Ramani, K. (2005). Shape-based searching for product lifecycle applications. *Computer-Aided Design*, 37(13), 1435–1446.

Jackson, C., & Buxton, M. (2007). The design reuse benchmark report: seizing the opportunity to shorten product development. *Aberdeen Group, Boston*.

Le, C., Norato, J., Bruns, T., Ha, C., & Tortorelli, D. (2010). Stress-based topology optimization for continua. *Structural and Multidisciplinary Optimization*, 41, 605–620.

Ma, Y.-S., & Tong, T. (2003). Associative feature modeling for concurrent engineering integration. *Computers in Industry*, 51(1), 51–71. doi:[https://doi.org/10.1016/S0166-3615\(03\)00025-3](https://doi.org/10.1016/S0166-3615(03)00025-3)

Monedero, J. (2000). Parametric design: a review and some experiences. *Automation in Construction*, 9(4), 369–377. doi:[https://doi.org/10.1016/S0926-5805\(99\)00020-5](https://doi.org/10.1016/S0926-5805(99)00020-5)

Myung, S., & Han, S. (2001). Knowledge-based parametric design of mechanical products based on configuration design

method. *Expert Systems with Applications*, 21(2), 99–107.  
doi:[https://doi.org/10.1016/S0957-4174\(01\)00030-6](https://doi.org/10.1016/S0957-4174(01)00030-6)

Patalano, S., Vitolo, F., & Lanzotti, A. (2013). *A graph-based software tool for the CAD modeling of mechanical assemblies*. In *International Conference on Computer Graphics Theory and Applications* (Vol. 2, pp. 60–69). SCITEPRESS.

Richter, T., Mechler, H., & Schmitt, D. (2002). *Integrated parametric aircraft design*. In *ICAS Congress, Toronto*.

Shah, J. J. (1991). Assessment of features technology. *Computer-Aided Design*, 23(5), 331–343.

Vardaan, K., & Kumar, P. (2022). Design, analysis, and optimization of thresher machine flywheel using Solidworks simulation. *Materials Today: Proceedings*, 56, 3651–3655.  
doi:<https://doi.org/10.1016/j.matpr.2021.12.348>

Wang, Yan, & Nnaji, B. O. (2005). Geometry-based semantic ID for persistent and interoperable reference in feature-based parametric modeling. *Computer-Aided Design*, 37(10), 1081–1093.

Wang, Yingjun, Xiao, M., Xia, Z., Li, P., & Gao, L. (2023). From Computer-Aided Design (CAD) Toward Human-Aided Design (HAD): An Isogeometric Topology Optimization Approach. *Engineering*, 22, 94–105.  
doi:<https://doi.org/10.1016/j.eng.2022.07.013>

Xu, S.-S., Xie, K.-X., & Li, S.-P. (2023). Optimization design study on a prototype Simple Solar Panel Bracket.

## CHAPTER II

### **An Overview of the Substantial Outputs of Forging Processes and the Generation of Loads Affected by Forging Parameters in Closed-Die**

**İsmail GÜRBÜZ<sup>1</sup>**  
**Seyit Murat Altunç<sup>2</sup>**  
**Abdulmecit GÜLDAŞ<sup>3</sup>**

#### **1. Introduction**

The Metal Forming term is defined by a group of manufacturing methods that transform a formless material or a material with simple geometry into a beneficial part without changing mass or composition. Metal parts manufacturing is split into five general areas in a simplified way; (1) primary forming (Casting, Melt Extrusion, Die Casting, and Metal Powder Pressing), (2) Metal forming processes (Rolling, Extrusion, Cold and Hot

---

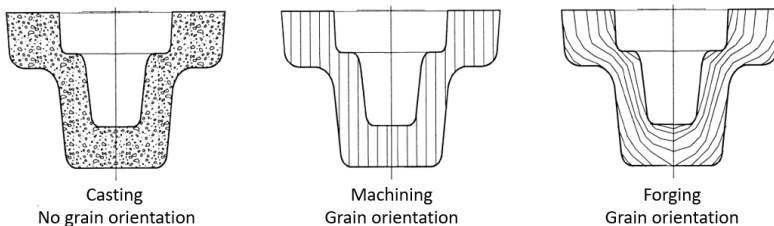
<sup>1</sup> Gazi Üniversitesi Fen Bilimleri Enstitüsü, İmalat Müh. Bölümü, Teknikokullar, Ankara-Türkiye  
ORCID ID: 0000-0002-1339-3427, [ismailgrbz9@gmail.com](mailto:ismailgrbz9@gmail.com)

<sup>2</sup> Evimetal Inox Yapı Çözümleri Tasarım Merkezi, Arnavutköy-İstanbul,  
ORCID ID: 0009-0006-6154-2817, [murat@evimetal.com.tr](mailto:murat@evimetal.com.tr)

<sup>3</sup> Gazi Üniversitesi Teknoloji Fakültesi, İmalat Müh. Bölümü, Teknikokullar, Ankara-Türkiye  
ORCID ID: 0000-0002-1865-2272, [aguldaz@gazi.edu.tr](mailto:aguldaz@gazi.edu.tr)

Forging, Bending), (3) Chip removal forming (Cutting, Turning, Milling and Broaching), (4) Heat treatment (Anodizing and Surface Hardening), (5) Joining processes (Welding, Soldering, Riveting, Shrinking, Mechanical Assembly).

Forging, (Dieter, 1986) which is considered one of the oldest metalworking arts, is one of the most important manufacturing processes in which a metal part in its simple initial form, such as rods, sheets, billets, and/or ingots, is formed into the desired shape by plastic deformation. It is also suitable for the production of individual sample parts as well as for mass production. Forging plays a significant role in the metal forming industry as it reduces the required machining processes and allows complex parts to be produced with the desired grain flow in forged parts. Because the ideal grain flow in the final products has been provided, they show better mechanical and metallurgical characteristics than parts manufactured by casting and machining processes (Groover, 2010) (Chen, et al., 2017) (Jo, Jeong, Lee, Moon, & Hwang, 2021). In addition to that, beneficial grain flow procures a longer fatigue life than parts manufactured by casting and machining (Chen, et al., 2017). The grain flow that occurs in parts manufactured by different manufacturing processes is shown symbolically in Figure 1.



*Figure 1: The grain orientation in different manufacturing methods.*

## **2. Forging**

### **Forging classification**

Fundamentally, forging consists of a group of manufacturing processes with deformation stages. The other stages are the separation and assembly processes. Forging processes are classified by machine type, workpiece type, forming temperature, and die set type.

#### **Machine type**

The forging process is classified by machine type into 3 main groups (press forging, hammer forging, and forming on the forging roller). The equipment used in forging (presses and hammers) affects the forging process as they impress strain rate and temperature conditions. Thus, they determine the manufacturing rate.

The demands of a specific forging technique need to align with the features of a specific forging device, including its load capacity, energy, time requirements, and precision. T. Altan et al. explained in detail the working principles and characteristics of traditional and special machine types used in forging (Altan, Ngaile, & Shen, Cold and Hot Forgings: Fundamentals and Applications, 2005).

#### **Material type**

The metals used in forging can be divided into ferrous (carbon steels, alloy steels, and stainless steels) and non-ferrous metals (aluminum, magnesium, and titanium alloys) according to their type. In the forging industry, ferrous steels are generally used extensively. However, with the increase in demand for forged non-ferrous metal products, especially in aviation and automotive, the

use of non-ferrous metal products in forging is increasing rapidly. The main reasons for this increase in demand are the lightness, long life, durability, and environmental friendliness of the forged non-ferrous final product (Cavaliere, 2004).

### Forming temperature

The temperature level and how it spreads are determined by the initial temperatures of the material and the dies, the friction-generated heat, and the heat exchange among the deformed material, dies, and the surroundings. It's noted that 90-95% of the energy used in forming processes is converted into heat (Atlan, Oh, & Gegel, 1983). Forging processes are divided into 3 groups bases on temperature; Cold forging, Hot Forging, and Warm Forging (Lange K. ). General temperature values for three different forging operations are illustrated in Figure 2.

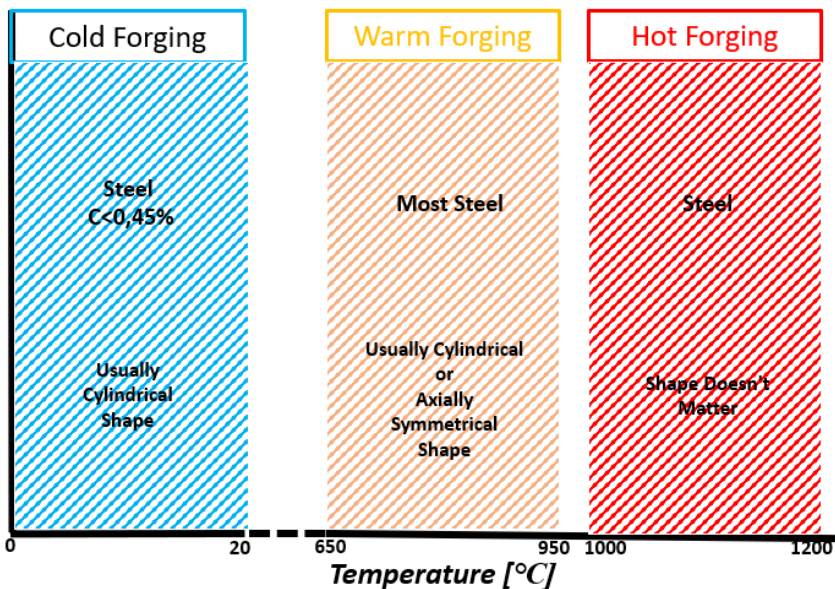


Figure 2: Forming temperature ranges

## **Cold forging**

Initially, the workpiece temperature is room temperature in cold forging. The forging process, in the design of the cold forging manufacturing process, may be considered a complex system that contains a workpiece that is affected by tribological and environmental conditions, and implicit interactions between tool and press. K.Lange indicates that the center of the system is the good surface conditions of a workpiece with a simple initial shape and the forging operation which enables the final product with a complex shape and correct dimensions (Lange K. , 1992). The advantages of cold forging compared to rival manufacturing processes are high material utilization, improved material properties, and an unaffected grain flow. The other advantages are also accuracy and high surface quality of manufactured compounds (Tekkaya & Hering, 2019) (Ishinaga, 1997) (Yanagimoto, Sugiyama, Yanagida, Iwamura, & Ishizuka, 2009). One of the most important factors in providing these advantages is the dislocations formed by high flow stress in the forged part. However, this high flow stress requires a high operation load, and only a limited number of patterns may be manufactured (Jo, jeong, Lee, Moon, & Hwang, 2021).

## **Hot forging**

Hot forging is carried out in a range of higher than recrystallization temperatures of the material to decrease flow stress and increase workpiece formability. After forming, which is carried out at higher than reforming temperatures, workpieces do not take place a permanent strain hardening (Lange K. ). Heat treatment is necessary for the workpiece to obtain the appropriate strength (Wernicke, et al., 2021). Even in this situation, high mechanical



loads come into existence during forming. High-forming load estimation is not possible because of Thermo-Elastic-Plastic effects and complex interactions between the tool and workpiece system (Behrens & Odening, 2009) (Maier, et al., 2019). Failure mechanisms for hot forging processes may be stated as corrosion, surface crack extension, plastic strain deposition, mechanical thermal fatigue, and thermal shocks. Despite the formability in hot forging being better than other forging processes, die corrosion is faster due to higher temperatures and compound pressure. Fast die corrosion negatively affects the die life, causing rising costs and decreasing manufacturing speed. For this reason, estimation of the die corrosion is critical for die life estimation (Davoudi, Nejad, Kolor, & Petru, 2021). Elastic springback caused by high thermo-mechanical stresses occurs after forging, leading to deviations from the actual geometry to undesirable geometry, and shrinkage behavior (Behrens, et al., 2020)

### **Warm forging**

During warm forging, the workpiece temperature is above room temperature and under the recrystallization temperature. The process may be accepted as a precise forming application that enables high-quality component manufacturing (Forcellese & Gabrielli, 2000). Intermediate temperature forging of high carbon and alloy steels is favored over cold forging due to its benefits, including reduced flow stress, enhanced ductility, minimized workpiece hardening, and improved toughness of the forged components (Fujikawa, Yoshioka, & Shimamura, 1992) (Hirscvogel & Dommelen, 1992) (S.Sheljaskov, 1994). Compared to hot forging, warm forging provides better material utilization, improved surface quality, and high dimensional accuracy (Shivpuri, Babu, Kini,

Pauskar, & Deshpande, 1994). In this context, the technique merges the accuracy of cold forging with the low yield stress and high formability characteristic of hot forging (Xinbo, Hongsheng, & Zhiliang, 2003). However, warm forging is more inconvenient than both traditional methods in terms of working conditions and environmental compatibility (Sheljaskov, 1994). In addition, die/tool corrosion is significant in warm forging. If the shape of the product desired to be obtained at the end of the operation is complex, the physical process that indicates the operation (metal flow, material characterization, and product qualification) is complicated and may not be analyzed systematically (Shivpuri, Babu, Kini, Pauskar, & Deshpande, 1994). Like in any of the three forging methods, understanding the metal's flow stress at warm forging temperatures is crucial for planning the process, designing the dies, selecting die materials, and determining press capacity.

### **Die set type**

Forging operations are generally non-stationary operations that occur consequent indirect pressure under three-dimensional stress and deformation conditions. There are several forging methods (flash/flashless closed die forging, open die forging, electric forging, forward/backward extrusion, radial forging, etc.) used in the industry depending on the type of die set, forging can be categorized into two primary groups: open die forging and closed die forging.

### **Open die forging**

In the most general definition, in the open die forging method, simple tools are used that have no concern with the final workpiece shape. Open die forging is a forming operation of hot metal with a hammer aid on a flat or simply contoured surface. The

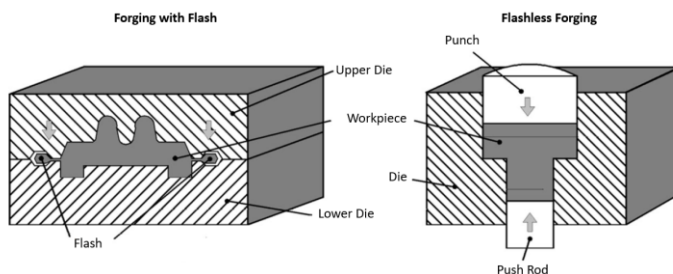
cross-section of the hot workpiece is reduced by compressing it between the upper die or hammer connected to a ram and a lower die connected to the press bed, and the length of the workpiece is increased by repeated and alternating forging. To minimize the number of machining required to obtain cylindrical steel components made in small quantities from large masses, such as turbine rotors, shafts, or rolling rolls, workpiece deformation is carried out in an open-die forging press to achieve approximate final geometry. (Choi, Chun, Tyne, & Moon, 2006). Open die forging is frequently conducted not only to shape the workpiece into its desired final form but also to enhance its mechanical properties by achieving a uniformly distributed fine grain size throughout the workpiece. (Wolfgarten, Rudolph, & Hirt, 2020). The tool sizes are relatively small in comparison to the overall dimensions of the forged workpieces. Because only a portion of the workpiece undergoes deformation at any given moment during forging, the necessary forging loads are lower than those needed to deform the entire workpiece. The primary purpose of this type of incremental forging process is to progressively compress or layer the material until it attains the ultimate desired shape. However, it is complicated to calculate the material flows in both the axial and lateral directions after each forming step of the workpiece. For this reason, to achieve the appropriate dimensional accuracy in the workpiece, geometric changes in the workpiece must be constantly observed and monitored by the operator who will perform the forming process, taking into account the flow behavior of the material (Aksakal, Osman, & Bramley, 2008) (Aksakal, Osman, & Bramley, 1997). It is a well-known fact that metal flow is affected by friction in forging processes. Metal flow is significantly affected by friction due to

using lubricants is difficult because of high temperatures in open-die forging. Therefore, the effect of friction in open die forging has attracted the attention of many researchers. R. Lakshmipathy and R. In their study, Sagar attempted to prevent the deterioration of the lubrication between the die and the workpiece by changing the surface topography of the die forging with a better-performance open die (Lakshmipathy & Sagar, 1992). E. Ghassemali et al. investigated the impact of lubricants with varying friction coefficients on material performance during the open die micro forging procedure (Ghassemali, Tan, Wah, Lim, & Jarfors, 2014).

The quality of open die forging relies on various control factors such as die width, die configuration, die overlap, die staging, ingot shape, temperature gradient, draft design, transition program, and more.

### **Closed die forging**

In closed die forging, tools that are closely related to the desired end product shape are used. Closed die forging is divided into two (with flash/flashless) in itself. Closed die forging systems with flash and flashless are shown in Figure 3 in simplified form.



*Figure 3: Simplified representation of flash and flashless closed die forging*

The quality of the part forged with the closed die depends on many parameters (process design, forging load, pre-die design, material flow stress, friction, equipment, etc.) (Shamasundar, 2003).

### **Closed die forging with flash**

Closed die type forging with flash is the forming process of a simple shaped (usually round or square bar) hot metal part in the form of a billet by plastic deformation in a die, usually consisting of two parts. During forming, waste material flows into the gutters outside the forging boundary of the die separation line. The flash geometry should fill the gutters when the two dies come into contact in the separation plane (Biswas & Rao, 1985). The flash gutter acts as a drain valve for the excess pressure that arises in closed dies. This gutter also acts as a brake to slow down the outflow of metal to allow it to be filled in the desired configuration (ASM HandBook, 1988). Closed forging dies can be made with one or more gutters, depending on the shape and dimensions of the workpieces to be forged. These gutters may be divided into several types according to their roles (forging finishing, pre-forging, cutting, etc.), and the workpiece shapes obtained with each gutter represent the forging stages (Luca, 2017).

As in other forging processes, it is important to know and control the flow behavior of the material in forging processes with flash to effectively fill the die gutter, surface quality, optimum load, and die wear and to avoid defects caused by material flow. In closed die forging with flash, the material flow mainly depends on 5 parameters (geometry of the flash gutter, initial and intermediate billet geometry, flash percentage, heat transfer between the tool and the billet) (Atlan, Oh, & Gegel, 1983).

Since material waste is one of the most crucial properties affecting the cost of forging, the correct calculation of flash gutter is critical in reducing the cost of forging (Sleeckx & Kruth, 1992). In forging with flash, flash gutters may be expressed in three basic geometries (parallel, wedged, and V-notch). G. Samolyk and Z. Peter, in their work, analyzed the effect of geometric parameters of the V-notched flash gutter on the forging process. They also conducted calculations aiming to ascertain the most advantageous measurements of the gutter based on the forging load and the degree of die gutter filling with metal. (Samolyk & Pater, 2005). F.F-Sanee and A.H. Hosseini investigated the impact of flash allowance and billet sizes on both forging load and material flow for two standard round components. One component had a vertical axis of symmetry (aligned with the ram direction of motion), while the other had a horizontal axis of symmetry. (F-Sanee & Hosseini, 2006).

In closed die hot forging, the quality of the finished part is widely determined by the design of the pre-die and the quality of the pre-shape. The purpose of the pre-die design is to achieve an optimal die shape, which allows the die gutter to be filled with effective forging force. (Dehghani & Jaferi, 2010) Furthermore, the correlation between the pre-forming volume and the final forging volume significantly influences the quality of the end product. When the pre-die geometry is intricate, the volume distribution within the pre-die becomes crucial to guarantee adequate metal flow during the final forging process. Thus, achieving precision forging necessitates the use of an accurate pre-die. (ASM HandBook, 1988).

## **Flashless closed die forging**

This forming operation has the advantage of lower material consumption and minimal machining tolerance due to the absence of flash in the final product. The purpose of this forming operation is to produce parts that are net shape or at least near net shape. This manufacturing method can be described as close tolerance forging (ASM HandBook, 1988). In the flashless closed die forging type, it is executed by permanently deforming a metal part in the form of a billet at room temperature or below the recrystallization temperature of the material with the help of a punch in a volume-controlled manner and filling it into the die gutter. In this forging process, the punch and die can consist of one or more parts and no material loss occurs. Flashless forged parts have an improved strength due to an uninterrupted grain flow (Stonis, Rüther, & Behrens, 2015).

Closed die cold forging is an extremely challenging metal forming application compared to other forging methods due to the high forming loads caused by the high flow stress of billet material. High die stresses due to high forming loads (surface pressure up to 3000 MPa (Geiger, Arbak, & Engel, 2008) (Ku & Kang, 2014)) cause wear on the application tools and reduce their service life. In addition, the success of cold forging processes depends on the properties of the tool material (high wear resistance, high strength, and high toughness) and its design. In addition, high operational loads cause elastic deformations of the operating systems, affecting the quality of the final product.

## **Forging defects**

When improper forming conditions are used in forging operations, forging defects often occur in the workpiece due to

complex deformation and complicated material flow. The most common forging defects are inadequate filling, cracks, surface defects, buckling, flowline protrusions, and swirls (Arentoft & Wanheim, 1997). These are widely known defects in forging operations, and it is significant to eliminate them to improve product, process design, and forming quality.

### **Buckling defect**

In die forging processes, buckling (folding) defect is one of the most common plastic flow defects. Figure 4 shows the buckling defect that occurs in an axisymmetric part manufactured using the cold forging method.



*Figure 4: The buckling defect in an axisymmetric part manufactured with the cold forging method. (W.L. Chan,2009)*

Flow-induced buckling defect prediction is crucial in product and design and has attracted the attention of many researchers. P. F. In their work, Gao et al. have developed a versatile approach to the prediction of buckling defects that is substantial for workpiece and forming design and improves the forming quality during the die-forging process (Gao, et al., 2019). W.L.Chan et al. proposed a dynamic change in tool geometry to control the buckling defect (Chan, Fu, Lu, & Chan, 2009). R. Balendra et al., in their studies, identified flow-related defects in the main configurations of injection forging with experiments to improve the efficiency of the injection



forging design of tubular materials. They found that forging defects such as plastic deformation instability of the workpiece, buckling, and improper axial/radial flow rate are due to different flow mechanisms of the materials. They also developed a pre-shaping procedure to prevent bucklings from developing (Balendra & Qin, 2000).

### **Metal flow lines**

The formation of metal flow lines among forging defects is due to the quality of the surfaces the toolset and the workpiece contact with, the coefficient of friction, and the die geometry. In mechanical parts manufactured by hot forging, where high strength and structural reliability are expected, M. K. Razali et al. emphasized the importance of friction effects in closed-die hot forging and carried out experimental and finite element method studies on the shaping of S45C steel with three-stage hot forging. They concluded that metal flow lines are greatly affected by friction conditions and that friction optimization improves metal flow lines (Razali, Kim, Irani, Kim, & Joun, 2021).

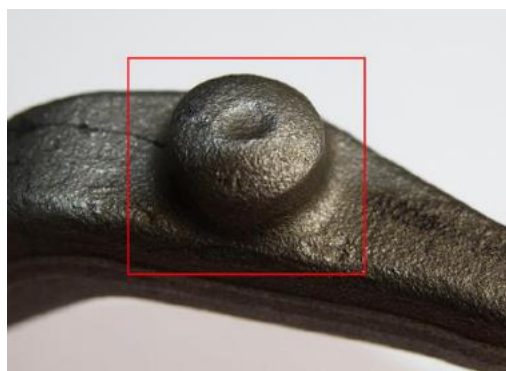
### **Side surface crack**

In forging processes, the flow direction and arrangement of the material play an important role in part quality. Y. H. Moon et al., in their studies, because the flow pattern of the material during forging may cause a side surface crack/error, developed velocity fields and power terms with upper bound analysis for double-ram axisymmetric forging. In the first of their two-part articles, they present the terms velocity domains and individual powers, derived based on flow patterns. In their second article, they present the criteria they have determined for side surface defects based on the

upper bond solution (Moon, Van Tyne, & Gordon, 2000) (Moon, Van Tyne, & Gordon, 2000). A.B.Abdullah et al. examined the effect of the conicity angle and distance to the edge on defect formation based on the flow model and stress distribution of the material, which will affect the quality and accuracy of the pin-shaped by cold embossing, with 2D simulations (Abdullah, Sapuan, Samad, T.Khaleed, & Aziz, 2013).

### **Inadequate filling**

Complete filling of the forging die is significant for forging operations. Figure 5 shows the inadequate filling error that occurred in the lever arm.



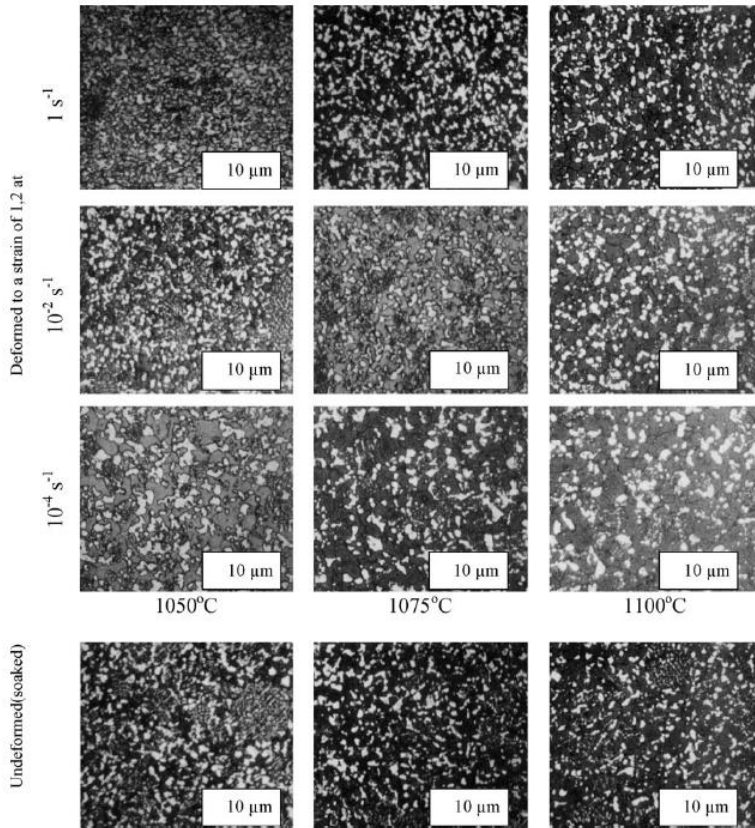
*Figure 5: Lever arm inadequate filling error (M. Hawryluk et al. 2015)*

The air gaps formed between the toolset and the workpiece are one of the substantial parameters that cause the die cannot be filled. Other important parameters in this defect formation may be shown as inaccurate pre-die design and incorrect material flow. M. Hawryluk et al. worked on the modeling of inadequate fillings (caused by air pockets between the workpiece and the tool) by the finite element method, which is seen as one of the major problems

in the closed die forging process. In their study, they observed the incorrect flow of material with the lever arm forging simulation. They also saw that the pre-die position had a significant impact on the proper filling of the die, and the correct die position helped to remove defects in the workpiece significantly with the lever arm forging simulation. In addition, in the lever arm forging simulation, they identified the incorrect flow of the material as the cause of the forging defect (Hawryluk & Jakubik, 2015). A. Kocanda et al. how the positioning of the die gap affects metal flow and the distribution of lateral forces within the die during the hot forging of aircraft engine turbine blades, utilizing simulation software based on the finite volume method. They also pointed to the effect of the torsional moment on the die offset brought about by these lateral forces (Kocanda, Czyzewski, & Mehdi, 2009). Y.Can et al. performed experimental investigations on conventional closed die forging, examining how the aspect ratios and indentation of the workpiece influence both forging load and die filling. They concluded that increased indentation and aspect ratio helped with better die filling overall. They also observed that they affect billet and punch diameters and punch ratios forging loads and die fill rates (Can, Altinbalik, & Akata, 2004). H. Ssemakula et al. have developed an alternative method of manufacturing large copper barrel lids with a much lower forging force for a forging company specializing in forging heavy parts. The main focus of their work is on the distribution of forming parameters such as load requirement, filling of the die gutter, and effective strain within the workpiece at different forming stages and temperatures (Ssemakula, Stahlberg, & Öberg, 2006).

## **Microstructure**

It is known that the material to be shaped using the forging method undergoes significant changes from the operation parameters (temperature, strain, and strain rate). M. O. Alniak et al. noted alterations in the microstructure resulting from plastic deformation in hot isostatically pressed (HIPed) P/M Rene 95 under isothermal conditions. Their research revealed that the microstructure transitions into a consistent coaxial fine-grained micro-duplex structure, at which point the flow forces become uniform. At this point, the ongoing deformation does not produce any further changes in grain size or flow strength. In this constant deformation state, the micro-duplex grain size and flow strength remain unaffected by the initial microstructure but are influenced by the strain rate at a specific temperature. When the strain rate decreases and/or the temperature rises, the steady-state grain size increases while the stable flow power decreases. Their study demonstrated that the microstructure undergoes significant changes during forging, and the grain size of both initially fine-grained and coarse-grained compacts is influenced by the applied strain rate, forging temperature, and strain. (Alniak & Bedir, 2006). Figure 6 shows how the material microstructure is affected by temperature and strain rate.



*Figure 6: The microstructural evolution of the material is affected by temperature and strain rate during the forging operation (M. O. Alniak et al. 2006)*

In this context, many studies have been carried out aimed at how the structural evolution of the material takes place and controlling it in forging operations. H-G. Yan et al. examined the microstructure and mechanical characteristics of the ZK21 alloy by conducting a multi-stage forging process at various strain rates in their research. (Yan, et al., 2012). W. Weronksi et al. analyzed grain growth by finite element method, which leads to a decrease in the mechanical properties of parts shaped by forging aluminum alloys.

The overlap of theoretical studies with industry practice has shown that it is possible to predict structural defects in the forging operations of aluminum alloys by the finite element method (Weronski, Gontarz, & Pater, 1999). M. J. Tan et al. investigated the interactive effect of grain size and sample sizes on material flow and microstructural evolution in a staged open-die micro-forming process (Tan, Ghassemali, Wah, Jarfors, & Lim, 2013).

T. Henke et al. propose a strategy that allows incorporating microstructure evolution uncertainties in material behavior into a microstructural model in their paper. They applied this model to the hot forging process design. They showed the probability distribution of the grain size value is asymmetrical and predicts the formation of grain sizes with a grand deviation from the most likely grain size (Henke, Bambach, & Hirt, 2013). G. Banaszek et al. studied stress density heterogeneity, material flow discontinuity, and elimination of metallurgical defects in free hot forging operations. They observed that the shapes and geometries of the tools contribute positively to the reduction of metallurgical defects on the workpiece by obtaining a uniform deformation character in the early stages of forging. They also found they are favorable for improving the homogeneity of stress concentrations over a forging cross-section. Besides, they observed significant controllability of the flow kinematics of the material with appropriate tool shape and appropriate forging technological parameters (Banaszek & Stefanik, 2006).

W.Li et al. observed the viscoplastic behavior of the AA7050 grade material as well as the temperature-dependent flow stress behavior of the material under various deformation conditions by

applying a series of compression tests with a physical simulator (Gleeble 3800). Additionally, they employed electron scattering diffraction technology to investigate the grain orientation map of the material and to examine potential dynamic recrystallization and grain size distribution during deformation. Their research aims to determine the optimal parameters for hot forging by analyzing the evolution of grain size during the process, and to offer guidance for the industrial manufacturing process of AA7050. (Li, et al., 2018). A.K. Padap et al. aimed to understand the microstructural improvement mechanisms that occur in the multiaxial warm forging stage of AISI 1016 steel in their study. In their paper, they utilized optical microscopy and electron-backscattered diffraction findings to examine the predominant mechanisms at different stress stages. They conducted an extensive investigation into the structural changes occurring in both ferrite and perlite components. (Padap, Chaudhari, Pancholi, & Nath, 2010).

## **Die fatigue**

As in all manufacturing processes, it is substantial to have sustainability, energy, and waste saving, therefore reducing environmental pollution in the forging method. Forging dies significantly affect the quality and cost of the forgings produced, and thus production sustainability as they exhibit an unstable and relatively short lifespan. In forging processes, the die cost may cover 15% to 35% of the total cost. M. Bayramoğlu et al. think that a 15% reduction in the total cost of the forging process may be achieved if the die life is increased by 100% (Bayramoğlu, Polat, & Geren, 2008). For this reason, studies to increase the durability of forging dies are the focus of attention of many researchers. While the main factors of die fatigue in hot forging are considered to be abrasive

wear and plastic deformation, one of the main causes of die fatigue in cold forging can be considered as fatigue cracks (Varquez, Hannan, & Altan, 2000). According to M. Hawryluk's literature search, forging tools indicate that the reasons for the failure of the tools used in hot forging are loss of dimension and fatigue cracks, which are a result of abrasive wear and plastic deformation (Hawryluk, 2016). They have discussed the wear mechanisms that affect the durability of hot forging tools through a comprehensive literature review and have extensively examined the most popular methods used to increase tool durability (Wildomski & Gronostajski, 2020).

A.A. Emamverdian et al. present methods for checking die tools and potentially extending die life, in addition to an extensive literature review of hot forging tool failures, including abrasion (abrasive wear, adhesive wear, oxidation, and thermal fatigue cracking), mechanical fatigue cracking, and plastic deformation, and related machining methods, including surface treatment (nitriding) in their studies (Emamverdian, Sun, Cao, Pruncu, & Wang, 2021). According to research, destructive mechanisms involved in die wear in hot forging processes (abrasive wear, adhesive wear, fatigue cracking, and plastic deformation) are also effective mechanisms in the wear of cold forging dies. However, it can be said that the main reason for the low tool strength used in cold forging is the high yield point of the material and the large forming loads (Cwikla & Tofil, 2019). In their study, M. Dalbosco et al. aimed to improve the fatigue life of an automotive part die manufactured by the cold forging method (Dalbosco, Lopes, Schmitt, & Pinotti, 2021). I. Valfolomeev et al. investigated the initiation and dispersion of fabrication defects in high-performance rotor steel under fatigue load



in their study (Varfolomeev, Moroz, Diegele, Kadau"K, & Amann, 2017). H. Y. Kim et al. aimed to obtain quantitative information in terms of material flow, die pressure, and temperature in the hot closed die forging process in their study. They considered using the information obtained in the design of pre-forming processes to reduce the forging load and extend the die life (Kim, Kim, & Kim, 1994).

### **Operation planning and scheduling**

As with other metal forming processes, forging requires estimating the maximum load, forming energy, and die stresses in the planning and programming of the operation. Maximum load and forming energy are the two basic parameters determining the press size and maximum production rate (Altan, O'Connell, Painter, & Maul, 1996). One of the most important parameters required for estimating these variables is the flow stress of the material. The effects on the flow stress of the metal can be divided into factors that are unrelated to deformation (chemical composition, metallurgical structure, etc.) and factors directly related to deformation (deformation temperature, strain, strain rate). The degree of dependence of the flow stress on the temperature may vary for different materials (Altan & Boulger, 1973). Flow stress is affected by temperature and strain rate. In hot forming processes of metals (Hot Forging), if the forging temperature is above the recrystallization temperature of the workpiece, the effect of strain on flow stress is insignificant. However, the effect of strain-velocity ratio on flow stress becomes substantial. T. Altan et al., in their study, mentioned that in conventional hot forging, specifically non-isothermal forging, temperature fluctuations within the deformed part impact metal flow and forging load. Additionally, they

highlighted that the temperatures are significantly influenced by the operational characteristics of the forging machines employed. (Altan, Varden, Im, & Shen, 1988).

In cold forging, the impact of the strain rate ratio on flow stress is minimal. (Altan, Ngaile, & Shen, 2005). In general, forging and forming operation(s) are planned with the assumption that the thermal effect is negligible for steels developed in accordance with cold forging operations. However, during operation, inherently high-strength materials can generate too much viscous heating, causing the operating temperature to rise to around 600°C (Eom, et al., 2014). In this case, there is a decrease in flow stress and forming load, especially in aluminum alloys and high-strength steels that generate a lot of heat during forming (Joun, Chung, & Hong, 2019) (Kim, Yoo, & Joun, 2019) (Byun, Lee, Park, Seo, & Joun, 2020). In addition, in forging processes, due to the effect of friction, the constraints of the die geometry, and the inhomogeneity of deformation, related stress, and forces are high. In cold forging, tools endure substantial loads, potentially leading to excessive friction between the workpieces and the tools. This friction can influence various aspects such as the deformation load, metal flow, deformation uniformity, internal structure and surface quality of the product, and die wear. Hence, it's crucial to comprehend, assess, and manage friction effectively. (Hu, Yin, & Zhao, 2017).

### **Finite element method**

In the late 1960s, the development of simulation technology with the finite element method began in the field of forging. In the 1970s and early 1980s, two-dimensional steady-state simulations were carried out, such as round bar drawing/extrusion and plane

strain plate rolling that did not require re-meshing (Lee & Kobayashi, 1973) (Oh, Chen, & Kobayashi, 1979). Especially in the aerospace part development phase, hot forging metal flow simulations were applied for 2D non-stationary state with manual re-meshing (Kim, Yagi, & Yamanaka, 2000).

Today, the finite element method is used extensively in the planning of metal forming operations. Biba et al. described the advantages of using FEM to analyze forging processes in their study (Biba, Stebounov, & Lishiny, 2001). To get effective results from simulation software, it is known the importance of accurate physical modeling of the operation(s) and the correct entry of the mechanical and thermal characteristics of the material into the system. Material flow curves serve as the primary data input for simulating metal forming processes. According to T. Altan et al., to ensure accurate finite element analysis, the flow curves of the material must encompass the process range being studied in terms of strain, strain rate, and temperature. (Altan & Vazquez, 1996). I. Gürbüz et al. studied creating simulation infrastructure to reduce die-lapping processes for mass production in the automotive industry. By fully characterizing the material mechanical properties, friction coefficients, and die elastic properties through a series of mechanical tests, they have shown that the negative deviations that may arise from mechanical conditions between the simulation environment and the physical environment are minimized, with the compatibility of simulation and physical data (Gürbüz, Altınel, & Karadoğan, 2013).

### **3. Forging (operation) load**

The effects of forging loads applied in the forging operations on product quality and operation systems during and/or after forming have been the subject of study for many researchers, as well as the parameters that the forging load is affected during the process. In this article, the studies of researchers focusing on the operational load in closed die forging forming processes regardless of the forming temperature are examined.

#### **Parameters affected by operational load**

The most substantial parameter required for estimating the maximum load and forming energy, which determines the maximum manufacturing rate in all metal forming operations, is the correct determination of the flow stress of the material. We have mentioned the parameters that flow stress is affected by forging operation types under the operation planning and programming heading of the article. This chapter focuses on the work of researchers who want to observe the impact of the flow stress of the material and the parameters directly related to deformation on the forging load.

#### **About flow stress and deformation (temperature, strain, strain rate)**

When the forging literature is examined, it is understood that the deviations in the load distribution that occur in forging operations are affected at most by the flow stress distribution of the material. Many researchers revealed that the flow stress of the material is directly affected by the parameters directly related to deformation (temperature, strain, and strain rate). P. Bereczki et al. examined how the strain rate affects flow stress development in Al 6082M grade alloy material during multiaxial forging, using a physical simulator

(Gleeble 3800) in their research. They found that the development of cyclic flow curves is non-monotonic, showing a notable decrease in flow tension as the forging direction changes. Their analysis of the strain rate effect led them to conclude that the kinetics of strain hardening varied depending on the applied strain rate. Also, as the strain rate increases, the saturation of the flow stress indicates that it occurs in the higher accumulated strain. However, they concluded that as the strain rate increases, it leads to an increase in the degree of strain softening between the forging passes (Bereczki, Krallics, & Renko, 2019).

H.J. Lee et al. present a new material flow strain model by improving the closed-form function model for the carbon steel S25C, which exhibits typical dynamic strain aging, in their research (Lee, Razali, Lee, & Joun, 2021). As a result of studies, it has been revealed that the flow stress of the material is affected by hardening mechanisms, as well as factors directly related to deformation. S. Nouri et al. developed a model in the flow stress studies of the alloy of three hardening mechanisms (solid solution, inhibiting the movement of dislocations, and density increase of statistically stored dislocations) that affect the hardening behavior of the alloy during plastic deformation of Al 2024 grade alloy. They applied this model to the finite element model to evaluate the development of the flow stress of the alloy after multiaxial forging (Nouri, Kazeminezhad, & Shadkam, 2020). Z. Xiao et al. investigated the effect of multi-stage forging forming parameters (degree of deformation, strain rate, number of stages, adiabatic thermal temperature) on the quality of products using a physical simulator (Gleeble 3500). With the results, they showed that the strain rate effect on microstructure and mechanical properties is low. They also emphasized that the number

of stages and the degree of deformation have a remarkable effect on the microstructure (Xiao, et al., 2015).

M. Irani and A. K. Taheri, in their study, determined the optimum temperature of a low-carbon steel in a precision forging operation (Irani & Taheri , 2008). R. Sirinivasan et al. investigated the effects of strain rate, workpiece temperature, and operation duration on deformation load in an experimental and simulation environment in which the die, workpiece, and ambient temperatures are different from each other (non-isothermal). Their research demonstrates that at extremely slow strain rates, the initial temperature may not notably impact deformation loads. Conversely, at very high strain rates, where there's insufficient time for substantial heat transfer to the surroundings, the behavior may resemble that observed in isothermal deformation. At slow strain rates, with prolonged deformation times, the workpiece temperature can stabilize. In such cases, the deformation load rises with the strain rate. However, at high strain rates, workpiece temperatures do not stabilize. Consequently, deformation loads can decrease at higher strain rates. (Srinivasan, Balathandayuthapani, & Yan, 2005).

C. D. Lang et al. have recently considered recent advances in electrically assisted manufacturing and have investigated the usability of this innovative approach in forging through a series of tests, based on the knowledge that it reduces flow strain and accordingly deformation force. With the test results in their studies, they exhibited the advantages of electrically assisted manufacturing in forging (decrease in flow voltage and increase in hardness, etc.) and disadvantages (increase in spring back) (Lang, et al., 2020). P. Vo et al. investigated the flow behavior and microstructural

development of IMI834 close to titanium under typical ingot cracking process conditions in their study. They also developed a comprehensive flow stress model valid in dual-phase temperature regimes for general close alloys. They validated the model for various alloys using experimental and literature data (Vo, Jahazi, Yue, & Bocher, 2007).

## **Tribology**

In metal forming processes, since the friction behavior between the die and the workpiece is one of the most significant parameters affecting metal flow, surface quality, and tool life, it has been the focus of attention of many researchers (Nielsen & Bay, 2017). In closed-die hot forging operations, the effects of high friction coefficients due to the high temperature and lubrication difficulties, in addition to die constraints on forming and operations are known. On the other hand, in cold forging, friction conditions become highly demanding because of the significant surface expansion and normal pressures at the interface between the tool and workpiece, despite the use of advanced lubrication systems (Andreas & Merklein, 2014). T. Altan, M. O'Connell et al. wanted to establish a guide for estimating accumulation loads and energies when creating accumulation with a closed die without flash in their study. They also investigated the sensitivity of the forging load to friction, part size, and average material stress using the finite element method (Altan, O'Connell, Painter, & Maul, 1996). Snape et al. investigated the change in the coefficient of friction in the area where the die interface contacts the workpiece using the finite element method. In their study, they observed that the estimated maximum forging load is highly sensitive to changes in the coefficient of friction (Snape, Clift, & Bramley, 1998). In another study, they observed that the

change in friction coefficient had a significant effect on strain and maximum forging load. The flow stress and friction between the empty die interfaces are found to have a significant effect on forging (Snape, Clift, & Bramley, 2002). T. Gangopadhyay et al. developed an expert fuzzy logic calculation-based system to estimate forging load and axial stress in their work on the knowledge that empty die interface friction has a significant effect on forging load and axial stresses and creates turbidity for the estimation of these parameters. (Gangopadhyay, Pratihari, & Basak, 2011)

C. Gilbert et al. concentrated on devising an analytical expression to compute forging forces during the compression of bimetallic components, focusing on an assembly comprising a ring made of AISI 1045 steel and a cylinder made of AISI 1015 steel. They aimed to enhance the calculation of forming loads in two-metal ring-cylinder assemblies by refining analytical models previously developed by M. Plancak et al. (Plancak, Kacmarcik, Vilotic, & Krsulja, 2012). Building upon earlier simplified models rooted in the Coulomb friction model, they devised two new analytical models incorporating the shear friction model to provide a more accurate simulation and approach to the real-world problem (Gilbert, Bernal, & Camacho, 2015). Q. Zhang et al. investigated the effect of friction and material flow change by comparing traditional cold forging and oscillating cold forging methods with experiments and simulations. With the results of simulations and experiments, they concluded that oscillating cold forging reduces the operational load by about 25% compared to traditional cold forging operations and contributes positively to friction. They also attributed the reason why the forged part surface quality is better than traditional cold forging to the fact



that low friction causes less metal accumulation (Zhang, Ben, & Yang, 2016).

N. Bay et al. determined frictional strain with typical lubricants for aluminum, steel, and stainless steel with a simulative tribology test system for varying normal pressure, surface expansion, slip length, and tool/workpiece interface temperature. The study results showed that friction was strongly influenced by normal pressure and tool/workpiece interface temperature, while other process parameters studied observed a small effect on friction (Bay, Eriksen, Tan, & Wibom, 2011). C. In their study, Hu et al. aimed to develop an alternative test to minimize the uneven deformations of the inner hole and hence measurement difficulties that occur in the ring compression test, which is often used to characterize the frictional behavior that necessarily occurs at the interface of the workpiece and the die or tool in metal forming. With the developed test method, by simply controlling the angle of inclination of the outer protrusion, they observed that the friction behavior at the workpiece and tool interface could be quantitatively evaluated (Hu, Ou, & Zhao, 2015). In another study, they examined the effect of tool surfaces obtained by machining an aluminum alloy differently in the cold forging process on friction conditions through two different test methods (Hu, Ding, Ou, & Zhao, 2018). In another study, they proposed a novel test based on combined forward and backward extrusion to determine the friction factor in cold forging (Hu, Yin, & Zhao, 2017).

K.H. Jung et al. determined the friction coefficients of Al2024 and 6061-o materials by size-reduced type test (Jung, Lee, Kim, Kang, & Im, 2012). M.S. Joun et al. examined the similarities

and differences between Coulomb's law of friction and the law of friction of constant shear by comparing finite element solutions involving friction-sensitive metal forming processes (accumulation processes with different aspect ratios, strip rolling, ring gear forging, multi-step extrusion, as well as pipe contraction and expansion) (Joun, Moon, Choi, Lee, & Jun, 2009).

## **Parameters affected by operational load**

### **Die fatigue**

N. Karunathilaka et al. investigated how cyclic contact pressure exerted on the tool surface during the forging process impacts the fatigue of the tool material. The samples were subjected to low, medium, and high forging pressures, and it was observed that the tensile strength and fatigue life of the samples forged with low and medium contact pressures increased compared to the non-forging sample. In contrast, the forging sample decreased with higher contact pressure.

Based on the assumption of sample homogeneity, they determined that the strength and fatigue life of the tool steel fluctuate according to the contact pressure applied to the tools during the forging process. (Karunathilaka, Tada, Uemori, Hanamitsu, & Kawato, 2018).

### **Pre-die design**

In forging processes (especially complex parts), the geometric design of the pre-die has a great influence on the forging load and material waste. M. Sedighi et al. have tried to present a suitable algorithm for the practical pre-die design of complex parts (Sedighi & Tokmechi, 2008). V. A. Pandya et al. aimed to observe the effect of the pre-die size on the stress and forging force on the

die during the closed-die forging of anchor clamp and transport pin used in a transmission line with the help of finite element analysis and to minimize die stress and forging force (Pandya & George, 2021) (Pandya & George, Effect of preform design on forging load and effective stress during closed die hot forging process of pin, 2020). A. Halouani et al. developed an optimization method that uses a free-surface method based on the final product shape for performing tool design in multi-stage cold forging processes. This optimization method aims to minimize the equivalent plastic stress and punch force during the forging process (Halouani, Li, Boussad, & Guo, 2012). H. S. Park et al. worked on the initial design and optimization of the pre-die shape for the bevel gear (Park, Ayu, & Kumar, 2018). N. Biba et al. developed the pre-existing isothermal surfaces method for pre-forging dies and developed special software to provide automatic bidirectional geometry data transfer between finite element method simulation software and computer-aided modeling program. They have applied this method in several forging cases. In the application results, they observed a reduction in surface defects and material waste (Biba, Vlasov, Krivenko, Duzhev, & Stebunov, 2020).

### **Elastic deformation (press-die-workpiece)**

Studies conducted by many researchers have shown that the quality of the final product obtained by forging is affected by many factors, such as the material properties of the workpiece and the tool, the elastic deformation behavior of the tools/dies, and the lubricant state between the workpiece and the tool. In addition to these studies, the effects of forging load on the system and part have been the focus of attention for many researchers. V. Krusic et al. analyzed the effect of the distribution of key input parameters (Mass, Flow Stress,

Friction, and Press Hardness) of four different forging processes (Backward Cup Extrusion, Upsetting, Closed Die Forging, and Forward Rod Extrusion) on the dimensional accuracy of the product and tool life for typical cold forging operations. In the study, it was stated that in backward cup extrusion and upsetting systems, the deviation in load distribution was mostly affected by the flow stress distribution of the material, and friction had a significant effect on the effective stress in the die. In addition, it has been stated that two of the most substantial parameters affecting dimensional accuracy in this system are the distribution of material values and press stiffness conditions. In closed-die forging, it has been noted that while the workpiece mass distribution has a great impact on dimensional accuracy, in the same process, the system load is most affected by the press stiffness, flow stress, and flow stress parameter. In the forward bar extrusion process, the distribution of the flow stress parameter and the press stiffness affected the dimensional accuracy of the product, while the system load was affected by the flow stress parameter and friction. In addition, it is emphasized that the effective stress distribution in the die is affected by flow stress and press stiffness. In addition, in the study, the effect of press stiffness on forging dies was investigated by working with presses with two different stiffnesses. It is emphasized that the stiff press increases the elastic deformation in the forging dies, and accordingly, the stiff press reduces the tool life (Krusic, Masera, Pristovsek, & Rodic, 2009).

In another study, V Krusic et al. studied both experimentally and analytically the effect of workpiece-tool-press and tool loads on product quality and optimization of these parameters in the multi-stage forging process (Krusic, Arentoft, Masera, Pristovsek, &

Rodic, 2011). H. Ou et al. investigated the effect of press and die deflections on the final product form in the forging of blade profiles using the finite element method. The results revealed distinct patterns and magnitudes of die surface deviations due to die and press elasticity. They also concluded that it is significant to consider press elasticity if achievable accuracy is to be improved in forging blade components (Ou & Armstrong, 2006). A. Chen et al. studied single-stage injection forging with a particular tool design as an alternative to traditional multi-stage forging processes for automobile fastener production. They have developed axisymmetric models to analyze forging force and energy requirements. Injection forging requires more load to complete the forming process compared to multi-stage forging. This excess load needed during forming will affect adversely effects on the tool's life and dimensional accuracy. However, the featured element in the study is the forming energy needed in injection forging is less than in multi-stage forging. In terms of forming errors, dimensional errors may be controlled by reducing the forming load at each stage of multi-stage forging (Chen, Qin, Chen, & Choy, 2017).

H.G. Zhang et al. created software to simulate the impact of process loads on press deflections in multi-stage forging procedures. In all stages single-stage, two-stage, and three-stage forgings performed on a vertical crank press may require several adjustment iterations before the correct settings are reached. This occurs because adjusting one station affects the forming load there, altering press/tool distortion and consequently, closing heights at other stations. Throughout production, wear on the intermediate-stage tool can enlarge the die cavity volume, leading to shorter workpieces. Adjusting the corresponding load can alter the dimensions of the

workpiece in the finishing die, thereby diminishing part accuracy. They worked to create a mathematical model of press/tool deviations that occur in multi-stage forging operations. By using a computer program developed from this model, they tried to predict the effect of variables such as workpiece dimensions, clamping height, press, and tool stiffness on product accuracy, and to minimize the press/tool setting times required at all stages of forging operations. The program validated its output through one-stage, two-stage, and three-stage physical forging experiments performed on a vertical crank press (Zhang & Dean, 1993). F. Jovane et al. devised a computerized method to aid users in assessing the appropriateness of forming sequences for multi-stage cold forging of rotationally symmetrical workpieces. The program is equipped with features such as automated analysis of sequences for forging both solid and hollow parts, identification of the specific processes within each step, assessment of load peak distribution across various forming stages, and estimation of the strain distribution accumulated in the final part with cavities. The most important meaning of using the program as a module of an integrated CAD system for cold forging is to perform a complete manufacturability check on the process planner and provide an appropriate tool to determine the optimal forging sequence. The benefits that can arise from the implementation of the program are the design of performing sequences consistent with the mechanical properties of the final product and the correct use of presses and tools (Jovane, BArriani, Benuzzi, & Knight, 1987).

R. Hino et al. studied a simulation-based optimization technique that aims to reduce the number of forming operations with multi-stage forging. This optimization technique has been applied in

the progressive reduction of the three-stage forging process of an axisymmetric aluminum billet. First, the focus is on forming load optimization, as the forming load increases significantly in the final stages of the forging processes, which negatively affects the quality of the surface that responds to this increased forming load. The second and third focuses were on breakage prevention and gap optimization, respectively (Hino, Sasaki, Yoshida, & Toropov, 2008). L. Capan et al. considered that the two metal forming methods were similar to each other because defects occurred in the material under the punch in backward cup extrusion by round-shaped closed die forging with flash, and the remaining material moved along the die walls. In their study, they calculated the required press force by dividing the workpieces into accretion areas for these two metals forming methods and also considering the die wall angles. They concluded that the backward extrusion method may be used to calculate the press load of round-shaped forgings (Capan & Baran, 2000). J. B. Renko et al. compared the results of a finite element method-based program with tests with a physical simulator (Gleeble 3800) for a multi-axis forging operation. They observed that the required operation load obtained from the virtual data was 5kN higher than the physical tests on average, and in both methods, the required operation load in the first forging stage was the highest and the required operation load in the second stage was the lowest. In addition, they observed that in the third stage and subsequent forging stages, the required operation load converged to the force-displacement curves from above in odd-numbered operations, while the required operation load converged from the bottom in even-numbered operations. As a result, they suggest that the incompatibility of physical tests and virtual data is due to the

applied linear hardening material model, which cannot handle the nonlinear structure of multi-axis forging (Renko & Krallics).

H.Ou et al. conducted simulations using finite element simulation to analyze the material flow during the forging process of wing sections (Aerofoil), forging force history, contact pressure distribution between the die and the component, and examined the elastic deflections of forging dies. They also proposed changing die profiles in response to die deviations based on compensation of elastic behavior of die and nominal dimensions of the forging dies. By using finite element analysis, they tried to minimize the form errors of the airfoil sections due to the die elasticity. They concluded that the precision forging of aerofoil sections enables the quantitative estimation of die elasticity and the technique of compensating for component-form errors to achieve the manufacturing net-shaped parts (Ou & Balendra, 1998). S.Y. Hsia ve P.Y. Shih investigated precisely how die wear, die stress, die interaction, and workpiece stresses are related in fastener manufacturing dies by finite element analysis method. In addition, in their study, they used different samples to evaluate the flow stress-strain curve and friction coefficient (Hsia & Shih, 2015).

#### **4. Results**

According to detailed literature research, it can be applied using more than one method in the manufacturing processes of metal components. When forging processes are carried out under less-than-ideal conditions, forging defects are inevitable. Examining and eliminating these defects as much as possible is critical in terms of the forging process and the final product to be reached as a result of this process.



During the application of the forging process, tribological and geometric effects and deformation should be considered as well as the operation load and die stresses.

The finite element method, which offers the opportunity to combine today's technologies with traditional manufacturing methods, is used extensively in the examination, development, and optimization of the forging process.

When the studies conducted to date are examined, it is clearly understood that many parameters affect the mechanical properties, dimensional accuracy, surface quality, formability, and operation planning of the workpiece in the forging process, which is the focus of this article. It is understood from research that forging operation loads are an important operational input that affects the ideal mechanical properties, dimensional accuracy, ideal surface quality, and ideal die tool life expected from the forged final product. In addition, it is understood that forming loads play a key role in the ideal forming energy and appropriate press/tool selection. Thus, it may be deduced that the requirement for the forming loads to be estimated and in the ideal range has a significant impact on the effective applicability of forging operations. In this context, the parameters affected by this substantial operational input have been of interest and studied in detail by many researchers. From the studies, it is understood that the flow stress of the material, die limitations, the effect of friction between the die and the workpiece, thermal effects, strain-rate, and press/tool hardness are important active parameters. When the studies conducted to date are examined, it is seen that while the forming load estimation, idealization, affected parameters, and factors in the first forming

stage of single-stage forging processes or multi-stage forging processes have been studied in detail and intensively, not much work has been done on the forming load estimation, idealization, affected parameters and factors in other stages of multi-stage forging operations.

## **Bibliography**

Abdullah, A., Sapuan, S. M., Samad, Z., T.Khaleed, H. M., & Aziz, N. A. (2013). Numerical investigation of geometrical defect in cold forging of an AUV blade pin head. *Journal of Manufacturing Processes*(15), 141-150.

Aksakal, B., Osman, F. H., & Bramley, A. N. (1997). Upper-bound analysis for the automation of open-die forging. *Journal of Materials Processing Technology*(71), 215-223.

Aksakal, B., Osman, F. H., & Bramley, A. N. (2008). Determination of experimental axial and sideways metal flow in open die forging. *Materials and Design*(29), 576-583.

Alniak, M. O., & Bedir, F. (2006). Change in grain size and flow strength in P/M Rene 95 under isothermal forging conditions. *Materials Science and Engineering B*(130), 254-263.

Altan, T., & Boulger, F. W. (1973). Flow Stress of Metals and Its Applications in Metal Forming. *Journals of Engineering for Industry*, 1009-1019.

Altan, T., & Vazquez, V. (1996). Numerical Process Simulation for Tool and Process Design in Bulk Metal Forming. *Scientific Technical Committee Paper Discussion Sessions, CIRP*(45), 599-615.

Altan, T., Ngaile, G., & Shen, G. (2005). *Cold and Hot Forgings: Fundamentals and Applications*. ASM International.

Altan, T., O'Connell, M., Painter, B., & Maul, G. (1996). Flashless closed-die upset forging-load estimation for . *Journal of Materials Processing Technology*(59), 81-94.

Altan, T., Varden, O., Im, Y. T., & Shen, G. (1988). Investigation of Metal Flow in Non-Isothermal Forging Using Ring and Spike Tests. *Annals of the CIRP* (37).

Andreas, K., & Merklein, M. (2014). Influence of surface integrity on the tribological performance of cold forging tools. *Procedia CIRP*(13), 61-66.

Arentoft, M., & Wanheim, T. (1997). *Journal of Materials Processing Technology*(69), 227-232.

*ASM HandBook*. (1988). ASM INTERNATIONAL.

Altan, T., Oh, S. I., & Gegel, H. (1983). Metal Forming-Fundamentals and. *American Society of Metals (ASM)*.

Balendra, R., & Qin, Y. (2000). Identification and classification of Flow-dependent defects. *Journal of Materials Processing Technology in the injection forging of solid billets*(106), 199-203.

Banaszek, G., & Stefanik, A. (2006). Theoretical and laboratory modelling of the closure of . *Journal of Materials Processing Technology metallurgical defects during forming of a forging*(177), 238-242.

Bay, N., Eriksen, M., Tan, X., & Wibom, O. (2011). A friction model for cold forging of aluminum, steel and stainless steel provided with conversion coating and solid film lubricant. *CIRP Annals - Manufacturing Technology*(60), 303-306.

Bayramoğlu, M., Polat, H., & Geren, N. (2008). Cost and performance evaluation of different surface treated dies for hot

forging process. *Journal Of Materials Processing Technology*(205), 394-403.

Behrens, B. A., & Odening, D. (2009). PROCESS AND TOOL DESIGN FOR PRECISION FORGING OF GEARED COMPONENTS . *International Journal of Material Forming*(2), 125-128.

Behrens, B.-A., Volk , W., Maier, D., Scandola, L., Ott, M., Brunotte, K., . . . Till, M. (2020). A Combined Numerical and Experimental Investigation on Deterministic Deviations in Hot Forging Processes. *Procedia manufacturing*(47), 295-300.

Bereczki, P., Krallics, G., & Renko, J. (2019). The effect of strain rate under multiple forging on the mechanical and microstructural properties. *Procedia Manufacturing*(37), 253-260.

Biba, N., Stebounov, S., & Lishiny, A. (2001). Cost Effective Implementation of Forging Simulation. *Journal of Materials Processing Technology*(113), 34-39.

Biba, N., Vlasov, A., Krivenko, D., Duzhev, A., & Stebunov, S. (2020). Closed Die Forging Preform Shape Design Using Isothermal Surfaces Method. *Procedia Manufacturing*(47), 268-273.

Biswas, S., & Rao, K. J. (1985). Flow of metal into the flash gap in the last stages of a plane-strain closed-die forging operation. *Journal of Mechanical Working Technology*(11), 319-331.

Byun, J. B., Lee, H. J., Park, J. B., Seo, I. D., & Joun, M. S. (2020). Fully Coupled Finite Element Analysis of an Automatic Multi-Stage Cold Forging Process. *Trans. Tech. Publication Ltd.*(311), 88-93.

Can, Y., Altinbalik, M. T., & Akata, H. E. (2004). An investigation on forging loads and metal flow in conventional closed-die forging of preforms obtained by open-die indentation. *Indian Journal of Engineering & Material Sciences*(11), 487-492.

Capan, L., & Baran, O. (2000). Calculation method of the press force in a round shaped closed-die forging based on similarities to indirect extrusion. *Journal of Materials Processing Technology*(102), 230-233.

Cavaliere, P. (2004). Isothermal forging of AA2618 reinforced with 20% of alumina particles. *Composites: Part A Applied Science and Manufacturing*(35), 619-629.

Chan, W., Fu, M. W., Lu, J., & Chan, L. C. (2009). Simulation-enabled study of folding defect formation and avoidance in axisymmetrical flanged components. *Journal of Materials Processing Technology*, 209(11), 5077-5086.

Chen, Q., Hu, H., Lin, J., Huang, S., Wu, Y., Shu, D., . . . Mingbo, Y. (2017). Multi-stage cold forging process for H68 brass cylindrical shell part with deep blind hole: simulation and experiment. *Int J Adv ManufTechnol*.

Chen, S., Qin, Y., Chen, J. G., & Choy, C.-M. (2017). A forging method for reducing process steps in the forming of automotive fasteners. *International Journal of MEchanical Sciences*.

Choi, S., Chun, M. S., Tyne, C. V., & Moon, Y. H. (2006). Optimization of open die forging of round shapes using FEM analysis. *Journal of Materials Processing Technology*(172), 88-95.

Cwikla, A., & Tofil, A. (2019). Analysis of wear of cold forging dies using the technique of focal differentiation microscopy. *IEEE*, 629-632.

Dalbosco, M., Lopes, G. S., Schmitt, P. D., & Pinotti, L. (2021). Improving fatigue life of cold forging dies by finite element analysis: A case study. *Journal of Manufacturing Processes*(64), 349-355.

Davoudi, M., Nejad, A. F., Koloor, S. R., & Petru, M. (2021). Investigation of effective geometrical parameters on wear of hot forging die. *Journals of Materials Research And Technology*(15), 5221-5231.

Dehghani, K., & Jaferi, A. (2010). Finite element stress analysis of forging dies to improve their fatigue life. *Material Science-Poland*, 28(1).

Dieter, G. E. (1986). *Mechanical Metallurgy*. Singapore: McGraw-Hill.

Emamverdian, A. A., Sun, Y., Cao, C., Pruncu, C., & Wang, Y. (2021). Current failure mechanisms and treatment methods of hot forging tools (dies) - a review. *Engineering Failure Analysis*(129).

Eom, J., Son, Y. H., Jeong, S. W., Ahn, S. T., Jang, S. M., Yoon, D. J., & Joun, M. S. (2014). Effect of strain hardening capability on plastic deformation behaviors of material during metal forming. *Materials and Design*(54), 1010-1018.

Forcellese, A., & Gabrielli, F. (2000). Warm forging of aluminium alloys: a new approach for time . *International Journal of Machine Tools & Manufacture compression of the forging sequence*(40), 1285-1297.

F-Saniee, F., & Hosseini, A. H. (2006). The effects of flash allowance and bar size on forming load and metal flow in closed die forging. *Journal of Materials Processing Technology*(177), 261-265.

Fujikawa, S., Yoshioka, H., & Shimamura, S. (1992). Cold- and warm-forging applications in the automotive industry. *Journal of Materials Processing Technology*(35), 317-342.

Gangopadhyay, T., Pratihari, D. K., & Basak, I. (2011). Expert system to predict forging load and axial stress. *Applied Soft Computing*(11), 744-753.

Gao, P., Fei, M. y., Yan, X. G., Wang, S. B., Li, Y. K., Xing, L., . . . Keyim, Z. (2019). Prediction of the folding defect in die forging: A versatile approach for three typical types of folding defects. *Journal of Manufacturing Processes*(39), 181-191.

Geiger, M., Arbak, M., & Engel, U. (2008). Material adapted tool design in cold forging exemplified by powder metallurgical tool steels and industrial ceramics. *German Academic Society for Production Engineering*(2), 409-415.

Ghassemali, E., Tan, M. J., Wah, C. B., Lim, A. V., & Jarfors, A. W. (2014). Friction effects during open-die micro-forging/extrusion processes: an upper bound approach. *Procedia Engineering*(81), 1915-1920.

Gilbert, C., Bernal, C., & Camacho, A. M. (2015). Improved analytical model for the calculation of forging forces during compression of bimetallic axial assemblies. *Procedia Engineering*(132), 298-305.



Groover, M. P. (2010). *Fundamentals of Modern Manufacturing: Materials, Processes, and Systems*. John Wiley & Sons, 2010.

Gürbüz, I., Altinel, S. A., & Karadoğan, C. (2013). PRACTICAL TECHNIQUES in VIRTUAL TRYOUT for AUTOMOTIVE SHEET METAL FORMING. 7. *International Design and Production of Machines and Dies/Mold*. Antalya.

Halouani, A., Li, Y. M., Boussad, A., & Guo, Y. Q. (2012). Optimization of cold forging perform tools using Pseudo Inverse Approach. *Trans. Nonferrous Met. Soc. China*(22), 207-213.

Hawryluk, M. (2016). Review of selected methods of increasing the life of forging tools in hot die forging processes. *Archives Of Civil Mechanical Engineering* , 16, 845-866.

Hawryluk, M., & Jakubik, J. (2015). Analysis of forging defects for selected industrial die forging processes. *Engineering Failure Analysis*.

Henke, T., Bambach, M., & Hirt, G. (2013). Quantification of uncertainties in grain size predictions of a microstructure-based flow stress model and application to gear wheel forging. *CIRP Annals - Manufacturing Technology*(62), 287-290.

Hino, R., Sasaki, A., Yoshida, F., & Toropov, V. V. (2008). A new algorithm for reduction of number of press-forming stages in. *International Journal of Mechanical Sciences forging processes using numerical optimization and FE simulation*(50), 974-983.

Hirsvogel, M., & Dommelen, H. V. (1992). Some applications of cold and warm forging. *Journal of Materials Processing Technology*(35), 343-356.

Hsia, S.-Y., & Shih, P.-Y. (2015). Wear Improvement of Tools in the Cold Forging Process for Long Hex Flange Nuts. *Materials*(8), 6640-6657.

Hu, C., Ding, T., Ou, H., & Zhao, Z. (2018). Effect of tooling surface on friction conditions in cold forging of an aluminum alloy. *Tribology International*.

Hu, C., Ou, H., & Zhao, Z. (2015). An alternative evaluation method for friction condition in cold forging by ring with boss compression test. *Journal of Materials Processing Technology*(15).

Hu, C., Yin, Q., & Zhao, Z. (2017). A novel method for determining friction in cold forging of complex parts using a steady combined forward and backward extrusion test. *Journal of Materials Processing Technology*.

Irani, M., & Taheri , A. K. (2008). Effect of forging temperature on homogeneity of microstructure and hardness of precision forged steel spur gear. *Materials Chemistry and Physics*(112), 1099-1105.

Ishinaga, N. (1997). An advanced press design for cold forging. *Journal of Materials Processing Technology*(71), 100-104.

Jo, A. R., jeong, M. S., Lee, S. K., Moon, Y. H., & Hwang, S. K. (2021). Multi-Stage Cold Forging Process for Manufacturing a High-Strength One-Body Input Shaft. *MDPI*(14), 532.

Jo, A. R., Jeong, M. S., Lee, S. K., Moon, Y. H., & Hwang, S. K. (2021). Multi-Stage Cold Forging Process for Manufacturing a High-Strength One-Body Input Shaft. *Multidisipliner Digital Publishing Institute*(14), 532.

Joun, M. S., Moon, H. G., Choi, L., Lee, M. C., & Jun, B. Y. (2009). Effects of friction law on metal forming processes. *Tribology International*(42), 311-319.

Joun, M., Chung, W. J., & Hong, S. M. (2019). Macroscopic Modelling of Metal Forming Processes by FEM. *Jinseam Media*.

Jovane, F., Bariani, P., Benuzzi, E., & Knight, W. A. (1987). Computer Aided Design of Multi-Stage Cold Forging Process: Load Peaks and Strain Distribution Evaluation. *Annals of the CIRP*.

Jung, K. H., Lee, H. C., Kim, D. K., Kang, S. H., & Im, Y. T. (2012). Friction measurement by the tip test for cold forging. *Wear*(286-287), 19-26.

Karunathilaka, N., Tada, N., Uemori, T., Hanamitsu, R., & Kawato, M. (2018). Effect of contact pressure applied on tool surface during cold forging on fatigue life of tool. *Procedia Manufacturing*(15), 488-495.

Kim, H. Y., Kim, J. J., & Kim, N. (1994). Physical and numerical modeling of hot closed-die forging to reduce forging load and die wear. *Journal of Materials Processing Technology*(42), 401-420.

Kim, H., Yagi, T., & Yamanaka, M. (2000). FE simulation as a must tool in cold/warm forging process and tool design. *Journal of Materials Processing Technology*(98), 143-149.

Kim, K., Yoo, J. D., & Joun, M. S. (2019). FE prediction of temperature variation of material and dies with number of strokes in aluminum yoke cold forging. *Proc. Kor. Soc. Tech. Plast. Conf.*, (pp. 105-106).

Kocanda, A., Czyzewski, P., & Mehdi, K. H. (2009). Numerical analysis of lateral forces in a die for turbine blade forging. *ARCHIVES OF CIVIL AND MECHANICAL ENGINEERING*, 9(4).

Krusic, V., Arentoft, M., Masera, S., Pristovsek, A., & Rodic, T. (2011). A combined approach to determine workpiece-tool-press deflections and tool loads in multistage cold-forging. *Journal of Materials Processing Technology*(211), 35-42.

Krusic, V., Masera, S., Pristovsek, A., & Rodic, T. (2009). Adjustment of stochastic responses of typical cold forging systems. *Journal of Materials Processing Technology*(209), 4983-4993.

Ku, T.-W., & Kang, B.-S. (2014). Hardness-controlled tool fabrication and application to cold forging of inner race with skewed ball grooves. *International Journal Of Manufacturing Technology*(74), 1337-1354.

Lakshmipathy, R., & Sagar, R. (1992). EFFECT OF DIE SURFACE TOPOGRAPHY ON DIE-WORK INTERFACIAL FRICTION IN OPEN DIE FORGING. *Int. J. Mach. Tools Manufact*, 32(5), 685-693.

Lang, C. D., Hasbrouck, C. R., Hankeys, A. S., Lynch, P. C., Allison, B. D., & Roth, J. T. (2020). Electrically-Assisted Manufacturing for Reduction in Forging Forces of Bearing Steels. *Procedia Manufacturing*(48), 349-357.

Lange, K. (1992). Some aspects of the development of cold forging to a high-tech precision technology. *Journal of Materials Processing Technology*(35), 245-257.

Lange, K. (n.d.). *Handbook of Metal Forming*. Michigan: Society of Manufacturing Engineers.

Lee, C., & Kobayashi, S. (1973). New Solutions to Rigid-Plastic Deformation Problems Using a Matrix Method. *Trans. ASME, J. Eng. Ind*(95), 865-873.

Lee, H., Razali, M. K., Lee, K. H., & Joun, M. S. (2021). Flow stress characterization of carbon steel S25C in the temperature range of cold forming with an emphasis on dynamic strain aging. *Materials Today Communications*(28).

Li, W., Liu, Y., Luan, Q., Li, Y., Gu, B., & Shi, Z. (2018). A study of thermomechanical behaviour and grain size evolution of AA7050 under hot forging conditions. *International Journal of Lightweight Materials and Manufacture*.

Luca, D. (2017). A numerical solution for a closed die forging process. *Matec Web Conferences*.

Maier, D., Hartmann, C., till, M., Büdenbender, C., Behrens, B., & Volk, W. (2019). Data-Driven Compensation for Bulk Formed Parts Based on Material Point Tracking. *Key Engineering Materials*(794), 277-284.

Moon, Y. H., Van Tyne, C. J., & Gordon, W. A. (2000). An upper bound analysis of a process-induced side-surface defect in forgings Part 1: The velocity fields and power terms. (99), pp. 169-178.

Moon, Y. H., Van Tyne, C. J., & Gordon, W. A. (2000). An upper bound analysis of a process-induced side-surface defect in forgings Part 2: Characteristics and criteria curves. *Journal of Materials Processing Technology*(99), 179-184.

Nielsen, C. V., & Bay, N. (2017). Overview of friction modelling in metal forming processes. *Procedia Engineering*(207), 2257-2262.

Nouri, S., Kazeminezhad, M., & Shadkam, A. (2020). Flow stress of 2024 aluminum alloy during multi-directional forging process and natural aging after plastic deformation. *Materials Chemistry And Physics*.

Oh, S. I., Chen, C. C., & Kobayashi, S. (1979). Ductile Fracture in Axisymmetric Extrusion and Drawing—Part 2: Workability in Extrusion and Drawing. *Trans. ASME, J. Eng. Ind*(101), 36-44.

Ou, H., & Armstrong, C. G. (2006). Evaluating the effect of press and die elasticity in forging of aerofoil sections using finite element simulation. *Finite Elements in Analysis and Design*(42), 856-867.

Ou, H., & Balendra, R. (1998). Die-elasticity for precision forging of aerofoil sections using finite element simulation. *Journal of Materials Processing Technology*(76), 56-61.

Padap, A., Chaudhari, G. P., Pancholi, V., & Nath, S. K. (2010). Warm multiaxial forging of AISI 1016 steel. *Materials and Design*(31), 3816-3824.

Pandya, V. A., & George, P. M. (2020). Effect of preform design on forging load and effective stress during closed die hot forging process of pin. *Materials Today, Proceedings*.

Pandya, V. A., & George, P. M. (2021). Analysis of die stress and forging force for DIN 1.2714 die material during closed die

forging of anchor shackle. *Materials Today, Proceedings*(45), 4695-4701.

Park, H. S., Ayu, F. R., & Kumar, S. (2018). Preform Optimization for Bevel Gear of Warm Forging Process. *Procedia CIRP*(72), 340-345.

Plancak, M., Kacmarcik, I., Vilotic, D., & Krsulja, M. (2012). Compression of bimetallic components—analytical and experimental investigation. *International Journals Of Engineering*(10), 1584-2665.

Razali, M. K., Kim, S. W., Irani, M., Kim, M. C., & Joun, M. S. (2021). Practical quantification of the effects of flow stress, friction, microstructural properties, and the tribological environment on macro- and micro-structure formation during hot forging. *Tribology International*(164).

Renko, J. B., & Krallics, G. (n.d.). Comparison of physical and virtual simulation of multi-axial forging processes on EN-AW 6082 aluminium alloy. *Materials Today*.

S.Sheljaskov. (1994). Current level of development of warm forging technology. *Journal of Materials Processing Technology*(46), 3-18.

Samolyk, G., & Pater, Z. (2005). Use of SLFET for design of flash gap with V-notched lands in a closed-die forging. *Journal of Materials Processing Technology*(162-163), 558-563.

Sedighi, M., & Tokmechi, S. (2008). A new approach to preform design in forging process of complex parts. *journal of materials processing technology*(197), 314-324.

Shamasundar, S. (2003). Process simulation based optimization of precision forging process. *International Seminar on Precision Forging*. Nagoya, Japan.

Sheljaskov, S. (1994). Current level of development of warm forging technology. *Journal of Materials Processing Technology*(46), 3-18.

Shivpuri, R., Babu, S., Kini, S., Pauskar, P., & Deshpande, A. (1994). Recent advances in cold and warm forging process modeling techniques: selected examples. *Journal of Materials Processing Technology*(46), 253-274.

Sleeckx, E., & Kruth, J. P. (1992). Review of flash design rules for closed-die forgings. *Journal of Materials Processing Technology*(31), 119-134.

Snape, G., Clift, S., & Bramley, A. (2002). Parametric sensitivity analyses for FEA of hot steel forging. *Materials Processing Technology*(125-126), 353-360.

Snape, R. G., Clift, S. E., & Bramley, A. N. (1998). Sensitivity of finite element analysis of forging to input parameters. *Materials Processing Technology*(82), 21-26.

Srinivasan, R., Balathandayuthapani, M., & Yan, W. (2005). Temperature changes and loads during hot-die forging of a gamma titanium–aluminide alloy. *Journal of Materials Processing Technology*(160), 321-334.

Ssemakula, H., Stahlberg, U., & Öberg, K. (2006). Close-die forging of large Cu-lids by a method of low force requirement. *Journal of Materials Processing Technology*(178), 119-127.



Stonis, M., R  ther, T., & Behrens, B.-A. (2015). Analysis of Material Characteristics and Forging Parameters for Flashless Forged Aluminum-Matrix Composites. *Materials And Manufacturing Process*(29), 140-145.

Tan, M.-J., Ghassemali, E., Wah, C. B., Jarfors, A. E., & Lim, S. (2013). Grain size and work piece dimension effect on material flow in an open-die micro-forging/extrusion process. *Materials Science & Engineering A*(582), 379-388.

Tekkaya, A. E., & Hering, O. (2019). Damage-induced performance variations of cold forged parts. *Journals of Materials Processing Technology*(19).

Varfolomeev, I., Moroz, S., Diegele, D., Kadam, K., & Amann, C. (2017). Study on fatigue crack initiation and propagation from forging defects. *Procedia Structural Integrity*(7), 359-367.

Varquez, V., Hannan, D., & Altan, T. (2000). Tool life in cold forging – an example of design improvement to increase service life. *Journal of Materials Processing Technology*(98), 90-96.

Vo, P., Jahazi, M., Yue, S., & Bocher, P. (2007). *Materials Science and Engineering A*(447), 99-110.

Wernicke, S., Hahn, M., Detzel, A., Tillmann, W., Stangier, D., Dias, N. L., & Tekkaya, A. E. (2021). Force reduction by electrical assistance in incremental sheet-bulk metal forming of gears. *Journal of Materials Processing Tech.*(296).

Weronski, W., Gontarz, A., & Pater, Z. (1999). The reasons for structural defects arising in forgings of aluminium alloys analysed using the finite element method. *Journal of Materials Processing Technology*(92-93), 50-53.

Wildomski, P., & Gronostajski, Z. (2020). Comprehensive Review of Methods for Increasing the Durability of Hot Forging Tools. *Procedia Manufacturing*(47), 349-355.

Wilson, F. (1965). *Die Design Handbook 2nd ed.* McGraw-Hill and Society of Manufacturing Engineers.

Wolfgarten, M., Rudolph, F., & Hirt, G. (2020). Analysis of process forces and geometrical correlations for open-die forging with superimposed manipulator displacements. *Journal of Materials Processing Tech.*(276).

Xiao, Z., Liu, H., Liu, B., Sun, H., Liu, D., & Liu, G. (2015). The effect of forming parameter on multi-stage cold forging with 20MnTiB steel. *Int J Adv Manuf Technol*.

Xinbo, L., Hongsheng, X., & Zhiliang, Z. (2003). Flow stress of carbon steel 08F in temperature range of warm-forging. *Journal of Materials Processing Technology*(139), 543-546.

Yan, H.-G., Wu, Y. Z., Chen, J. H., Du, Y. G., Zhu, S. Q., & Su, B. (2012). Microstructure and mechanical properties of ZK21 magnesium alloy fabricated by multiple forging at different strain rates. *Materials Science & Engineering A*(556), 164-169.

Yanagimoto, J., Sugiyama, S., Yanagida, A., Iwamura, N., & Ishizuka, M. (2009). Control of ultrafine microstructure by single-pass heavy deformation and cold forging of metal. *journal of materials processing technology*(209), 679-685.

Zhang, H. G., & Dean, T. A. (1993). COMPUTER MODELLING OF TOOL LOADS AND PRESS/TOOL DEFLECTIONS IN MULTISTAGE FORGING. *Int. J. Mach. Tools Manufact*, 35(1), 61-69.

Zhang, Q., Ben, N., & Yang, K. (2016). Effect of variational friction and elastic deformation of die on oscillating cold forging for spline shaft. *Journal of Materials Processing Technology*.

## CHAPTER III

### Replacement of Cross-Car Beam Steel Parts with a Carbonfibered Composite Material in a Vehicle

*Cem İÇİER<sup>1</sup>*

*Tevfik Can ÖZGÜR<sup>2</sup>*

*Gökay PİRLEPELİ<sup>3</sup>*

*Gökçe EKEN<sup>4</sup>*

#### Introduction

The cross-car beam (CCB) of the vehicle is a structural component. It is located under a vehicle's instrument panel. It spans the interior of the car below the instrument panel. CCB provides structural rigidity absorbs impact forces in collisions for occupant safety and serves as a stable mounting point for a variety of interior components such as the instrument panel and steering column. Figure 1. shows the CCB. The steering column carrier group, shown

---

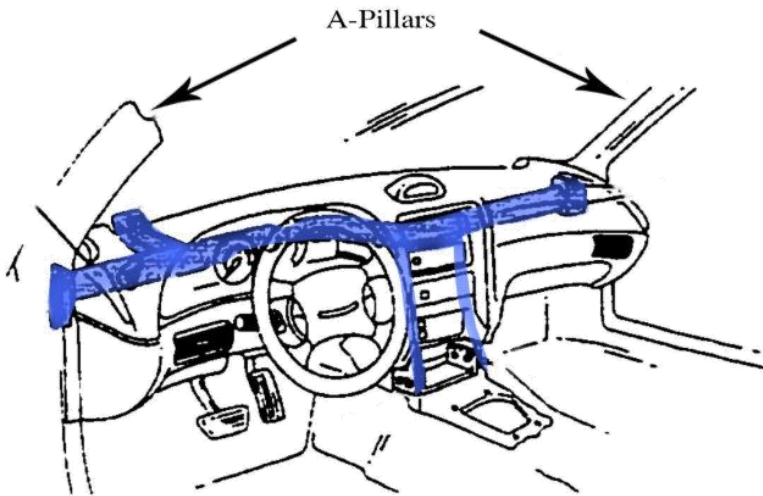
<sup>1</sup> Researcher, TOFAŞ Türk Otomobil Fabrikası A.Ş R&D Center, Bursa, Türkiye

<sup>2</sup> Researcher, TOFAŞ Türk Otomobil Fabrikası A.Ş R&D Center, Bursa, Türkiye

<sup>3</sup> Researcher, TOFAŞ Türk Otomobil Fabrikası A.Ş R&D Center, Bursa, Türkiye

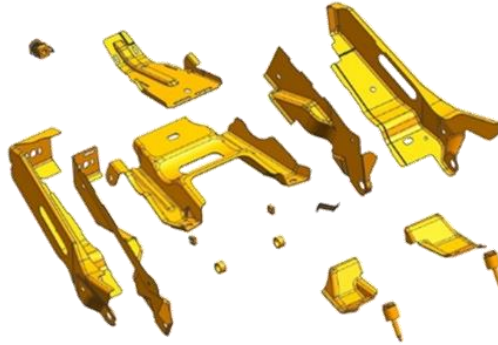
<sup>4</sup> Researcher, TOFAŞ Türk Otomobil Fabrikası A.Ş R&D Center, Bursa, Türkiye - Researcher, Yıldız Technical University Advanced Materials Research Group, İstanbul, Türkiye

in Figure 2. provide structure for steering column mounting. It generally provides retention to body-in-white. It is included to CCB. The steering column carrier group helps ensure the steering column is securely fastened, allowing for consistent steering control while also improving safety by reducing intrusion into the passenger area.



**Figure1.** *Cross-car beam (Rahmani,2013)*

CCB is generally heavy due to its material and worries about fulfilling safety requirements. A heavy car means more fuel efficiency and less sustainable vehicles. Vehicle designers and producers that are one of the most fuel consumers always push for lighter designs (Ebrahimi,2015).



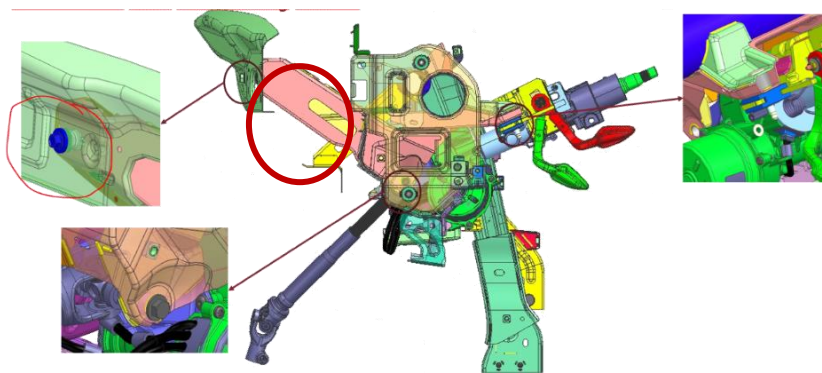
**Figure2.** *Steering column carrier group in cross-car beam*

## Methods

One of the best options that have an indirect effect on an end-user is material changing for lightweighting. However, finding an equivalent material that fulfils requirements is a challenge (Cunha,2013). The conventional material for CCB is steel. Hot rolled such as DD13 and cold rolled steels such as DC03 are generally used in CCB. The stamping process is used for the sheet metal manufacturing process. The roll-forming process is used for the production of the tubes. Each separate part has welded each other with the arc welding method. The aim of this proceeding is to investigate the effects of weight reduction in cross-car beams by changing the material of the steering column carrier group. In this manner, the material benchmark was done. Around 15 materials from 6 suppliers were analysed. PA 6.6 - Akromid A3 ICF 40 black (5116) was selected as a material due to achieving properties defined in the specification report.

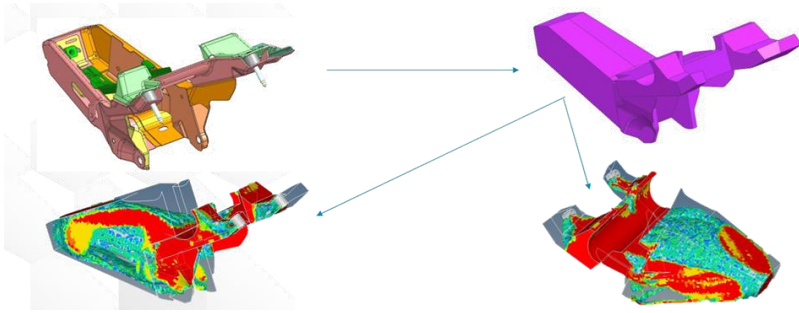
In this study, the transition from five separate steel parts to a single-piece composite-enhanced polyamide part was achieved. One of the most important considerations during part design was to

preserve the connection points with surrounding components. Connection locations with surrounding models can be seen in Figure 3. The front of the part features a connection to the front body, while the bottom has a connection to the steering mechanism. Attention was paid to preserving these connections during the part design process.



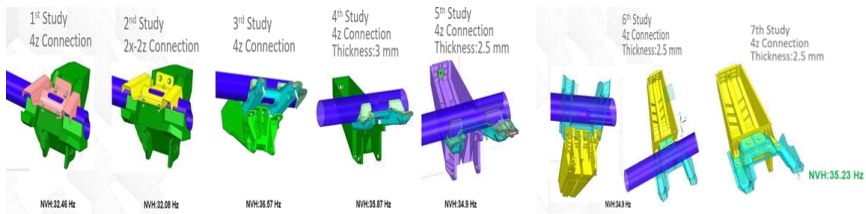
***Figure3. Connections with Surrounding Models***

Additionally, due to the material change, welding processes were not possible, so screw connections were provided for the assembly of the part to the cross-car beam. Methods such as topology optimization modal NVH analysis and crash analysis were used to achieve the best design. Thanks to these studies some parameters were defined. Critical regions, optimum screw connection locations, and part thickness were determined. Figures related to the topology optimization and modal NVH analysis conducted are available in Figures 4. and 5. Vibrations inside the vehicle reduce passenger and driver comfort.



**Figure4. Topology Optimization**

The steering column carrier group may also be one of the reasons for this vibration. A vibration in the steering column carrier group is directly detected by the driver. Therefore, it is significant to perform NVH analysis at the design stage. (Pinto et al., 2015). Crash analysis is something that reflects the physical crash test at a much lower cost and without causing any casualties and shows the safety status of the people inside the vehicle at the time of the accident and to what extent the components were affected by the accident. (Huang, 2002)



**Figure5. NVH Analysis**

After completing the design process, the injection mold was manufactured by a supplier. Then, the part was produced by injection molding method.

To validate the project, some technical tests were conducted. Heat aging test, thermal cycle test, humidity aging test. These tests



are used to determine the service temperatures for a product by using a thermal cycle or heat to accelerate the aging process. Except for these, a cold impact resistance test was done to observe withstanding an impact at the areas defined below after being exposed to cold temperatures.

A dimensional quality test was made to see whether the component was compliant with the released drawing or not. The fogging test and olfactory test were another physical test for the project.

## **Results**

At the end of the study, carbon fiber-reinforced composite material was successfully integrated into the CCB.

After this study, approximately 30% weight reduction was achieved for the steering column carrier group in CCB.

Thermal cycle test, on the steering column carrier group part was carried out within the scope of the project, according to the PSA standards. There were no geometrical changes observed with measurement.

Cold impact, olfactory, and fogging tests on the steering column carrier group part were carried out within the scope of the project, according to PSA standards. In these tests, it was seen that the requirements were fulfilled.

Heat aging test, on the steering column carrier group part was carried out within the scope of the project, concerning PSA standards. According to the result of the test, it can be said that geometrical changes are in tolerance.

Torquable fastener requirements were checked. The serviceability of the part was also checked. No deflection or deformation was observed.

The dimensional quality of the part was measured to check if there were any changes in the dimensions of the part compared to the 2D model and the real part. No incompatibility was observed after measurements.

To sum up, according to conducted tests, it can be said that there is no physical obstacle to the transition of the material in the steering column carrier group from steel to carbon fiber reinforced polyamide.

## References

Ebrahimi, M. (2015). Design and Optimization of Aluminum Cross-Car Beam Assemblies Considering Uncertainties. University of Toronto (Canada).

Rahmani, M. (2013). Multidisciplinary design optimization of automotive aluminum cross-car beam assembly (Doctoral dissertation, University of Toronto).

Cunha, R. (2013). Early Phase of the Cross Car Beam Concept Development.

Pinto, A. F., Tavares, S. M. O., César de Sá, J. M., & de Castro, P. M. S. T. (2015). Structural analysis of a cross car beam using finite element models. *International Journal of Structural Integrity*, 6(6), 759-774.

Huang, M. (2002). Vehicle crash mechanics. CRC press.

## **CHAPTER IV**

### **Living Hinge Design on Automotive Glovebox Mechanism**

**Gökay PİRLEPELİ<sup>1</sup>**  
**Abdullah HELVACI<sup>2</sup>**  
**Gökçe EKEN<sup>3</sup>**  
**Cem İÇİER<sup>4</sup>**

#### **1.Introduction**

A dashboard is a unit located in the front of the vehicle cabin. As well as carrying vital components for the use of the vehicle, such as the steering wheel and gearshift, the dashboard also contains many assistants that provide information and comfort to the driver, such as an entertainment unit, ventilation controllers, and many

---

<sup>1</sup> Researcher, TOFAŞ Türk Otomobil Fabrikası A.Ş. R&D Center, Bursa, Türkiye

<sup>2</sup> Researcher, TOFAŞ Türk Otomobil Fabrikası A.Ş. R&D Center, Bursa, Türkiye

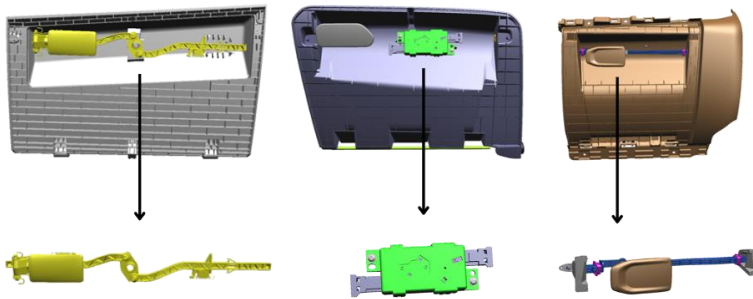
<sup>3</sup> Researcher, TOFAŞ Türk Otomobil Fabrikası A.Ş. R&D Center, Bursa, Türkiye - 2  
Researcher, YITU Advanced Materials Research Group, İstanbul, Türkiye

<sup>4</sup> Researcher, TOFAŞ Türk Otomobil Fabrikası A.Ş. R&D Center, Bursa, Türkiye

others. One of these assistants is the glovebox, which is positioned in front of the front passenger seat and used to store some items.

Gloveboxes have clutch mechanisms in the lids so that the glovebox does not open at undesirable moments due to the weight of the objects inside or due to road shocks. The lock opens and closes with the force provided by the user. Clutch mechanisms might have a single or double lock, depending on their construction, and can consist of 4–9 pieces.

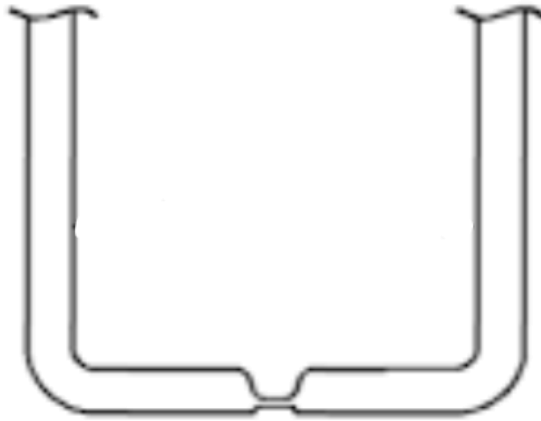
Most modern-generation passenger vehicles include a double-locked clutch mechanism due to perceived quality requirements. Some clutch mechanism examples are shown in figure 2.



***Figure 1. Clutch Mechanism Examples from Various Vehicles***

The production process of clutch mechanisms consists of the production of injection molds for each piece, plastic injections, spring production if the mechanism has one, assembly of pieces, and lastly, assembly of the glovebox lid. This process costs quite some money and time. In order to avoid these, a new type of clutch mechanism was designed by TOFAS engineers, aiming to minimize mold cost and assembly time.

A special geometry, the living hinge, was used for the design of the new clutch mechanism. Living hinge geometry is also used in different applications, such as bottle caps and container lids. The difference between a living hinge and a normal hinge is that while normal hinges have a pin and two pieces of body, living hinges consist of only one part and rotate around an arc.



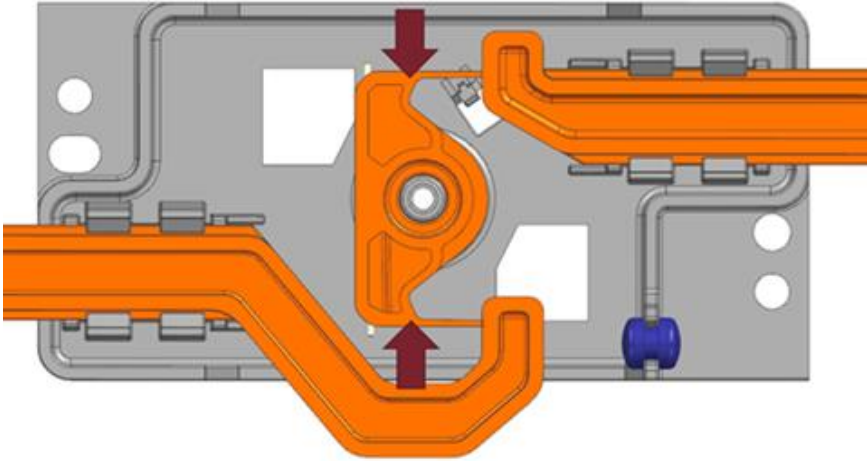
**Figure 2.** *Living Hinge (MIT, Design Issues on Living Hinges)*

The arc, mentioned in the previous paragraph, is the thinnest section of the hinge, which allows the hinge to fold and carries the stress. Most of the living hinges are made of polymers like PP and PE, have a 0.2–0.5 mm thickness, and have a very small radius (Brannon, P. J.,2003).

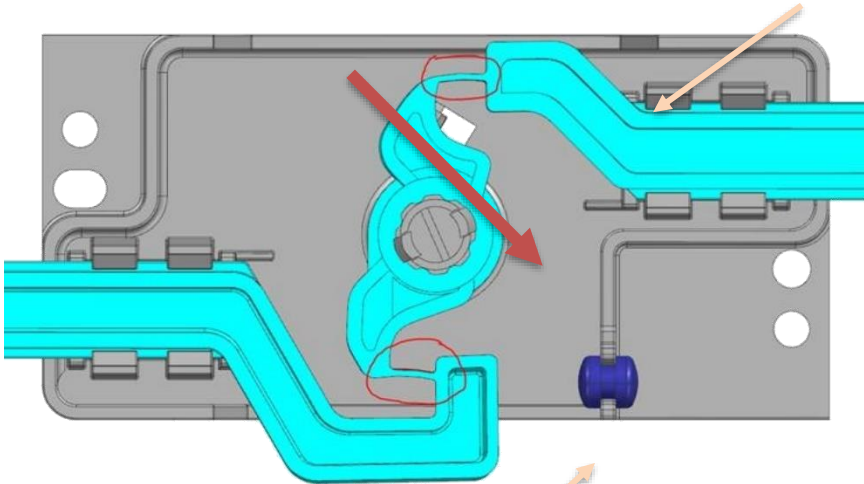
## **2.Design**

As first step of design, a component has designed with the same dimentions as the older mechanism. To determine the needed curve radius and thickness dimentions, stress analysis carried out

using FEA programs for different rotations of hinge. In all designs, PA6 (polyamide) material used due to its good fatigue ability, ease to manufacture and accesability.



**Figure 3.** *First Version of Mechanism Without Living Hinges*

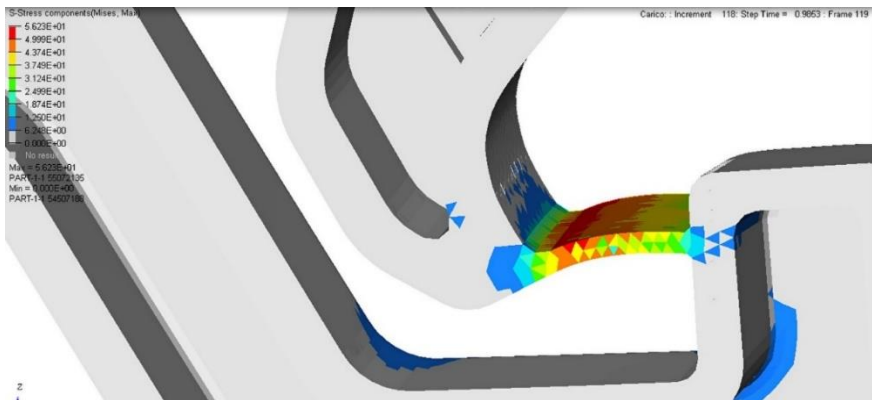


**Figure 4.** *Second Version of Design With Hinges*

In Figure 3, a new mechanism construction is given without using living hinges. This design is used to investigate if the

mechanism transmits the motion or not, without concern about fatigue life. Test results showed that motion transmission was successful, but stress amounts were different on the top half and bottom half (around +5). After these results, the design changed and curves for hinges were added. Wing-like structures were rotated in order to minimize the stress difference between the two sides. Also, some material was removed (the area shown with the orange arrow in Figure 4) to have a more compact component.

This design's stress analysis results showed that stress distribution is more even now, but corners of hinges (shown with lime arrows in Figure 4) were carrying too much stress. Stress analysis is given in Figure 5.

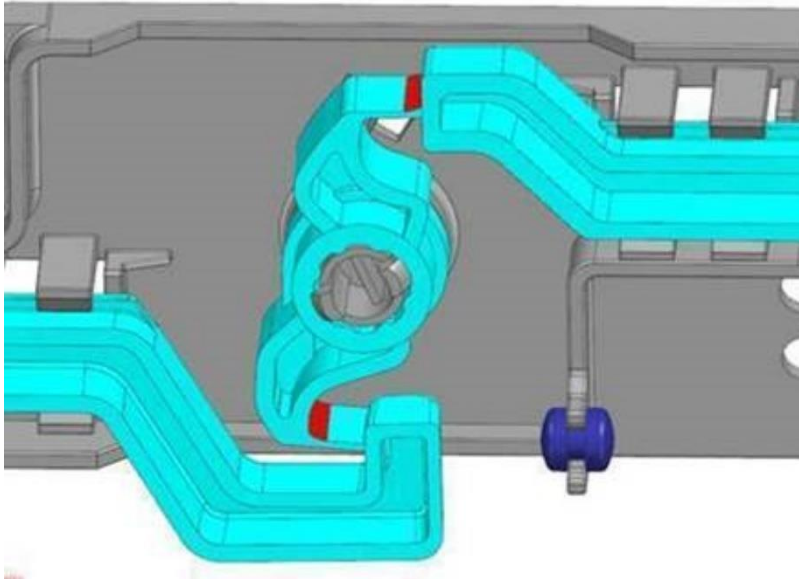


**Figure 5. Stress Analysis of Second Design**

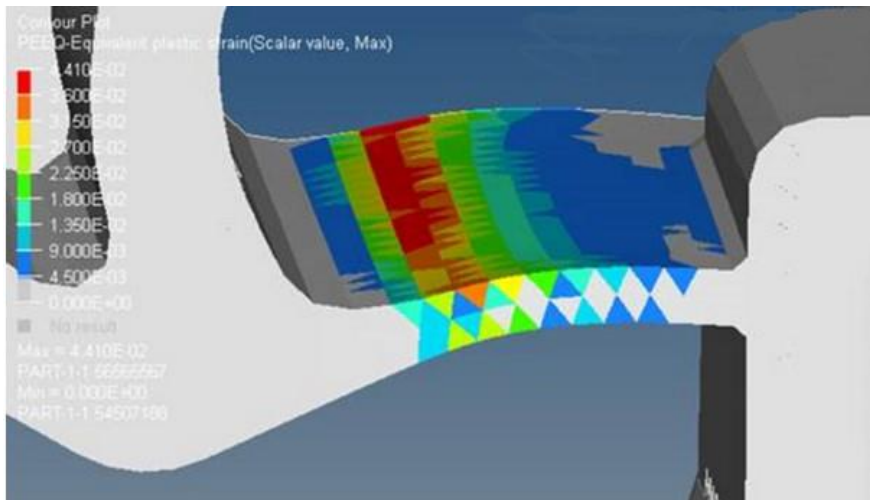
In the stress analysis of the third version design, it was clearly seen that stress distribution was more evenly distributed and there was no high stress piling in any area. The results of the stress analysis are given in Figure 7.

Since high stress in these areas will affect fatigue strength negatively, these areas were designed again by adding radiuses.





**Figure 6.** *Third Version of Design With Hinges and Radiuses*



**Figure 7.** *Stress Analyses Results for Third Version of Design*

After the stress analysis results turned out to be suitable for the usage, a fatigue test was carried out using Fiat norms. Norms are given in Table 1:

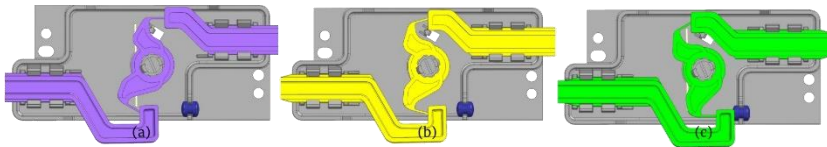
**Table 1.** *Lower Glove Box Duty Cycle Test Conditions*

Number of Cycles (One Life)	8000
Cycles at Room Temperature	5920
Cycles at High Temperature	200
Cycles at High Relative Humidity	1680
Cycles at Low Temperature	200

Test results came as suitable to use, since there was no failure or obvious damage like whitening in material.

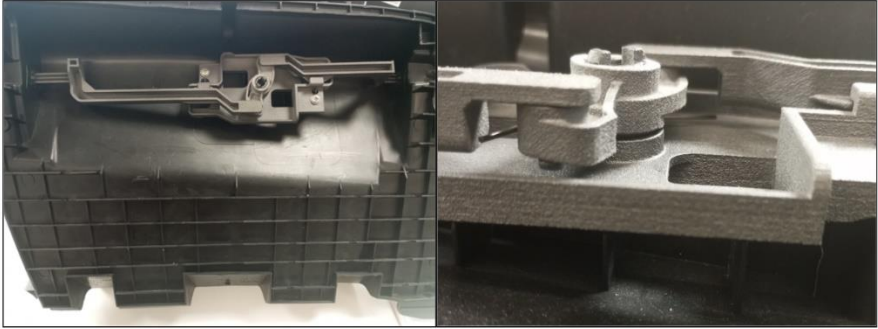
### 3.Results

As a result of this study, a new type of clutch mechanism for glovebox compartment has been developed, using FEA and fatigue tests. This new mechanism is given in Figure 8 in various rotation degrees.



**Figure 8.** *New Clutch Mechanism at (a) 0°, (b) 15° (c) 30°*

As this mechanism is a single part, it saves a lot of cost, material, and time for the manufacturer compared to the old mechanism, which was 4 parts. A real photo of the old mechanism is given in Figure 9.



***Figure 9: Current Mechanism***

## References

<https://stuff.mit.edu/afs/athena/course/2/2.75/resources/random/Living%20Hinge%20Design.pdf> (Accessed at 26.03.2024)

Brannon, P. J. (2003). A study of failure prediction in polypropylene living hinges. University of Massachusetts Lowell.

## CHAPTER V

### Additive Manufacturing in Plastic Injection Moulding

**Mehmet ALTUĞ<sup>1</sup>**  
**Yunus ASLAN<sup>2</sup>**  
**Yakup YILMAZ<sup>3</sup>**

#### 1. Introduction

Additive manufacturing (AM) processes produce three-dimensional physical objects from digital data, one piece, surface, or layer at a time. (Altuğ, 2022; Kanbur et al., 2022; Seepersad, 2014; Weinert et al., 2023; Zhang et al., 2018). Additive manufacturing processes use raw materials to create a final part by placing, bonding, and transforming volumetric elements. The shape, size, and strength of the bonds between the elements are determined by the raw material(s), manufacturing equipment settings, and process

---

<sup>1</sup> Assoc. Prof. Dr., Inonu University, Malatya OIZ Vocational High School, Malatya/Turkey, Orcid: 0000-0002-4745-9164, mehmet.altug@inonu.edu.tr

<sup>2</sup> Lecturer, Inonu University, Malatya OIZ Vocational High School, Malatya/Turkey, Orcid: 0000-0003-0929-5047, yunus.aslan@inonu.edu.tr

<sup>3</sup> Mechanical Engineer, Inonu University, Malatya/Turkey, Orcid: 0000-0001-5712-0650, yk.yilmaz4488@gmail.com

parameters. (Thompson et al., 2016; Weinert et al., 2023). Additive manufacturing technologies have the potential to reduce the number of manufacturing steps required by producing parts without the need for intermediate shaping tools.(Gibson et al., 2015; Seepersad, 2014; Thompson et al., 2016; Weinert et al., 2023) Additive manufacturing allows for the creation of complex internal features, improving the functionality and performance of injection tooling. The most significant benefit of additive manufacturing over traditional machining methods for injection mould tools is the ability to incorporate conformal cooling channels into the part design during layer-by-layer construction.(Gibson et al., 2015; Seepersad, 2014; Thompson et al., 2016) The use of additive manufacturing (AM) techniques, either alone or in combination with conventional manufacturing methods, can overcome the design and manufacturing constraints that arise when using traditional techniques. (Arman & Lazoglu, 2023; Evens et al., 2019; Hatos et al., 2018; Kovács et al., 2015; Papadakis et al., 2020; Zink & Kovács, 2017) Recent developments in additive manufacturing (AM) technology have made it possible to produce complex and effective products in an affordable way, unlike traditional machining tools. Therefore, additive manufacturing can be effectively applied to plastic injection moulding processes due to the design and manufacturing flexibility of AM tools.(Kanbur et al., 2022; Rajamani et al., 2021; Zhang et al., 2018)

Additive manufacturing, has become an essential technology in various industries, including the plastic injection moulding sector. In recent years, the plastic injection moulding industry has also adopted additive manufacturing technologies to improve their products' design, performance, and production processes. This

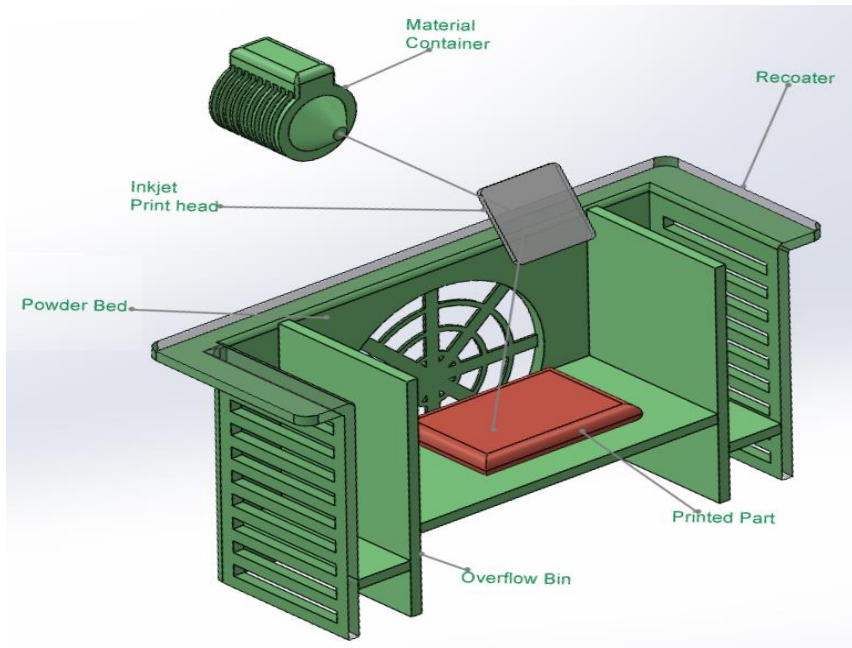
research aims to explore the use of AM technologies in the plastic injection moulding industry and their potential benefits and challenges. Plastic injection mouldings are gaining significant popularity due to their eco-friendliness and fuel efficiency. Additive manufacturing technologies offer unique advantages that make them attractive for the plastic injection moulding industry, including the ability to produce complex geometries and lightweight parts with high precision and accuracy.

## **2. Additive manufacturing methods**

### **2.1 Selective laser sintering (SLS)**

It is a form of additive manufacturing, also referred to as 3D printing, that utilises a high-powered laser to selectively fuse powdered material together layer-by-layer in order to construct a tangible object. The schematic representation of this system is given in figure 1. The first step in the SLS process is to prepare the material. SLS uses powdered materials, typically plastics such as nylon, polyethylene, or polypropylene. These materials are loaded into a powder bed that is spread out in a thin layer. A high-powered laser is then used to selectively heat and fuse the powdered material according to the design of the object being printed. The laser scans the powdered material, melting it and fusing it together to create a solid layer. Once the first layer is complete, the powder bed is lowered, and a new layer of new powder is spread on top. The laser then scans and selectively sinters this new layer, fusing it to the previous layer. This process is repeated layer by layer until the entire object is printed. After the object is fully printed, it is allowed to cool down and solidify. The excess, unfused powder acts as a support structure, helping to hold the printed object in place during the

printing process. Once the object is cooled, it is removed from the powder bed, and the excess powder is typically brushed off or blown away. The printed object may then undergo further post-processing, such as sanding, polishing, or additional heat treatment, depending on the desired finish and properties of the final part.



*Figure 1: Selective laser sintering (SLS) method diagram.*

SLS has several advantages as a rapid prototyping method. It allows for the creation of complex, functional parts with high precision and accuracy. It also does not mandate the use of support structures, as the unfused powder acts as temporary support during printing, which can save time and effort in post-processing. SLS is a popular manufacturing method used in a variety of industries, such as aerospace, automotive, consumer goods, and medical, for quickly creating prototypes and producing low volumes

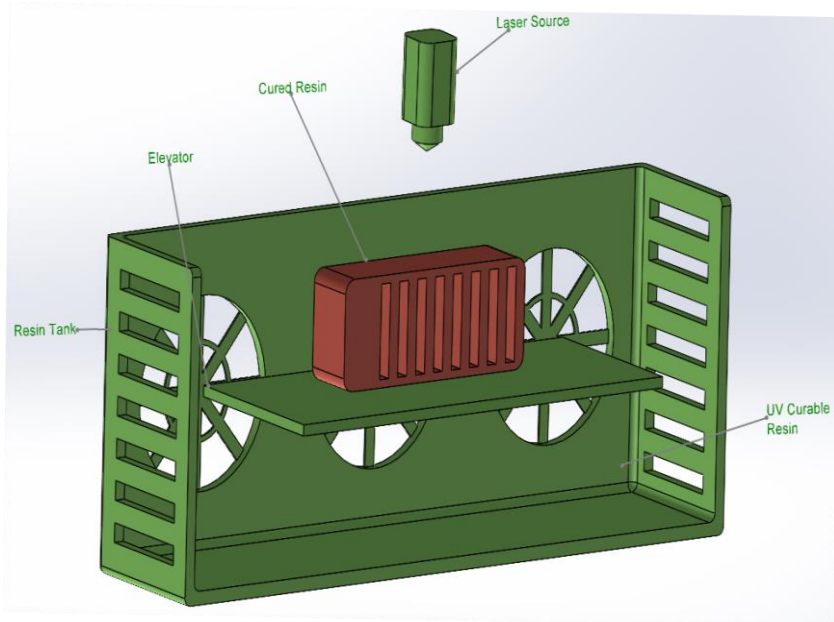


of parts with intricate geometries. However, 3D printing using SLS technology also has some limitations, including a restricted range of material options, higher costs compared to some other 3D printing methods, and the requirement for specialized equipment and safety measures due to the use of lasers and powdered materials.

## **2.2 Stereolithography (SLA)**

It was developed in the 1980s and is based on the principle of photopolymerization, where a liquid resin is cured layer-by-layer using a focused UV laser to create a solid 3D object. The first step in SLA is to create a 3D model of the desired object using Computer-Aided Design (CAD) software. The model is typically saved in a standard STL file format, which represents the object as a collection of triangular facets. Next, a suitable liquid resin is selected based on the required properties of the final object, such as color, transparency, flexibility, or strength. There are various types of resins available for different applications, including standard resins, engineering resins, and specialty resins. The 3D model is slice into thin layers (typically 0.04-0.25 mm thick) using specialized software. These slices are then sent to the SLA machine for printing. The SLA machine consists of a vat of liquid resin, a tray that can move up and down, and a UV laser. The process starts by lowering the platform into the vat of resin, just above the surface. The UV laser then scans the first layer of the object on the surface of the liquid resin, selective curing the resin in the shape of the first layer according to the sliced data. The schematic representation of this system is given in figure 2. Once the first layer is cured, the platform is lifted by a fraction of the layer thickness, and the process is recursive for the next layer. This layer by layer process is repeated until the entire object is built. Once the printing is complete, the

object is typically removed from the SLA machine and washed in a cleaning solution to remove any uncured resin. Depending on the type of resin used, additional post-processing steps may be required to achieve the desired surface finish and properties. These steps may include curing under UV light, sanding, polishing, or painting.



*Figure 2: Stereolithography (SLA) method diagram.*

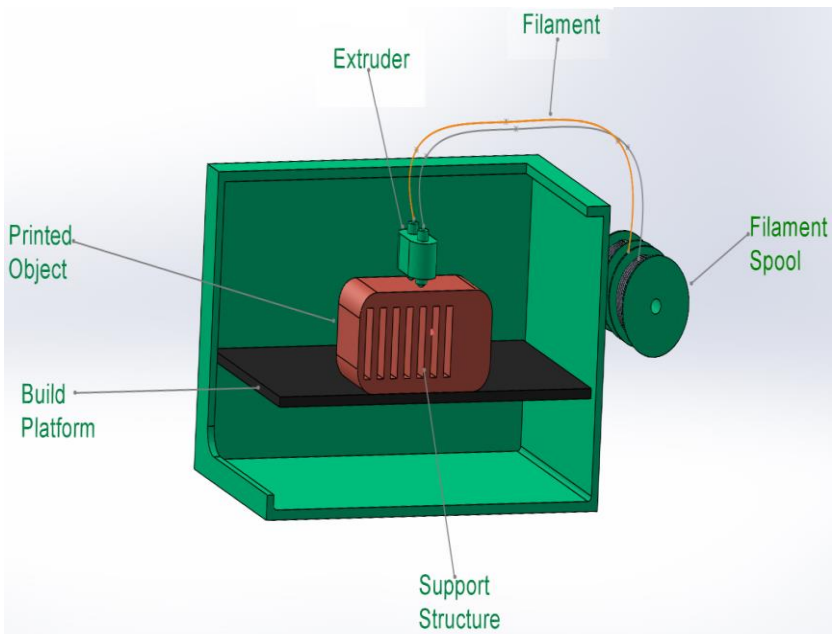
The SLA offers significant advantages. SLA offers a wide range of resin materials with different properties, including various colors, transparency, flexibility, and mechanical strength, allowing for versatile material choices for different applications. High Precision, SLA is capable of producing highly detailed and complex parts with very fine features and tight tolerances, making it suitable for prototyping intricate geometries and functional parts. Surface Quality, SLA parts typically have a smooth surface finish right out of the printer, requiring minimal post-processing to achieve a high-

quality appearance. SLA is known for its fast printing speeds, allowing for quick turnaround times in the prototyping process.

### **2.3 Fused deposition modeling (FDM)**

Fused Filament Fabrication (FFF) is a widely used rapid prototyping technique that involves depositing melted thermoplastic materials layer by layer to create three-dimensional objects. Fused Deposition Modelling (FDM) is a popular technique used across a range of industries for rapid prototyping, modelling and manufacturing. Fused Deposition Modelling (FDM) utilises a thermoplastic material that is heated to a semi-liquid state and then extruded through a nozzle onto a build platform. The two most commonly used materials in FDM are ABS (Acrylonitrile Butadiene Styrene) and PLA (Polylactic Acid), although other materials, such as PETG and TPU, are also available. FDM begins with a 3D model that is converted into machine-readable code (G-code) using specialized software. The G-code contains instructions for the FDM machine to move the print head, control the temperature, and lay down the material layer by layer. The FDM machine has a heated build platform to ensure proper adhesion of the material to the platform. The FDM machine moves the print head in the X and Y directions while simultaneously extruding the melted thermoplastic material through the nozzle in the Z direction onto the build platform. The material quickly solidifies upon deposition, forming a solid layer. The build platform is then lowered by a precise amount to create space for the next layer, and the process repeats until the complete object is built up layer by layer. In cases where the object being printed has overhangs or complex geometries that cannot be printed without support, FDM machines can also generate support structures made of the same material or a different, dissolvable

material. These support structures provide temporary support to the overhanging features during the printing process and can be removed after the print is complete. Once the object is fully printed, it is typically left to cool on the build platform. Afterward, any support structures can be removed, and the object may undergo additional post-processing steps such as sanding, polishing, painting, or assembly to achieve the desired finish or functionality. The schematic representation of this system is given in figure 3.



*Figure 3: Fused deposition modeling (FDM) method diagram.*

Advantages of FDM offers a wide range of thermoplastic materials to choose from, making it versatile for various applications and industries. FDM is relatively more affordable compared to other rapid prototyping methods, making it accessible to a broader range of users and applications. FDM has a straightforward workflow, with

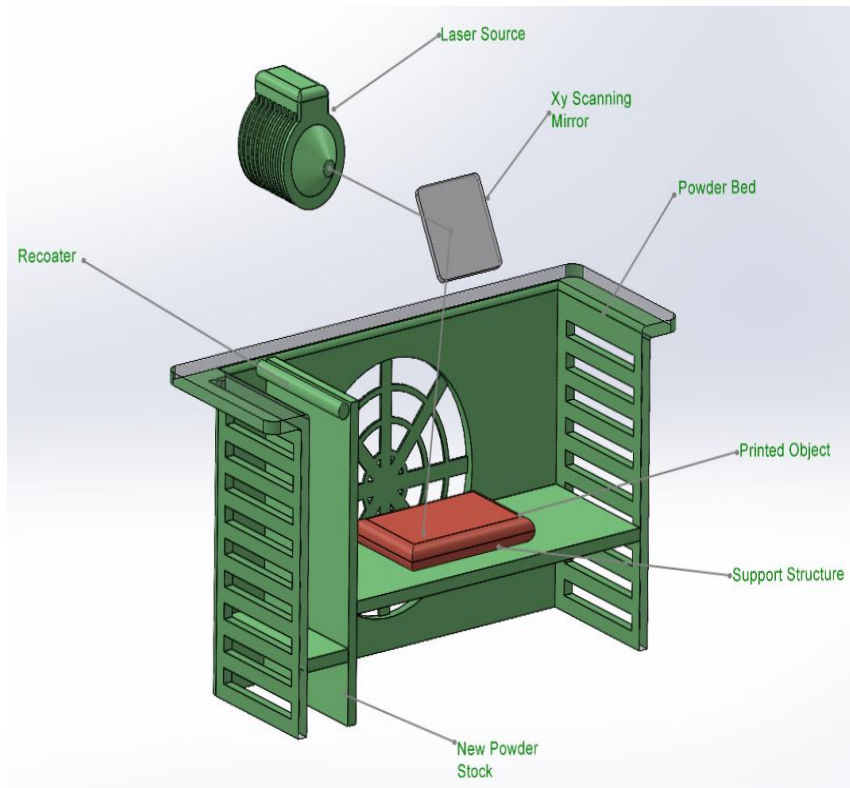
minimal setup and easy-to-use software, making it user-friendly for both beginners and experienced users. FDM machines come in different sizes, allowing for the production of large-scale prototypes or parts in a single print.

Applications of FDM, is widely used for functional prototyping, allowing designers and engineers to create physical prototypes of parts or products for fitment testing, form validation, and functional testing. FDM is used for creating concept models and mockups to visualize and validate design concepts before moving to full-scale.

## **2.4 Selective laser melting (SLM)**

Selective Laser Melting (SLM) is a type of additive manufacturing technology that falls under the category of powder bed fusion methods. The process involves using a high-powered laser to selectively melt and fuse metallic powders layer by layer, resulting in the creation of three-dimensional objects. SLM is renowned for its capability to manufacture fully dense, intricate, and operational metal components with high precision and exceptional mechanical characteristics. The process starts with preparing a 3D computer-aided design (CAD) model of the required part. The CAD model is then sliced into thin layers, typically ranging from 20 to 100 microns in thickness, to create a digital representation of the part's cross-sections. Metallic powders, typically in the form of spherical particles, are loaded into a powder bed inside the SLM machine. The powder bed is spread evenly and leveled to a precise thickness using a recoater, which is a movable blade or roller. A high-powered laser, usually a fiber laser, is used to selectively melt and fuse the metallic powders according to the cross-sections of the CAD model. The

laser is controlled by a computer to scan and trace the outlines of the part's cross-section onto the powder bed. The laser energy is absorbed by the powder particles, causing them to melt and fuse together. After scanning and fusing a layer, the powder bed is lowered by the thickness of one layer, and a new layer of metallic powders is spread on top using the recoater. This process is repeated until the object is complete. The laser scanning process is repeated to selectively melt and fuse the new layer to the previous layer. This layer-by-layer building process is repeated until the entire part is completed. After the part is fully built, it is allowed to cool and solidify inside the powder bed. This helps in preventing deformation and warping of the part due to thermal stresses. Once the part has cooled down, the excess, unfused metallic powders are removed from the powder bed using various methods such as brushing, air blowing, or vacuuming. The schematic representation of this system is given in figure 4. The manufactured components may require additional processing to achieve the desired surface finish, dimensional accuracy, and mechanical properties. Post-processing may involve heat treatment, machining, polishing, or other finishing processes, depending on the specific requirements of the part.



*Figure 4: Selective laser melting (SLM) method diagram.*

Advantages of Selective Laser Melting, Ability to produce fully dense and functional metal parts with complex geometries. The material exhibits excellent mechanical properties, such as high strength, toughness, and fatigue resistance. Design flexibility, allowing for the production of customized and optimized parts. The ability to manufacture components from a variety of metal alloys, such as stainless steel, titanium, and aluminium, among others. The production time is faster compared to traditional manufacturing methods because it eliminates the need for tooling or molds.

## **2.5 Direct metal laser sintering (DMLS)**

Direct Metal Laser Sintering (DMLS) is an additive manufacturing technique, also known as Selective Laser Melting (SLM). It uses a high-powered laser to fuse metal powders layer by layer, resulting in the production of three-dimensional objects. DMLS is widely used in industries such as aerospace, automotive, medical, and tooling, where complex metal parts with high precision and durability are required. DMLS uses metal powders as the raw material. The metal powders are typically fine and have specific properties suitable for the DMLS process, such as high melting points and good thermal conductivity. Common materials used in DMLS include stainless steel, titanium, aluminum, cobalt-chrome, and inconel. Before the DMLS process begins, the 3D model of the object to be printed is converted into machine-readable code (G-code) using specialized software. The G-code contains instructions for the DMLS machine, including the layer-by-layer geometry and the laser parameters. The Direct Metal Laser Sintering (DMLS) machine features a build platform coated with a thin layer of metal powder. The metal powder is selectively melted by the high-powered laser, following the instructions in the G-code, which fuses the particles together to form a solid layer. The build platform is lowered by a precise amount, and a new layer of metal powder is spread over the previous layer. The object is formed by repeating the process layer by layer until it is complete. The laser used in DMLS generates a significant amount of heat, which causes the metal powders to melt and fuse together. After each layer is melted, it is rapidly cooled to solidify the metal and create a solid part. This controlled heating and cooling process helps to achieve good metallurgical properties in the final part. Similar to other additive manufacturing methods, DMLS



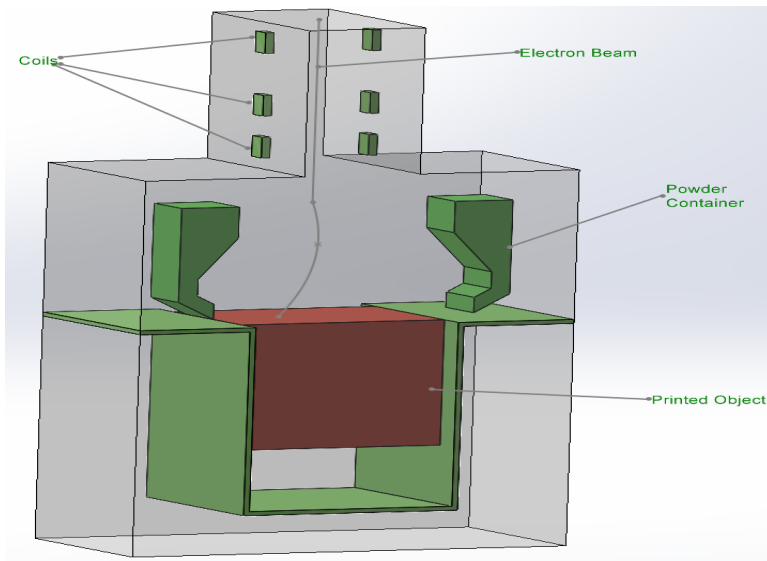
may require support structures to hold up overhanging or complex geometries during the printing process. Support structures are usually made of the same material as the part or a sacrificial material that can be removed after printing is complete. After the object has been fully printed, it may undergo post-processing steps such as removing support structures, surface finishing, and heat treatment to optimize its mechanical properties. Post-processing is crucial to attain the intended surface finish, precision, and mechanical properties of the final product.

DMLS enables the production of intricate geometries that may be difficult or unfeasible to achieve with conventional manufacturing techniques, such as CNC machining. DMLS can produce parts with high accuracy and fine details, making it suitable for applications that require tight tolerances and precise dimensions. DMLS produces fully dense metal parts with excellent mechanical properties, including high strength, good thermal conductivity, and corrosion resistance. The parts are comparable to traditionally manufactured metal parts. DMLS is a rapid prototyping method that allows for quick iteration and design validation. It can also be used for small-scale production of complex metal parts without the need for tooling.

## **2.6 Electron beam melting (EBM)**

Electron Beam Melting (EBM) is an additive manufacturing process that utilises an electron beam to liquefy metal powders and construct three-dimensional objects layer by layer. EBM is similar to Selective Laser Melting (SLM) in that it is a powder bed fusion process, but it uses an electron beam instead of a laser as the energy source. The process of EBM commences with an even layer of metal

powder being spread across a build platform. An electron beam is then used to selectively melt the powder in the desired areas, based on a computer-generated 3D model of the part. The electron beam is precisely controlled and scans the powder bed, melting it and creating solidified metal layers. After each layer is finished, the build platform is lowered by one layer thickness. Then, a new layer of metal powder is spread over the previous layer that has been melted. The process is repeated step by step until the final layer is complete. One of the unique aspects of EBM is that it operates in a vacuum or near-vacuum environment. This is because the electron beam requires a vacuum to travel through to avoid scattering, and also to prevent oxidation of the metal powder during the melting process. The vacuum environment ensures that the parts are produced with minimal contamination and optimal material properties. The schematic representation of this system is given in figure 5.



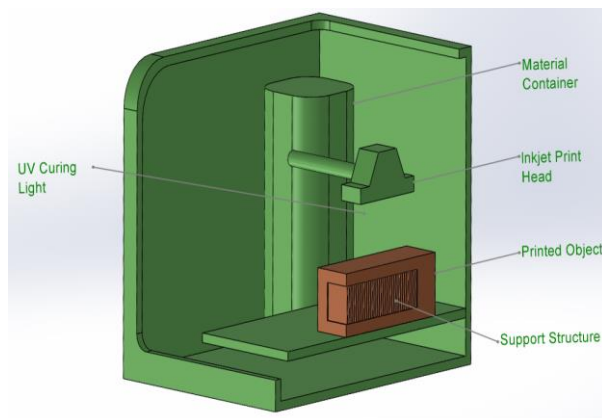
*Figure 5: Electron beam melting (EBM) method diagram.*

Advantages of EBM can achieve faster build speeds compared to some other additive manufacturing processes due to the high energy density of the electron beam, which allows for rapid melting and solidification of metal powders. EBM machines generally have large build volumes, which enables the production of large and complex parts in a single build, reducing the need for assembly or joining of multiple smaller parts. EBM produces parts with excellent material properties, including high density, good mechanical properties, and high-quality surface finish. EBM can process a wide range of high-temperature materials, such as titanium alloys, nickel alloys, and cobalt-chromium alloys, which are commonly used in aerospace, automotive, and medical applications. EBM can produce parts with intricate geometries, such as internal features, overhangs, and undercuts, without requiring support structures. This allows for the production of intricate and lightweight parts.

## **2.7 Polyjet**

PolyJet is a rapid prototyping method that uses an inkjet-style process to create 3D objects by jetting and curing liquid photopolymer materials layer by layer. Stratasys, a leading manufacturer of 3D printers, developed the PolyJet technology. It is widely used in various industries for rapid prototyping, product development, and manufacturing of complex and detailed parts. Photopolymer materials are used in PolyJet technology. These materials are liquid polymers that are cured or solidified when exposed to ultraviolet (UV) light. The materials are typically supplied in cartridges or tanks, and they can be loaded into the 3D printer. The PolyJet printer uses inkjet-style printheads to jet tiny droplets of liquid photopolymer materials onto a build platform.

These droplets are precisely deposited layer by layer, and each layer is cured or solidified using UV light immediately after it is jetted. The cured layers bond together to create a solid object. PolyJet printers can also jet a support material alongside the model material. The support material is used to support overhanging or complex geometries during the printing process. The support material can be easily removed after printing, leaving behind the final 3D object. PolyJet technology allows for high precision and resolution printing, with layer thicknesses typically ranging from 16 to 30 microns. Additionally, PolyJet printers can print with multiple materials in a single print job, allowing for the creation of parts with varying colors, textures, or material properties in a single print. After printing, the 3D object may require post-processing, such as washing to remove excess photopolymer materials or support material, and UV curing to fully solidify the object. The schematic representation of this system is given in figure 6. Some PolyJet printers also offer additional post-processing options, such as smoothing, polishing, or painting, to achieve desired surface finishes or aesthetics.



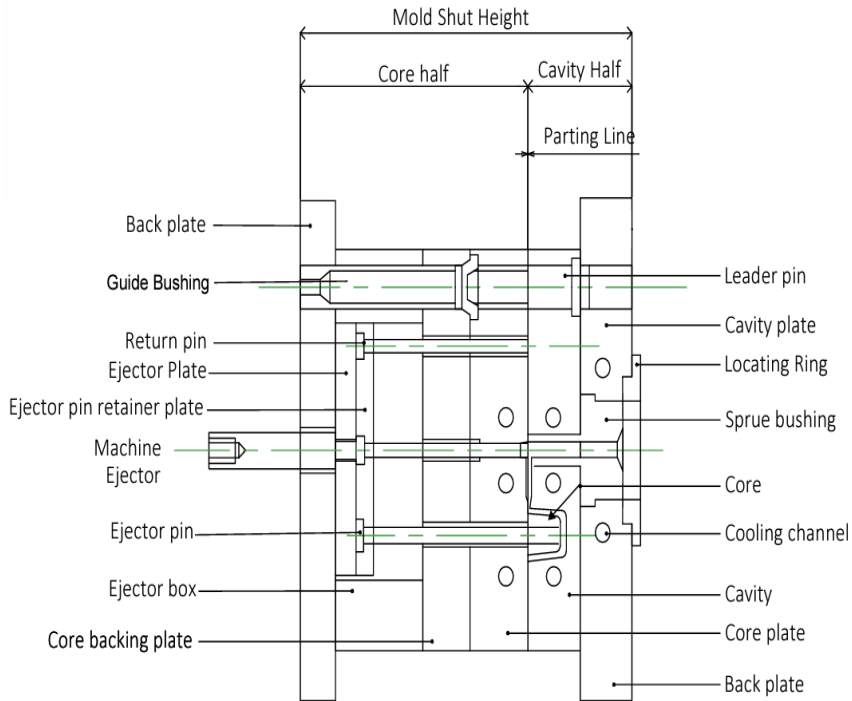
*Figure 6: Polyjet method diagram.*

Advantages of PolyJet, high precision and resolution printing, allowing for the creation of complex and detailed parts. Multi-material printing capability, allowing for parts with varying colors, textures, or material properties. Wide range of available photopolymer materials with different properties, such as transparency, flexibility, and durability. Support material can be easily removed, leaving behind smooth surfaces. Fast printing speeds, making it suitable for rapid prototyping and iterative design processes. Suitable for producing parts with fine details, smooth surfaces, and high-quality aesthetics.

### **3. Plastic injection molding**

Plastic injection molding (PIM) is a highly efficient and widely used manufacturing technique for producing plastic parts. (Çallışkan et al., 2023; Zhou et al., 2021) The injection molding method is utilised to manufacture parts of various sizes and intricate shapes. The injection molding process can improve product quality and reduce cycle times depending on the mold design and plastic part geometry. This technique is commonly used in various fields, including automotive, aviation, biomedical, packaging, electronics, and toy production. (Deepika et al., 2020; Mercado-Colmenero et al., 2021).

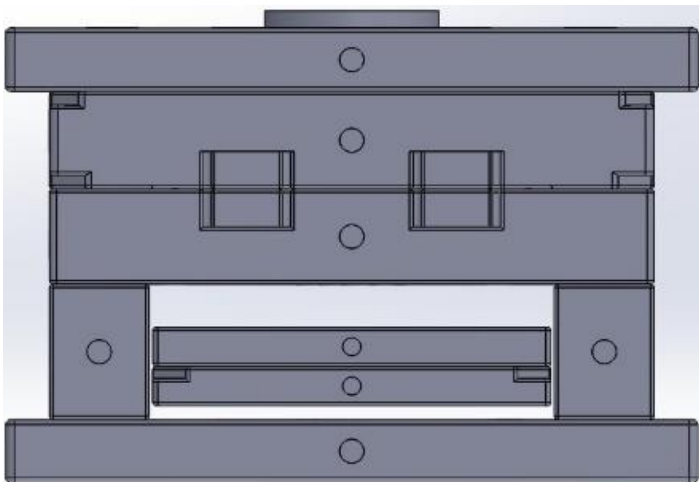
Plastic injection molding is a manufacturing process that creates three-dimensional plastic parts by injecting molten plastic material into a mold cavity. Injection moulding is a highly efficient, cost-effective, and versatile technique for mass-producing plastic parts. Concepts related to plastic injection molding terminology are shown in figure 7 (Catoen and Rees, 2021).



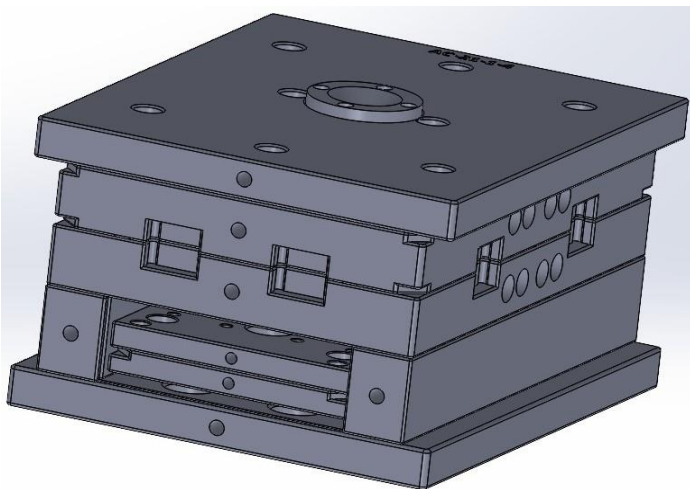
*Figure 7: Injection mold terminology.*

*Source: Catoen and Rees, 2021*

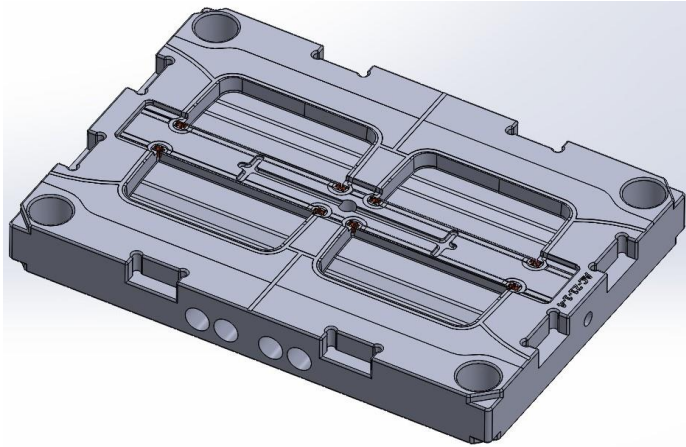
Plastic injection molding can produce parts with complex geometries, precise dimensions, and various material properties, making it suitable for a wide range of applications in industries such as automotive, consumer goods, electronics, medical, and more. The representation of a plastic injection mold assembly and mold core is given in Figure 8.



*a)*



*b)*



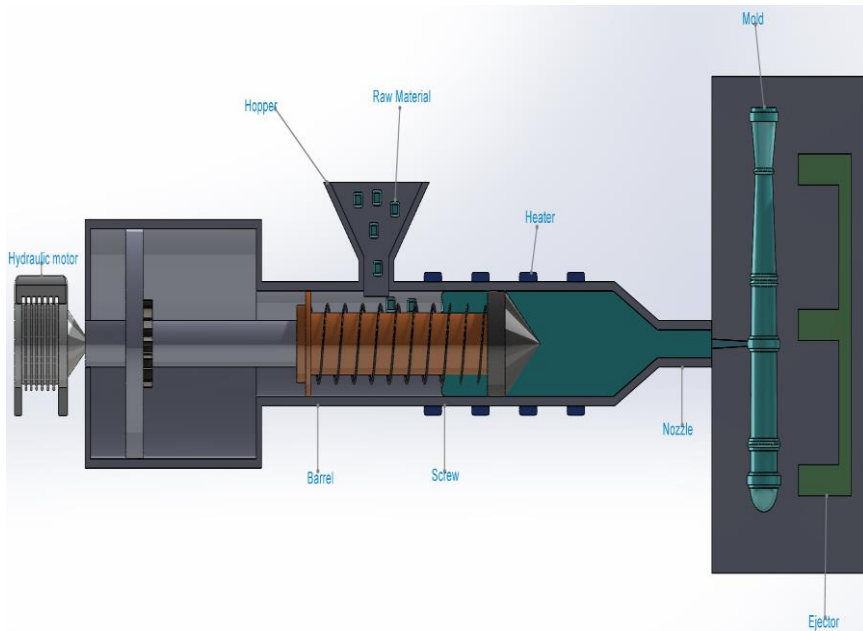
c)

*Figure 8: (a,b) Plastic injection mold assembly, (c) Plastic injection mold core.*

The process of plastic injection molding typically involves the some phase. The first phase in plastic injection molding is product design. The next phase is to select the appropriate plastic material for the injection molding process. There are various types of plastics available with different properties, such as thermoplastics (ABS, PP, PE, PC) and thermosetting plastics (epoxy). The material selection depends on the desired characteristics of the final part, such as strength, flexibility, heat resistance, and more. After selecting the product and plastic material for deformation molding, the next phase is mold design. The mold, also known as the tool or die, is a hollow cavity that defines the shape and features of the final plastic part. It is typically made of steel or aluminum and consists of two halves, the cavity and the core, which are precision machined to create the desired part geometry. After the design, production and assembly stages, the replacement process begins. The selected plastic material is then fed into the injection molding machine (Figure 9), where it is



heated to its melting point and converted into a molten state. The molten plastic is typically mixed with additives, such as colorants, fillers, and stabilizers, to achieve the desired properties of the final part. Once the molten plastic is ready, it is injected into the mold cavity under high pressure using a reciprocating screw or a plunger. The plastic material fills the mold cavity and takes the shape of the mold, forming the part's desired geometry. After the injection, the mold is cooled to solidify the molten plastic material and allow it to take the shape of the mold cavity. Cooling time depends on the material and part geometry and is carefully controlled to prevent deformations or warping of the part. Once the plastic part has solidified, the mold is opened, and the part is ejected from the mold cavity using ejector pins or other mechanisms. The part is then trimmed and any excess material, known as flash, is removed. The above phases are repeated to produce a large number of identical parts in a continuous cycle. Injection molding machines can operate in a high-speed, automated manner, allowing for efficient and cost-effective production of large quantities of plastic parts.



*Figure 9: Plastic injection machine.*

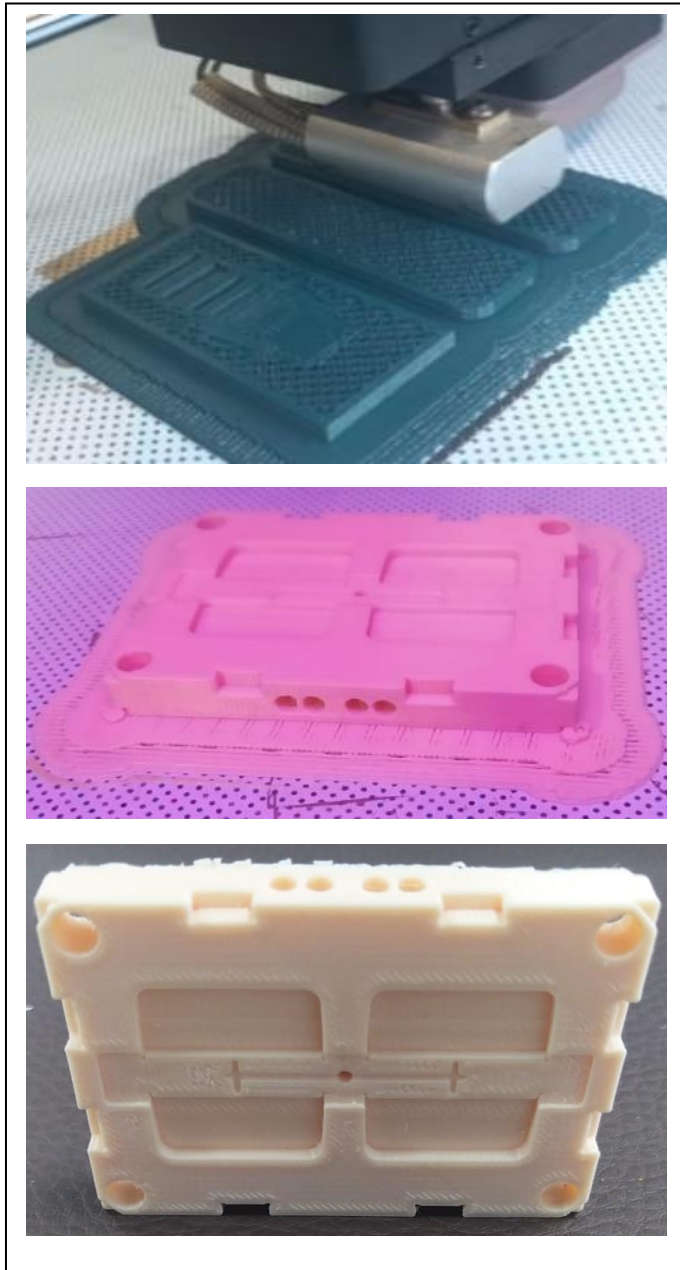
Plastic injection molding offers several advantages, including. Injection molding allows for high-volume production of plastic parts with fast cycle times, making it highly efficient for mass production. Injection molding can produce parts with complex geometries, tight tolerances, and various surface finishes, offering design flexibility and versatility in creating a wide range of parts with different shapes and sizes.

#### **4. Use of additive manufacturing in plastic injection molding**

Injection molding is a versatile process that can handle a wide range of plastic materials, including both thermoplastics and thermosetting plastics. This allows for flexibility in material selection to achieve the desired properties in the final product. Injection molding is a cost-effective method for producing plastic

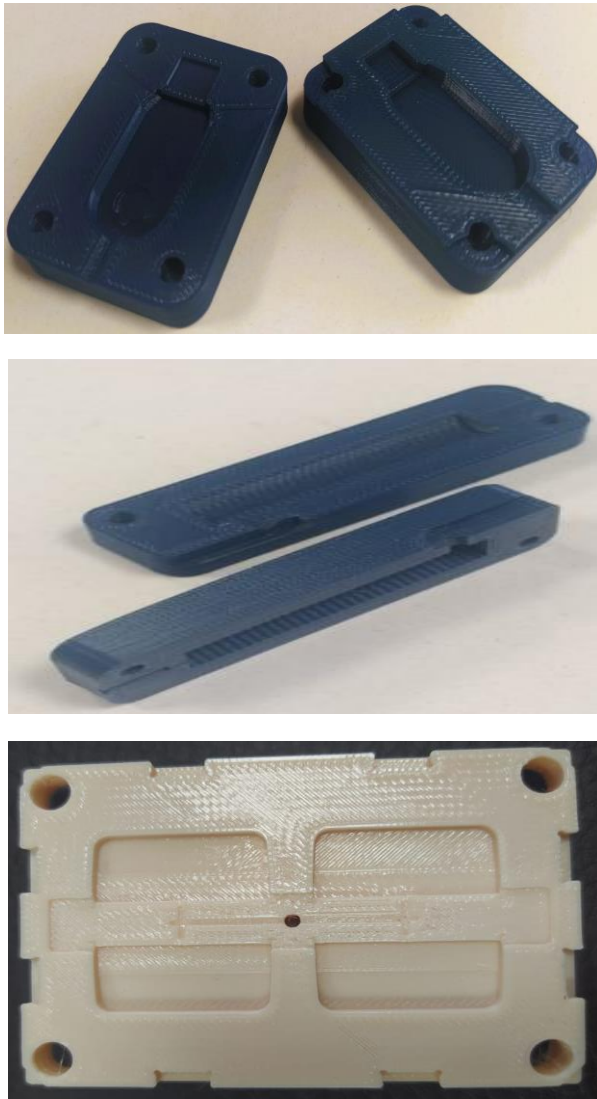
parts in large quantities, as the per-part cost decreases with higher production volumes. Injection molding offers high repeatability and consistency in part quality, as the process parameters can be precisely controlled and monitored, resulting in consistent parts.

However, there are also some limitations to plastic injection molding, including. The design and fabrication of molds for plastic injection molding can be expensive, especially for complex parts or low-volume production. The molds need to be precise and durable, adding to the initial tooling cost. This can make it less suitable for small-scale or prototype production runs. The design and fabrication of molds for plastic injection molding can take time, ranging from weeks to months, depending on the complexity of the part and the availability of resources. This lead time can delay the overall production timeline, especially for new product development or time-sensitive projects. In this context, additive manufacturing has created an important vision in plastic injection molding in terms of both speed and precision. The production of mold core samples using a 3D printer is shown in figures 10 and 11.



*Figure 10: Production of mold core samples using 3D printer.*

Injection molding has certain design limitations, such as draft angles, wall thickness, and undercuts, which need to be considered during the design process. These limitations can affect the design freedom and may require design modifications or additional tooling features, adding complexity and cost to the process. While injection molding can process a wide range of plastic materials, there may be limitations in terms of the material properties that can be achieved. For example, certain high-temperature or high-performance materials may require specialized equipment or processing techniques, which can add to the overall cost. Plastic injection molding involves the use of plastic materials, which can raise environmental concerns related to plastic waste, recycling, and sustainability. Proper disposal or recycling of plastic waste generated during the process is important to mitigate the environmental impact of plastic injection molding.



*Figure 11: Examples of mold cores produced with 3D printers.*

There are some examples from around the world where additive manufacturing has been used in plastic injection molding. Volkswagen Autoeuropa, an automotive manufacturing plant in

Portugal, has integrated additive manufacturing into its plastic injection molding processes to produce custom tools, jigs, and fixtures. By leveraging 3D printing, they have been able to optimize their production processes, reduce tooling costs, and improve production efficiency (<https://additive-x.com>). BMW Group, a leading automobile manufacturer, has implemented additive manufacturing in plastic injection molding for producing complex tooling inserts and core pins with conformal cooling channels. This has allowed them to achieve faster cooling times, reduced cycle times, and improved part quality (<https://www.press.bmwgroup.com>). IKEA, a global furniture retailer, has utilized additive manufacturing in plastic injection molding to produce customized components for its furniture products. This has enabled them to offer unique designs, improve product performance, and reduce costs associated with traditional tooling methods (<https://www.voxelmatters.com>). HP Inc., a leading technology company, has incorporated additive manufacturing in plastic injection molding to produce customized tooling inserts for their inkjet printhead manufacturing process. This has resulted in improved print quality, reduced production time, and increased efficiency (<https://www.industryweek.com>). Adidas, a renowned sportswear and footwear brand, has integrated additive manufacturing in plastic injection molding to produce customized midsoles for their running shoes. This has allowed them to offer personalized footwear with enhanced comfort and performance, and also enabled rapid design iterations for faster product development (<https://www.cnet.com>).

## **5. Conclusion**

Despite the limitations, plastic injection molding remains one of the most widely used and versatile methods for mass production of plastic parts. Its advantages in terms of efficiency, design flexibility, material variety, and cost-effectiveness make it suitable for a wide range of applications in various industries. However, careful consideration of the design, tooling, material, and environmental aspects is necessary to ensure successful implementation of plastic injection molding for specific projects or applications. In this context, additive manufacturing has brought about extremely important and significant improvements for plastic injection molding.

Additive manufacturing, has been increasingly used in plastic injection molding to complement or enhance the traditional injection molding process. Additive manufacturing offers unique advantages in the plastic injection molding workflow, including the ability to produce complex geometries, create rapid prototypes, produce tooling components, and manufacture small quantities of custom parts. Here are some specific uses of additive manufacturing in plastic injection molding.



## References

Altuğ, M. (2022). A comparison study in terms of dimensional accuracy and precision of 3d modeling. *International Journal of Innovative Engineering Applications*, 6(1). <https://doi.org/10.46460/ijiea.1012067>

Arman, S., & Lazoglu, I. (2023). A comprehensive review of injection mold cooling by using conformal cooling channels and thermally enhanced molds. In *International Journal of Advanced Manufacturing Technology* (Vol. 127, Issues 5–6). Springer London. <https://doi.org/10.1007/s00170-023-11593-w>

Çalışkan, C. I., Özer, G., Koç, E., Sarltaş, U. S., Yıldız, C. F., & Çiçek, Ö. Y. (2023). Efficiency Research of Conformal Channel Geometries Produced by Additive Manufacturing in Plastic Injection Mold Cores (Inserts) Used in Automotive Industry. *3D Printing and Additive Manufacturing*, 10(2), 213–225. <https://doi.org/10.1089/3dp.2021.0062>

Catoen, B., & Rees, H. (n.d.). *Sample Pages Injection Mold Design Handbook*. <http://www.sciencedirect.com:5070/book/9781569908150/injection-mold-design-handbook>

Deepika, S. S., Patil, B. T., & Shaikh, V. A. (2020). Plastic injection molded door handle cooling time reduction investigation using conformal cooling channels. *Materials Today: Proceedings*, 27, 519–523. <https://doi.org/10.1016/j.matpr.2019.11.316>

Evens, T., Six, W., De Keyzer, J., Desplentere, F., & Van Bael, A. (2019). Experimental analysis of conformal cooling in SLM produced injection moulds: Effects on process and product quality.

*AIP Conference Proceedings*, 2055(October 2017).  
<https://doi.org/10.1063/1.5084861>

Gibson, I., Rosen, D., & Stucker, B. (2015). Additive Manufacturing Technologies. In *Additive Manufacturing Technologies: 3D Printing, Rapid Prototyping, and Direct Digital Manufacturing, Second Edition*. Springer New York.  
<https://doi.org/10.1007/978-1-4939-2113-3>

Hatos, I., Fekete, I., Ibriksz, T., Kovács, J. G., Maros, M. B., & Hargitai, H. (2018). Surface modification and wear properties of direct metal laser sintered hybrid tools used in moulds. *Journal of Mechanical Engineering*, 64(2), 121–129.  
<https://doi.org/10.5545/sv-jme.2017.4942>

Kanbur, B. B., Zhou, Y., Shen, S., Wong, K. H., Chen, C., Shocket, A., & Duan, F. (2022). Metal additive manufacturing of conformal cooling channels in plastic injection molds with high number of design variables. *Materials Today: Proceedings*, 70, 541–547. <https://doi.org/10.1016/j.matpr.2022.09.555>

Kovács, J. G., Szabó, F., Kovács, N. K., Suplicz, A., Zink, B., Tábi, T., & Hargitai, H. (2015). Thermal simulations and measurements for rapid tool inserts in injection molding applications. *Applied Thermal Engineering*, 85, 44–51.  
<https://doi.org/10.1016/j.applthermaleng.2015.03.075>

Mercado-Colmenero, J. M., Torres-Alba, A., Catalan-Requena, J., & Martin-Doñate, C. (2021). A new conformal cooling system for plastic collimators based on the use of complex geometries and optimization of temperature profiles. *Polymers*, 13(16). <https://doi.org/10.3390/polym13162744>

Papadakis, L., Avraam, S., Photiou, D., Masurtschak, S., & Falcón, J. C. P. (2020). Use of a holistic design and manufacturing approach to implement optimized additively manufactured mould inserts for the production of injection-moulded thermoplastics. *Journal of Manufacturing and Materials Processing*, 4(4). <https://doi.org/10.3390/jmmp4040100>

Rajamani, P. K., Ageyeva, T., & Kovács, J. G. (2021). Personalized mass production by hybridization of additive manufacturing and injection molding. *Polymers*, 13(2), 1–19. <https://doi.org/10.3390/polym13020309>

Seepersad, C. C. (2014). Challenges and Opportunities in Design for Additive Manufacturing. *3D Printing and Additive Manufacturing*, 1(1), 10–13. <https://doi.org/10.1089/3dp.2013.0006>

Thompson, M. K., Moroni, G., Vaneker, T., Fadel, G., Campbell, R. I., Gibson, I., Bernard, A., Schulz, J., Graf, P., Ahuja, B., & Martina, F. (2016). Design for Additive Manufacturing: Trends, opportunities, considerations, and constraints. *CIRP Annals*, 65(2), 737–760. <https://doi.org/10.1016/j.cirp.2016.05.004>

Weinert, A., Tormey, D., O'Hara, C., & McAfee, M. (2023). Condition Monitoring of Additively Manufactured Injection Mould Tooling: A Review of Demands, Opportunities and Potential Strategies. *Sensors*, 23(4). <https://doi.org/10.3390/s23042313>

Zhang, Y., Wu, L., Guo, X., Kane, S., Deng, Y., Jung, Y. G., Lee, J. H., & Zhang, J. (2018). Additive Manufacturing of Metallic Materials: A Review. *Journal of Materials Engineering and Performance*, 27(1), 1–13. <https://doi.org/10.1007/s11665-017-2747-y>

Zhou, H., Zhang, S., & Wang, Z. (2021). Multi-objective optimization of process parameters in plastic injection molding using a differential sensitivity fusion method. *International Journal of Advanced Manufacturing Technology*, 114(1–2), 423–449. <https://doi.org/10.1007/s00170-021-06762-8>

Zink, B., & Kovács, J. G. (2017). The effect of limescale on heat transfer in injection molding. *International Communications in Heat and Mass Transfer*, 86(June), 101–107. <https://doi.org/10.1016/j.icheatmasstransfer.2017.05.018>

## **CHAPTER VI**

### **Performance Improvement of Vapor Compression Refrigeration System Using Nanofluid**

**Metin YILMAZ<sup>1</sup>**  
**Canan CİMŞİT<sup>2</sup>**  
**Elif ÖĞÜT<sup>3</sup>**

#### **Introduction**

Today's rapid technological developments have made the concept of energy even more important. With these developments, energy demand has increased in industry, daily life, and many other areas. However, although fossil resources are known as the main energy source of today's world, their reserves are decreasing and their environmental damages are also known. Refrigeration systems are now widely used in almost every industry and in our daily lives.

---

<sup>1</sup> Kocaeli University, Institute of Natural and Applied Sciences, Department of Mechanical Engineering, Umuttepe, Kocaeli, Turkey, metinyilmaz@outlook.com.tr

<sup>2</sup> Kocaeli University, Golcuk Vocational School, Golcuk, Kocaeli, Turkey, ccimsit@kocaeli.edu.tr

<sup>3</sup> Kocaeli University, Faculty of Engineering, Department of Mechanical Engineering, Umuttepe, Kocaeli, Turkey, elif.ogut@kocaeli.edu.tr

Considering the energy consumption of industrial systems, it is important to conduct efficiency studies on these systems. The refrigeration systems in the industrial sector are critical in terms of energy consumption. Therefore, efficiency studies should be carried out.

There are 3 main factors affecting energy efficiency in the refrigeration system. The first step is to take appropriate measures for the existing system and system elements. The second is the use of alternative cycles using alternative energy sources. The analysis of absorption-vapor compression cascade refrigeration systems created by combining absorption and conventional vapor compression refrigeration systems, which are considered as alternative cycles, is seen in literature (Jain et al. 2013; Colorado and Velázquez 2013; Zhang et al. 2023; Cimsit and Ozturk 2014). The third factor is the selection of the appropriate refrigerant for the refrigeration system. Nanofluids are a new technology that is becoming increasingly important in the refrigeration systems because of their high heat transfer. These fluids are formed by dispersing nanoparticles in the fluid. The use of nanofluids in refrigeration systems offers a more environmentally sustainable option by providing high efficiency and lower energy consumption. In the studies conducted with the use of nanofluid in vapor compression refrigeration systems, it was concluded that the COP values of the system increased (Bilen et al 2021; Pawela et al. 2017; Babarinde et al. 2018). (It has been observed that the performance of the system has increased in studies by adding  $\text{Al}_2\text{O}_3$  nanoparticles to the R134A fluid used in the vapor compression refrigeration cycle (Ajayi et al. 2019; Aly et al. 2019; Hussain et al. 2018). Adelekan et al. (2019) examined the effect of adding titanium dioxide ( $\text{TiO}_2$ )

nanoparticles to a system using an R600a refrigerant on the system performance. The results showed that the nanoparticle-doped system performed better than the plain system. In another experimental study by Jatinder et al. (2019), the effect of TiO<sub>2</sub> nanoparticles was investigated in two different refrigerant systems using R600a and LPG. The results showed that the system using TiO<sub>2</sub> doped R600a performed better than the system using LPG under the same conditions.

Nair et al. (2020) experimentally investigated the effect of the addition of aluminium oxide (Al<sub>2</sub>O<sub>3</sub>) nanoparticles on system performance in a system using an R134A refrigerant. The results of the research showed a 6.5% improvement in the COP value with the addition of nanoparticles. The effect of addition of diamond nanoparticles on the performance of a system using R32 refrigerant was experimentally investigated. In the research, it was reported that the nanoparticle additive increased the refrigeration capacity by 5% and the COP value by 0.5%. Adelekan et al. (2021) experimentally investigated the effect of TiO<sub>2</sub> addition on performance in a system using R600a, and as a result, the COP value reached the highest value of 4.2 with the contribution of nanoparticles. In a system using R134a and R600a refrigerants, Joshi et al. (2021) examined the effect of Al<sub>2</sub>O<sub>3</sub> addition on performance. In the research, it was stated that the COP value of the system with R600a containing 0.1% Al<sub>2</sub>O<sub>3</sub> by mass increased by 37.2% compared with that of the system using R134a. Senthilkumar and Anderson (2021) experimentally investigated the effect of SiO<sub>2</sub> addition on the performance of a system using R410a. Because of this research, it has been reported that the addition of nanoparticles improves the performance of the system.

Due to increasing energy consumption and environmental concerns in refrigeration, the performance of the refrigeration system needs to be improved. If a reduction in compressor work can be achieved in the vapor compression refrigeration system, the performance parameter can be improved. In this direction, the aim of this study is to investigate the improvement of the performance of a vapor compression refrigeration system using nanorefrigerants with a theoretical approach. In this study, the effects of adding  $\text{Al}_2\text{O}_3$  and  $\text{CuO}$  nanoparticles to the R134A refrigerant used in the vapor compression refrigeration cycle on the system have been theoretically investigated. A detailed thermodynamic analysis was carried out at different evaporator and condenser temperatures and mass fractions. The results obtained are given in tables and graphs.

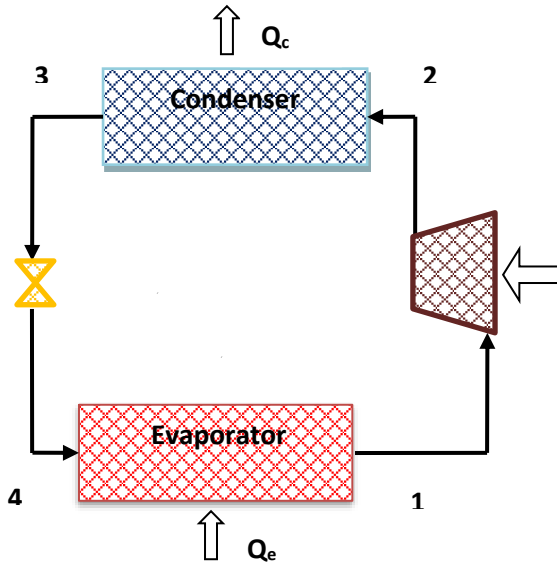
## **Material And Methods**

The method used in this study is based on a review of similar studies in the literature to develop a theoretical approach suitable for the use of nanorefrigerants in the vapor compression refrigeration cycle (Bilen et al 2021; Aktemur and Ozturk 2022; Kumar et al. 2016). To better understand the theoretical model, an ideal vapor compression cycle is first considered and explained using basic thermodynamic equations. Figure 1 shows the vapor compression refrigeration cycle.

This theoretical model is based on similar studies in the literature and studies by Aktas et al. (2015) and Kumar et al. (2016). In the system, the fluid is assumed to be superheated vapor from the evaporator and compressed liquid from the condenser. In a simplified model, the heat loss and pressure drop of the working fluid during heat transfer are not considered. The refrigerant and



nanoparticles have the same temperature inside each component. In this study, the isentropic efficiency of the compressor is considered because the COP of the system is directly dependent on the energy consumption of the compressor. For the vapor compression refrigeration cycle given in Figure 1, the energy balance is written per unit mass, and the calculations are made using the relations valid under steady regime conditions. The related relations for the cycle are given below. The isentropic efficiency of the compressor is calculated using Equation (4) (Elakdhar et al. 2007).



*Figure 1. The vapor compression refrigeration cycle*

The equations are given used in thermodynamic analysis below (Bejan et al. 1996):

General mass and energy balance:

$$\Sigma \dot{m}_{in} = \Sigma \dot{m}_{out} \quad (1)$$

$$\dot{Q} - \dot{W} = \Sigma \dot{H}_{out} - \Sigma \dot{H}_{in} \quad (2)$$

$$q_e = h_1 - h_4 \quad (3)$$

$$q_c = h_2 - h_3 \quad (4)$$

$$\eta_{is} = 0,874 - 0,0135 \frac{P_c}{P_e} \quad (5)$$

$$w_{net} = h_2 - h_1 \quad (6)$$

$$COP = \frac{h_1 - h_4}{h_2 - h_1} \quad (7)$$

$$\rho_{nr} = \omega - \rho_{np} + (1 - \omega)\rho_{pr} \quad (8)$$

The properties of nanofluids are given in the Table 1 (Kosmadakis and Neofytou 2019).

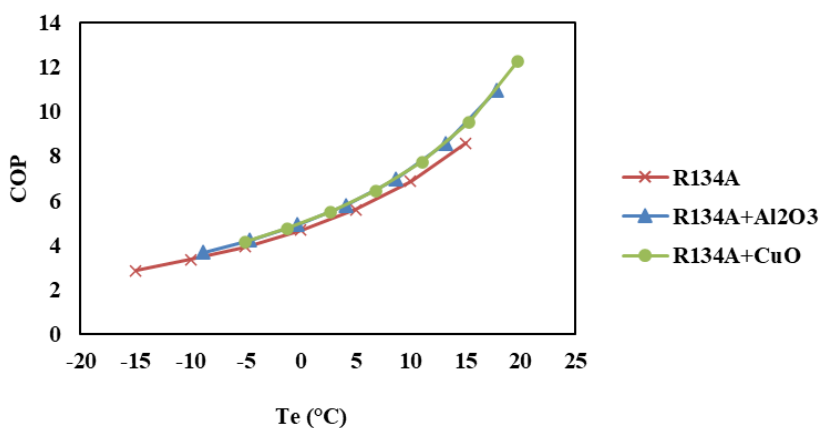
*Table 1. Properties of the nanoparticles at 25°C*

Nanoparticle	Thermal Conductivity (W.m-1.°C-1)	Density (kg.m-3)	Specific Heat (kJ.kg-1.°C-1)	Particle Size (nm)
Al2O3	38,7	3690	0,765	48
CuO	33,0	6315	0,530	77

Nanofluid properties can be obtained using the method used in Aktaş et al. [17]. The properties of a nanorefrigerant are determined by parameters such as density and enthalpy of the working fluid.

## Results And Discussion

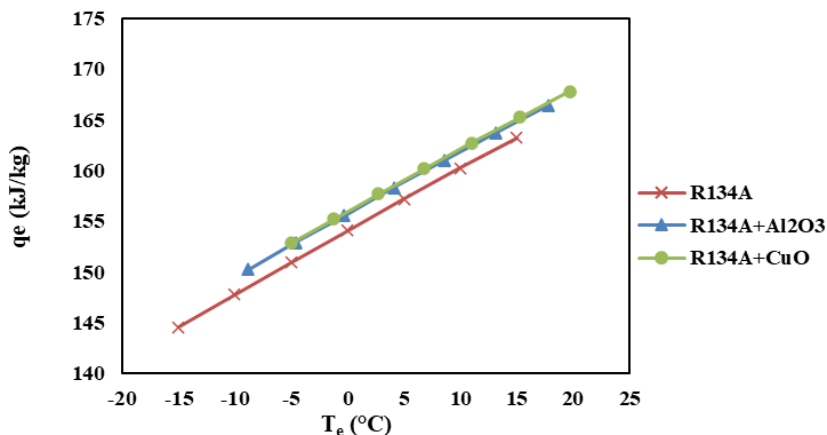
In this study,  $\text{Al}_2\text{O}_3$  and  $\text{CuO}$  the nanoparticles were added to the R134A fluid, and their effects on the system were theoretically analyzed. First law analyses were performed and COP values were obtained and compared with R134A fluid. The variation of the system parameters was investigated for different evaporator temperatures in this study. The condenser temperature was kept constant at  $40^\circ\text{C}$  for the R134A fluid and mixtures. The mass fractions of  $\text{Al}_2\text{O}_3$  and  $\text{CuO}$  the nanoparticles were kept constant at 0.006. As can be seen in Figure 2, the COP value increases as the evaporator temperature increases for the R134A, R134A+ $\text{Al}_2\text{O}_3$ , and R134A+ $\text{CuO}$  fluids. On the other hand, the COP values of R134A+ $\text{CuO}$  fluid are slightly higher than those of R134A and R134A+ $\text{Al}_2\text{O}_3$ . The lowest COP values were observed in R134A.



*Figure 2. Variation of COP with the evaporation temperature*

In Figure 3, the evaporator capacity increases as the evaporator temperature increases. This is because the enthalpy of the fluid leaving the evaporator increases in direct proportion to evaporation. It has been observed that the evaporator capacities of

R134A+ Al<sub>2</sub>O<sub>3</sub> and R134A+CuO fluids are higher than those of R134A.



*Figure 3. Variation of the evaporator capacity with the evaporation temperature*

In Figure 4, similar to the evaporator capacity, the enthalpy of the fluid entering the compressor increases as the evaporator temperature increases. On the other hand, the compressor needs to compress the fluid less. It has been observed that the compressor works of R134A+Al<sub>2</sub>O<sub>3</sub> and R134A+ CuO fluids are less than R134A. As can be seen from Figure 5, the same result was observed for the compression ratios.

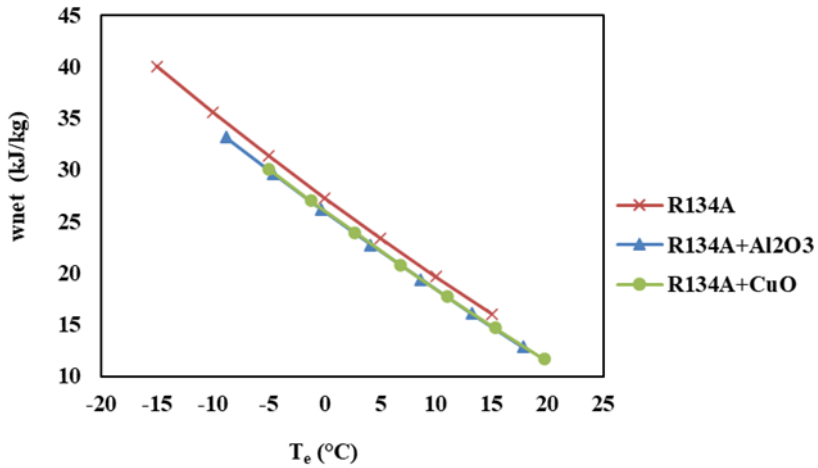


Figure 4. Variation of the compressor work with evaporation temperature

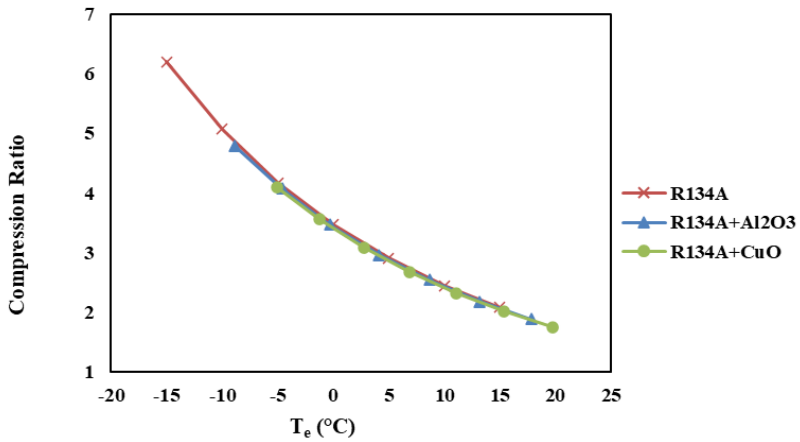
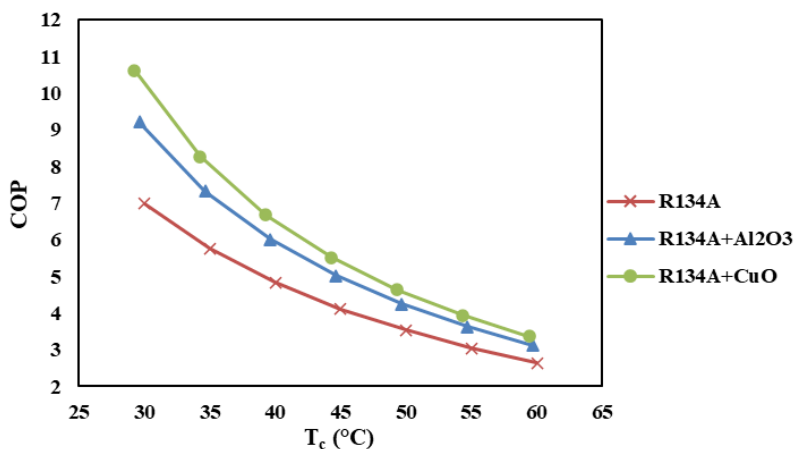


Figure 5. Variation of the compression ratio with evaporation temperature

The variation of the system parameters was investigated for different condenser temperatures in this study. The evaporator temperature was kept constant, and the mass fraction of

nanoparticles in the mixtures was determined as 0.006. According to the results show in Figure 6, the COP values for the R134A, R134A+Al<sub>2</sub>O<sub>3</sub>, and R134A+CuO fluids decrease as the condenser temperature increases. The COP values of R134A+CuO fluid are slightly higher than those of the R134A and R134A+Al<sub>2</sub>O<sub>3</sub> fluids. The lowest COP values were determined for R134A.



*Figure 6. Variation of COP with condenser temperatures*

According to the results show in Figure 7, as the condenser temperature increases, the enthalpy of the fluid leaving the compressor increases. Also, the compressor has to compress the fluid more. The compressor work of R134A+Al<sub>2</sub>O<sub>3</sub> and R134A+CuO fluids is lower than that of R134A. According to the results show in Figure 8, the same trend has been observed in compression ratios.

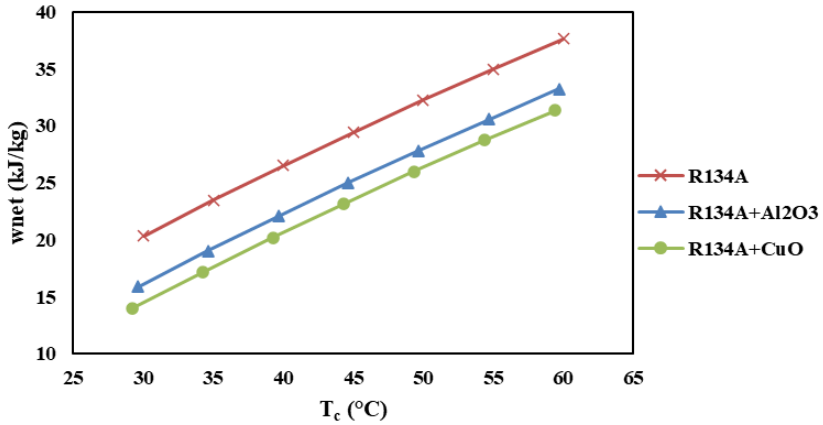


Figure 7. Variation of the compressor work with condenser temperature

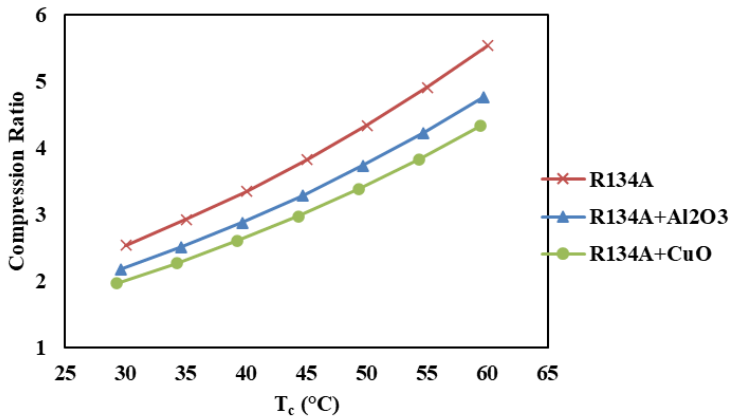


Figure 8. Variation of the compression ratio with condenser temperature

The variation of the system parameters was investigated for different mass fraction in this study. The evaporator temperature was kept constant at 1°C and the condenser temperature was kept constant at 40°C for the R134A fluid and mixtures. As can be seen in Figure 9, the COP value increases as the mass fractions

temperature increases for R134A+Al<sub>2</sub>O<sub>3</sub> and R134A+CuO fluids. On the other hand, the COP values of R134A+CuO fluid are slightly higher than R134A+Al<sub>2</sub>O<sub>3</sub>. The work in the compressor decreases as the mass fraction increases (Figure 10). In this respect, the COP value increases. As can be seen in Figure 11, the evaporator capacity increases with the nanoparticle mass fraction.

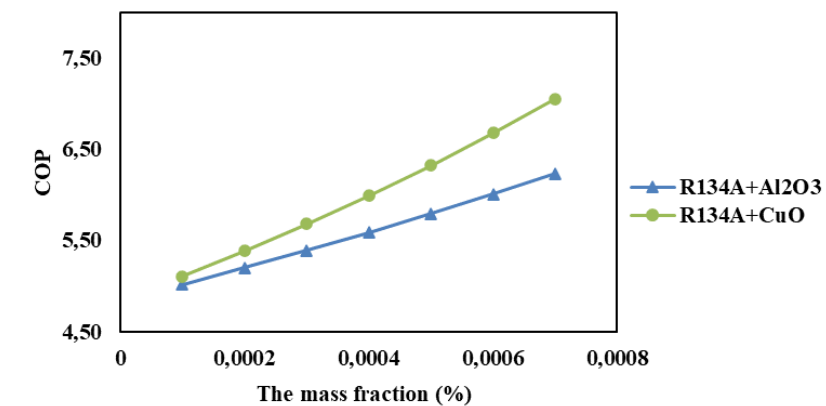


Figure 9. Variation of the COP with different mass fraction

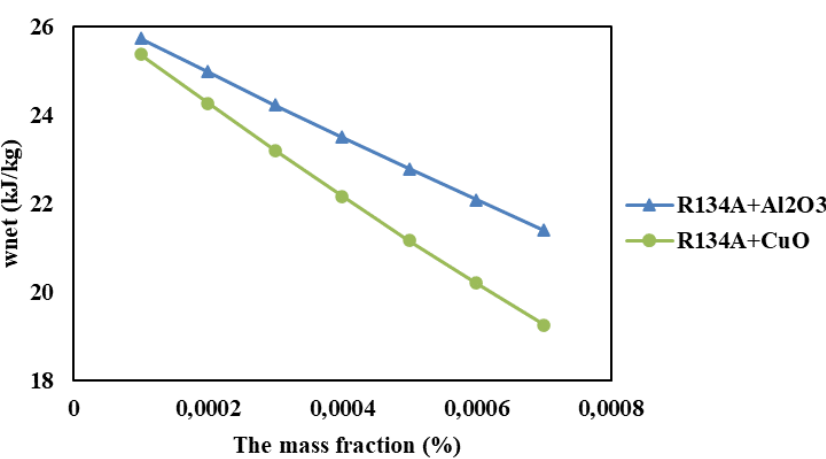
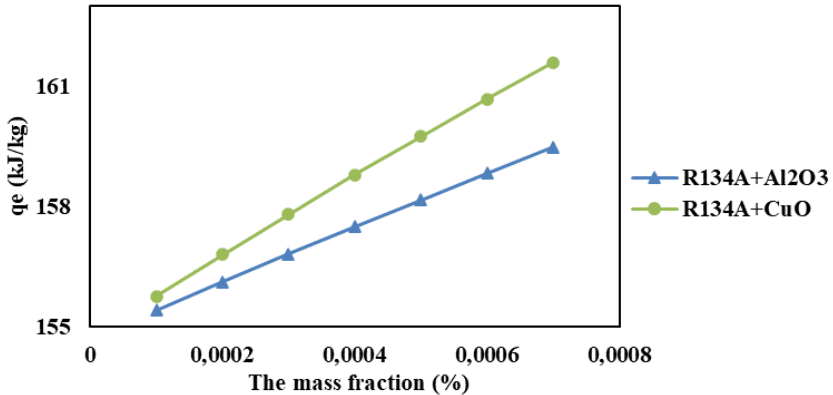


Figure 10. Variation of the compressor work with different mass fraction





*Figure 11. Variation of the evaporator capacity with mass fraction*

## Conclusions

$\text{Al}_2\text{O}_3$  and  $\text{CuO}$  nanoparticles were added to R134A fluid and theoretically analyzed in vapor compression refrigeration cycle. As a result of the addition of nanoparticles to the refrigerant, an increase in the COP and evaporator capacity of the system was observed. On the other hand, a decrease in the compressor power consumption was observed. For the same concentration values and,  $\text{CuO}$  nanoparticles gave better results than  $\text{Al}_2\text{O}_3$  nanoparticles.

The addition of nanoparticles significantly affects the thermal, physical, and heat transfer properties of the refrigerant. These fluids are formed by dispersing nanoparticles in the liquid. The application of nanoparticles as additives in refrigerants and as lubricants in the vapor compression refrigeration system is positive and promising. The use of nanofluids in refrigeration systems provides high efficiency and lower energy consumption. It also offers an important alternative from an environmental view point. Thus, with these nanofluids, both lower energy consumption and higher environmental protection are achieved.

To reduce energy consumption in the vapor compression mechanical refrigeration cycle and to ensure environmental protection, the determination of the refrigerants that may be suitable and the system elements that meet desired criteria will increase energy efficiency in these systems.

### **Nomenclatura**

COP : Cooling Performance Coefficient

$h$  : Enthalpy (kJ/kg)

$P$  : Pressure (bara)

$\dot{Q}$  : Heat flow rate (kW)

$T$  : Temperature (°C)

$\dot{W}$  : Compressor work (kW)

#### Subscripts

$c$  : condenser

$e$  : evaporator

$in$  : inlet

$out$  : Streams leaving a component

#### Greek Symbols

$\omega$  : Mass fraction

$\eta_{is}$  : Isentropic efficiency

$\rho$  : Density (kg/m<sup>3</sup>)

## References

Jain V, Kachhwaha SS, Sachdeva G. 2013. Thermodynamic performance analysis of a vapor compression–absorption cascaded refrigeration system, *Energy Conversion and Management* 75: 685-700.

Colorado D, Velázquez V.M. 2013. Exergy analysis of a compression–absorption cascade system for refrigeration, *International Journal of Energy Research* 37: 1851-1865.

Zhang H, Pan X, Chen J, Xie J. 2023. Energy, exergy, economic and environmental analyses of a cascade absorption-compression refrigeration system using two-stage compression with complete intercooling, *Applied Thermal Engineering* 225: 120185.

Cimsit C, Ozturk I.T. 2014. The vapour compression-absorption two stage refrigeration cycle and its comparison with alternative cycles, *Journal of Thermal Science and Technology* 34: 1, 19-26.

Bilen K, Dagidir K, Arcaklioglu E. 2021. Theoretical Analysis of Usage of R1234yf Refrigerant and R1234yf/Al<sub>2</sub>O<sub>3</sub> and R1234yf/CNTs Nanorefrigerants instead of R134a in the Vapor Compression Refrigeration Cycle in terms of I. and II. Laws of Thermodynamics, *Gazi Journal of Engineering Sciences* 3: 183-195 (Turkish).

Pawale K T, Dhupal A H, Kerkal G. M. 2017. Performance Analysis of VCRS with Nano-Refrigerant, *International Research Journal of Engineering and Technology (IRJET)* 04: Issue: 04.

Babarinde T O, Akinlabi S A, Madyira D M. 2018. Enhancing the Performance of Vapour Compression Refrigeration

System using Nano Refrigerants: A review, *IOP Conf Ser Mater Sci Eng.* 413: 1-8.

Ajayi O, Ukasoanya DE, Ogbonnaya M, Salawu E Y, Okokpujie I P, Akinlabi S A, Akinlabi E T, Owoeye F T. 2019. Investigation of the Effect of R134a/Al<sub>2</sub>O<sub>3</sub>–Nanofluid on the Performance of a Domestic Vapour Compression Refrigeration System, *Procedia Manufacturing* 35:112–117.

Aly M A, Soliman A, Ali K, Rahman A, Ookawara S. 2019. Enhancement of vapor compression cycle performance using nanofluids, *Journal of Thermal Analysis and Calorimetry* 135:1507–1520.

Hussain T, Khan F, Ansari A, Chaturvedi P, Mohd Yahya S. 2018. Performance improvement of vapour compression refrigeration system using Al<sub>2</sub>O<sub>3</sub> nanofluid, *IOP Conf. Series: Materials Science and Engineering* 377: 012155.

Adelekan DS, Ohunakin OS, Gill J, Atiba OE, Okokpujie IP, Atayero AA. 2019. Experimental investigation of a vapour compression refrigeration system with 15 nm TiO<sub>2</sub>-R600a nano refrigerant as the working fluid, *Procedia Manufacturing* 35:1222-1227.

Jatinder G, Ohunakin OS, Adelekan DS, Atiba OE, Daniel AB, Singh J, Atayero A. 2019. Performance of a domestic refrigerator using selected hydrocarbon working fluids and TiO<sub>2</sub>-MO nanolubricant, *Applied Thermal Engineering* 160:114004.

Nair V, Parekh AD, Tailor PR. 2020. Experimental investigation of a vapour compression refrigeration system using

R134a/Nano-oil mixture, *International Journal of Refrigeration* 112: 21-36.

Adelekan DS, Ohunakin OS, Oladeinde MH, Jatinder G, Atiba OE, Nkiko MO, Atayero AA. 2021. Performance of a domestic refrigerator in varying ambient temperatures, concentrations of TiO<sub>2</sub> nanolubricants and R600a refrigerant charges, *Heliyon* 7: 1-13.

Joshi Y, Zanwar D, Joshi S. 2020. Performance investigation of vapor compression refrigeration system using R134a and R600a refrigerants and Al<sub>2</sub>O<sub>3</sub> nanoparticle-based suspension, *Materials Today: Proceedings* 44: 1511-1519.

Senthilkumar A, Anderson A. 2021. Experimental investigation of SiO<sub>2</sub> nanolubricants for R410A vapour compression refrigeration system, *Materials Today: Proceedings* 44: 3613- 3617.

Aktemur C, Ozturk IT. 2022. Thermodynamic performance enhancement of booster assisted ejector expansion refrigeration systems with R1270/CuO nano-refrigerant, *Energy Convers. Manag.* 253:115191.

Kumar VPS, Baskaran A, K.M Subaramanian KM. 2016. A performance study of vapour compression refrigeration system using ZrO<sub>2</sub> nano particle with R134a and R152a, *International Journal of Scientific and Research Publications* 6: no. 12, 410-421.

Aktas M, Dalkilic AS, Celen A, Cebi A, Mahian O, Wongwise S. 2015. A theoretical comparative study on nanorefrigerant performance in a single-stage vapor-compression refrigeration cycle, *Advances in Mechanical Engineering* 7: 1-12.

Elakdhar M, Nehdi E, Kairouani L. 2007. Analysis of a compression/ejection cycle for domestic refrigeration, *Ind. Eng. Chem. Res.* 46: (13) 4639–4644.

Bejan A, Tsatsaronis G, Moran M. 1996. Thermal Design & Optimization, Wiley, New York.

Kosmadakis G, Neofytou P. 2019. Investigating the effect of nanorefrigerants on a heat pump performance and cost-effectiveness, *Therm. Sci. Eng. Prog.* 13:100371

